Measurement of charged fragments production cross sections (dσ/dE) in the interactions of C-ions with C,H,O targets

Episode II: forward angles

IlaMi for Roma and Milano, June 2020

Experimental SETUP

CNAO

Thin Targets based on C,H and O elements: PMMA, Graphite and Plastic Scintillator

- The fragments production (Z=1) has been measured as a function of the kinetic energy for 4 angles;
- The Time of Flight in thin plastic scintillators and the energy deposit in the inorganic crystals has been used for PID and kinetic energy measurements;

The thin targets (1-2 mm) do not require, as a first approximation, the implementation of a correction for the fragments absorption inside the target.

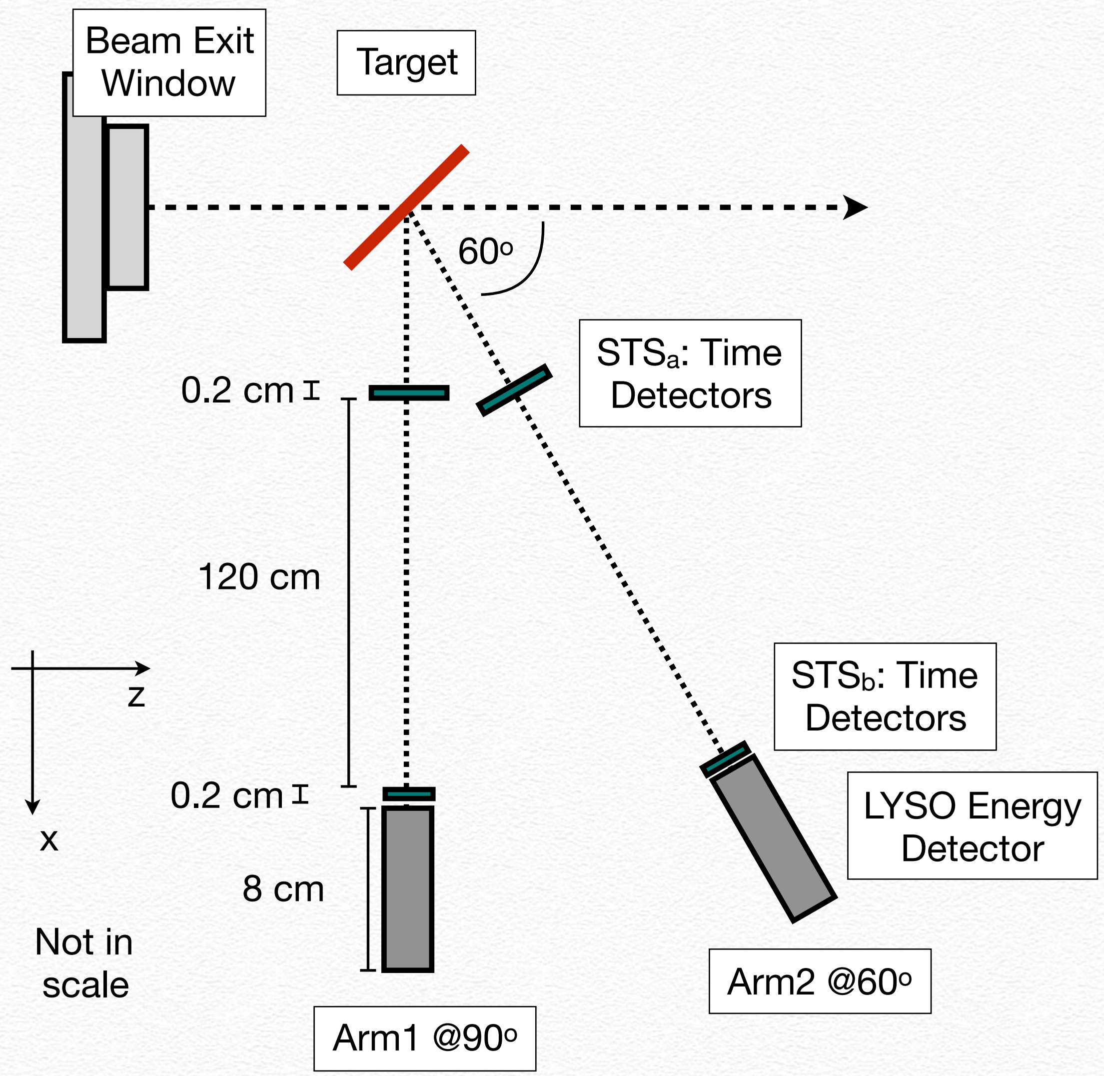

- 4 STS: thicknesses 2 mm for ToF measurements (Time Resolution ~400-600 ps) and Deposited Energy measurements (dE)
- 2 LYSO: 8 cm thick for Deposited Energy measurements (E)

Episode I: 90/60°

Experimental SETUP

CNAO

Thin Targets based on C,H and O elements: PMMA, Graphite and Plastic Scintillator

- The fragments production (Z=1) has been measured as a function of the kinetic energy for 4 angles;
- The Time of Flight in thin plastic scintillators and the ene
use

The thin targets (1-2 mm) do not require, as a first approximation, the implementation of a correction
bsorption
get.

“FORWARD” ANGLES:
50° ± 2° and 32° ± 2°

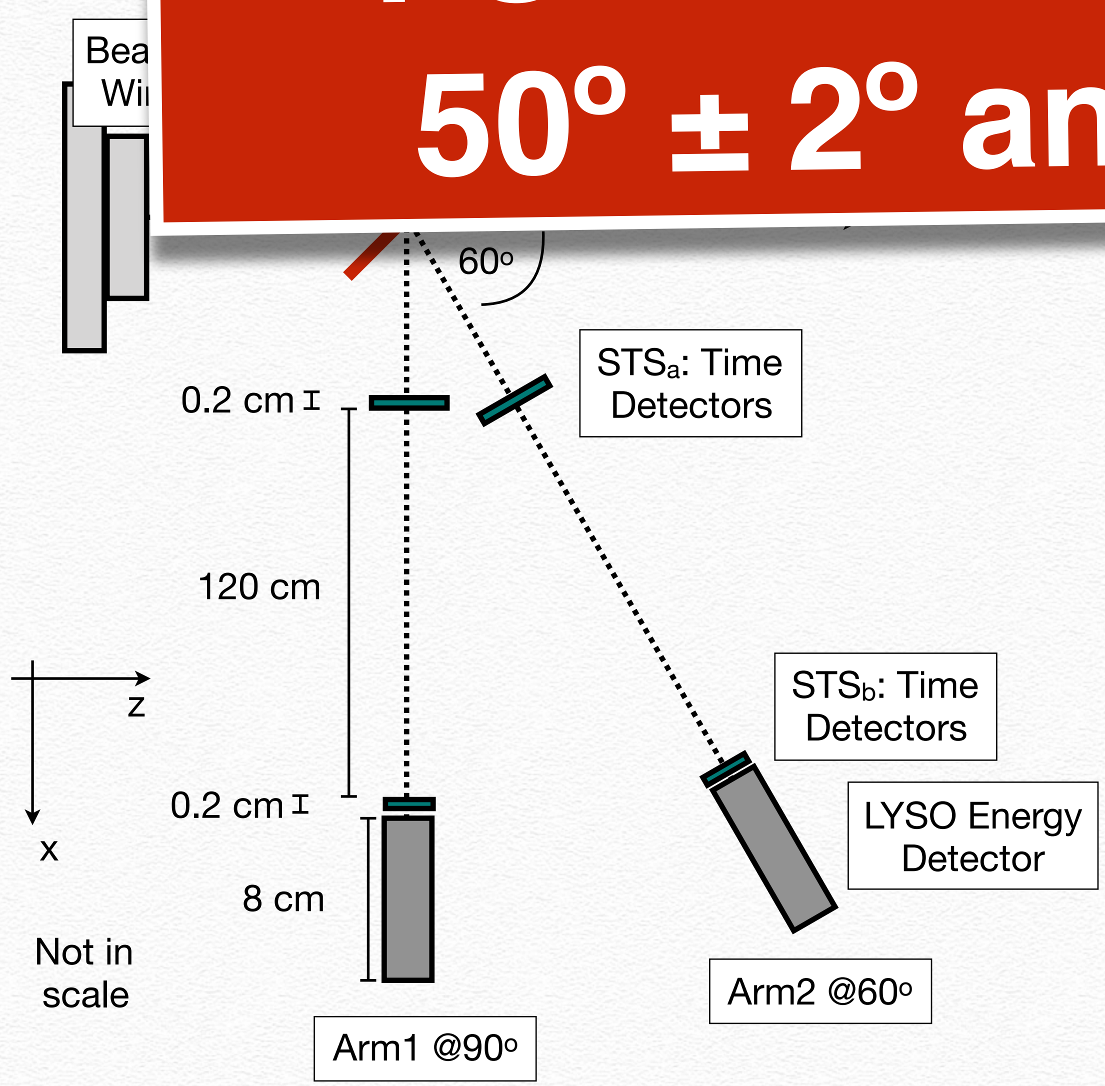

n for ToF measurements (Time Resolution ~400-600 ps) and Deposited Energy measurements (dE)

- 2 LYSO: 8 cm thick for Deposited Energy measurements (E)

Episode II: 50/32°

Cross section

The ^{12}C fragmentation cross sections for a $^{A}_{Z}X$ fragment are obtained as:

$$\frac{d\sigma}{dE_k}({}^{A}_{Z}X) = \frac{\boxed{N_{{}^{A}_{Z}X}(E_k)}}{N_{^{12}C}} \cdot \frac{1}{N_Y} \cdot \frac{1}{\epsilon}$$

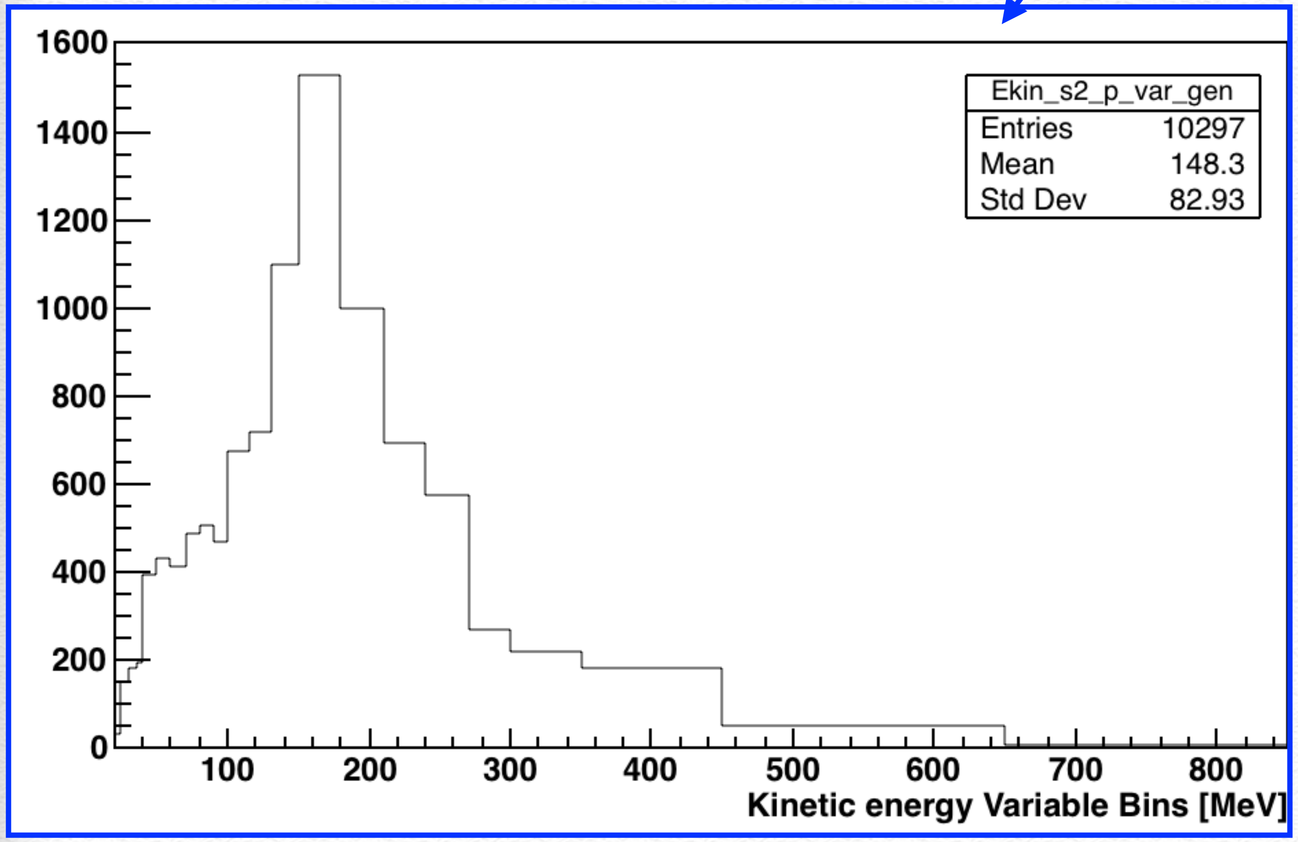

Ekin at generation

The energy loss by the fragments has been taken into account: we evaluate via MC the fragments (p,d,t) energy loss in target, air and sts1 and then we corrected the measured Ekin up to the energy at generation.

Cross section

The ^{12}C fragmentation cross sections for a $^{A}_{Z}X$ fragment are obtained as:

$$\frac{d\sigma}{dE_k}(^{A}_{Z}X) = \frac{\boxed{N_{^A_ZX}(E_k)}}{\boxed{N_{^{12}C}}} \cdot \boxed{\frac{1}{N_Y}} \cdot \frac{1}{\epsilon}$$

From CNAO
Dose Delivery

dose-current conversion systematic uncertainty. The relative uncertainty on $N_{^{12}C}$ (4%) is hence the convolution of the uncertainty on the stopping power determination [20] and on the dose measurements [21]. A possible additional contribution to the systematic uncertainty, coming from the monitoring system measurement stability [22], was found to be negligible

$N_{^{12}C}$	$\cdot 10^6$	$\cdot 10^6$	$\cdot 10^6$	$\cdot 10^6$	$\cdot 10^6$
Target	115 [MeV/u]	153 [MeV/u]	222 [MeV/u]	281 [MeV/u]	353 [MeV/u]
PMMA	49866	46512	49395	49601	42000
Graphyte	49454	46583	47484	47288	49328
Plast. Scint.	49728	50600	49347	49787	49653

Information of the target composition:

Target	Composition	Thickness $[mm]$	Density $[g/cm^3]$
PMMA	$C_5O_2H_8$	2	1.19
Graphite	C	1	0.94
Plas.Scint.	C_bH_a	2	1.024

$$N_Y = \frac{\rho_Y \cdot th_Y \cdot N_A}{A_Y}$$

thy=thy*sqrt(2)

Cross section

The ^{12}C fragmentation cross sections for a $^{A}_{Z}X$ fragment are obtained as:

$$\frac{d\sigma}{dE_k}({}^{A}_{Z}X) = \frac{\boxed{N_{{}^{A}_{Z}X}(E_k)}}{\boxed{N_{^{12}C}}} \cdot \boxed{\frac{1}{N_Y}} \cdot \frac{1}{\boxed{\epsilon}}$$

$$\epsilon = \epsilon_{Det} \cdot \epsilon_{Sel} \cdot \epsilon_{DT}$$

Solid angle and efficiencies

Protons, deutons and tritons impinged on the experimental setup to calculate the geometrical acceptance and the trigger+detection efficiency

Measurements of the DAQ dead time for each run (rate dependent)

Full simulation (C on Targets and fragments production). On the E (and dE) vs ToF distributions application of the PID selections tuned from data: evaluation of fragments (p, d, t) mis-identification.

Particle Identification

Protons Deutons and tritons have been selected from all other particles exploiting **deposited Energy vs ToF**, Edep vs 1/ToF, dE vs E and dE vs ToF information.

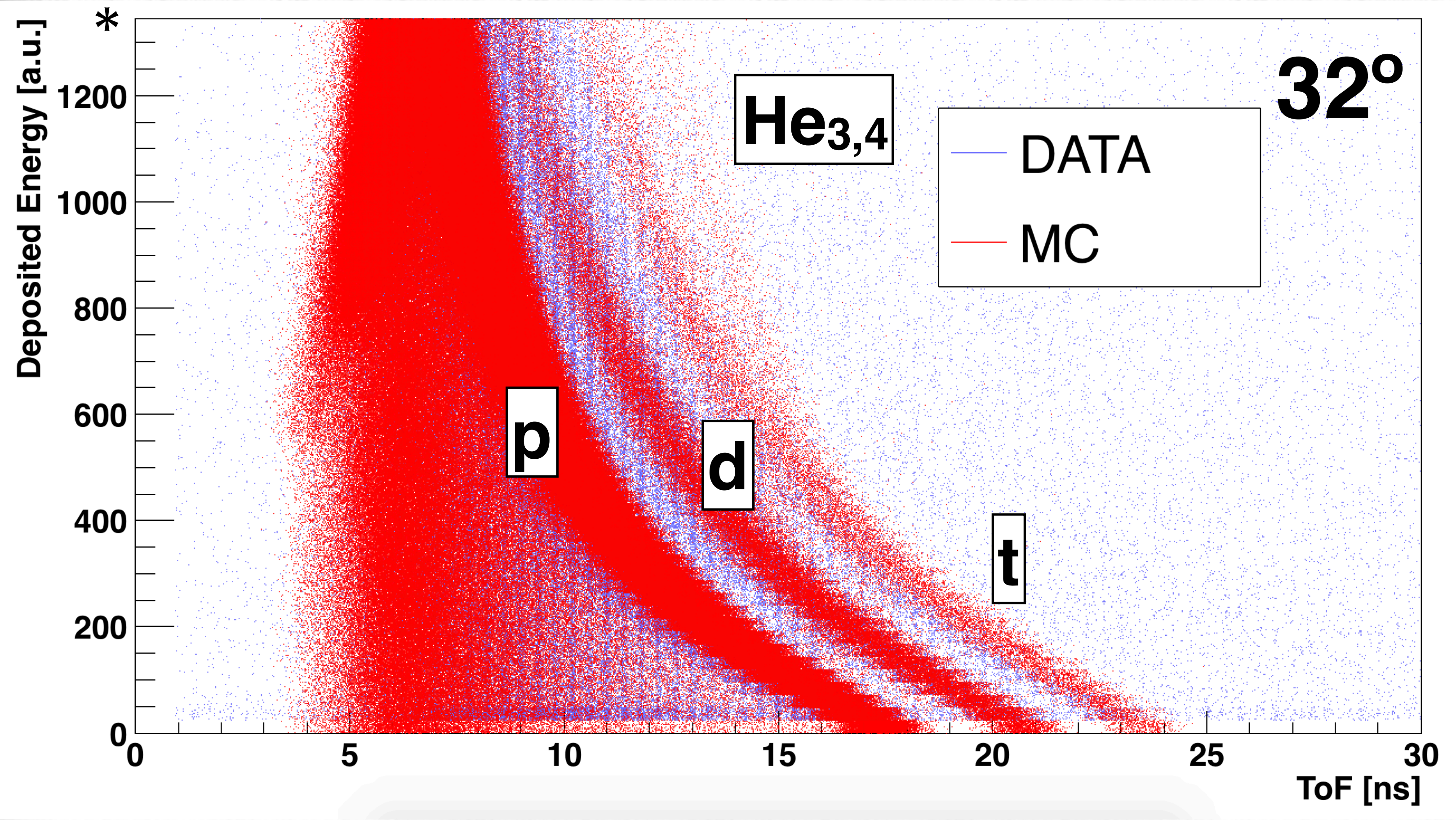

The use of MC allows to clearly identify the fragments and define our identification strategy.

The He contribution is visible.. see next slide for the Z>2 separation.

***QDC saturation @ 1350pC**

The deposited energy in the LYSO crystal is shown as a function of the time of flight of the measured particles for data and MC-data. For the data and the MC, the deposited energy is in arbitrary units. The fragments identity is shown in order to confirm the described data selection strategy.

Particle Identification

Protons Deutons and tritons have been selected from all other particles exploiting deposited Energy vs ToF, Edep vs 1/ToF, dE vs E and **dE vs ToF** information.

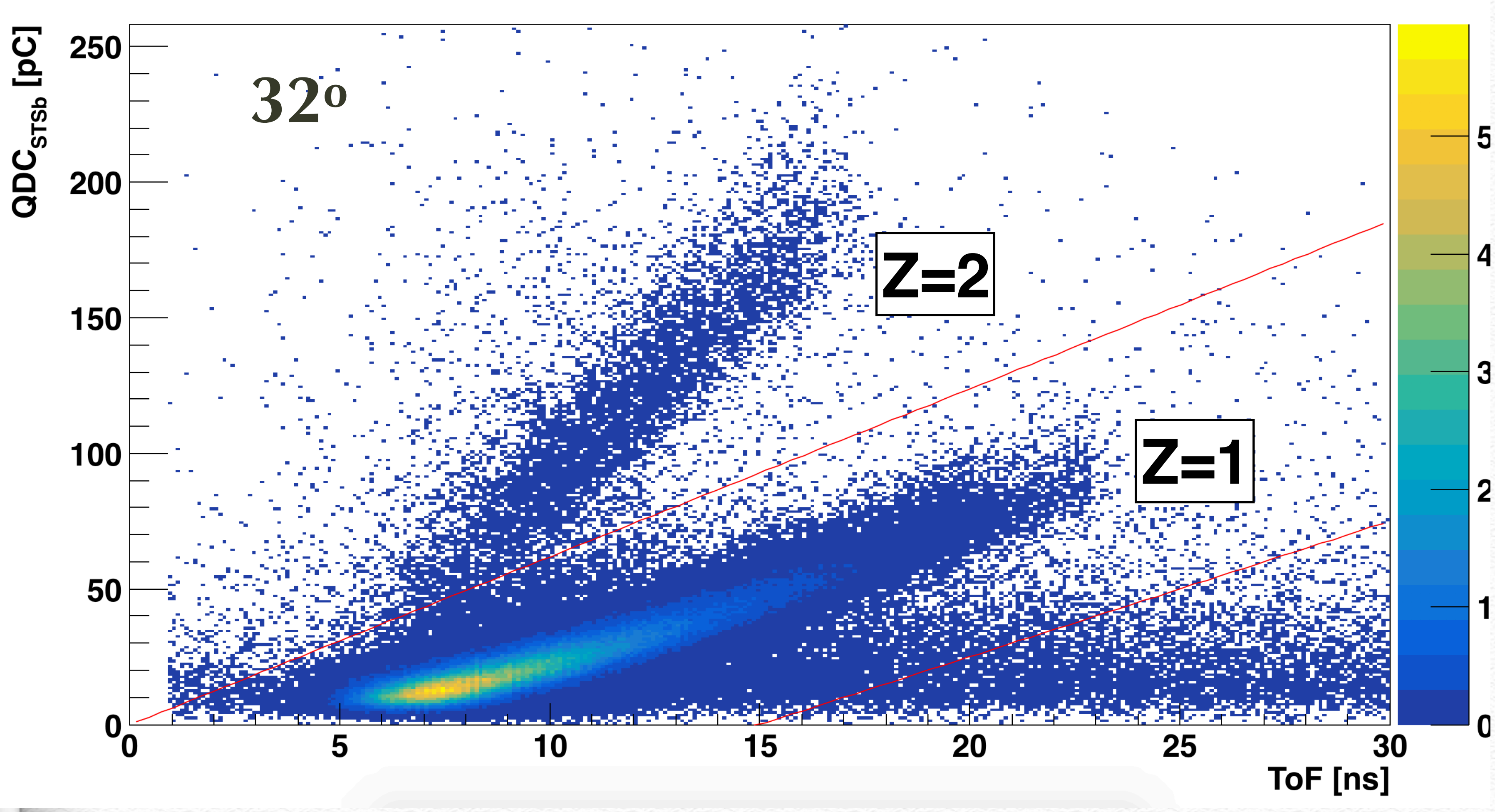

The helium fragments, as well as tritons, do not represent a statistically significant sample: only about 2% of the fragments are Z=2, at 32º. No cross section analysis has been performed for Z>1 fragments. They have been removed from the analysed data sample.

The energy loss in the STSb (in pC) is shown as a function of the time of flight of the measured particles. The populations of Z=1 and Z=2 at 32 degrees are clearly separated by the red line.

Particle Identification

32º

Protons Deutons and tritons have been selected from all other particles exploiting deposited Energy vs ToF, **Edep vs 1/ToF**, dE vs E and **dE vs ToF** information.

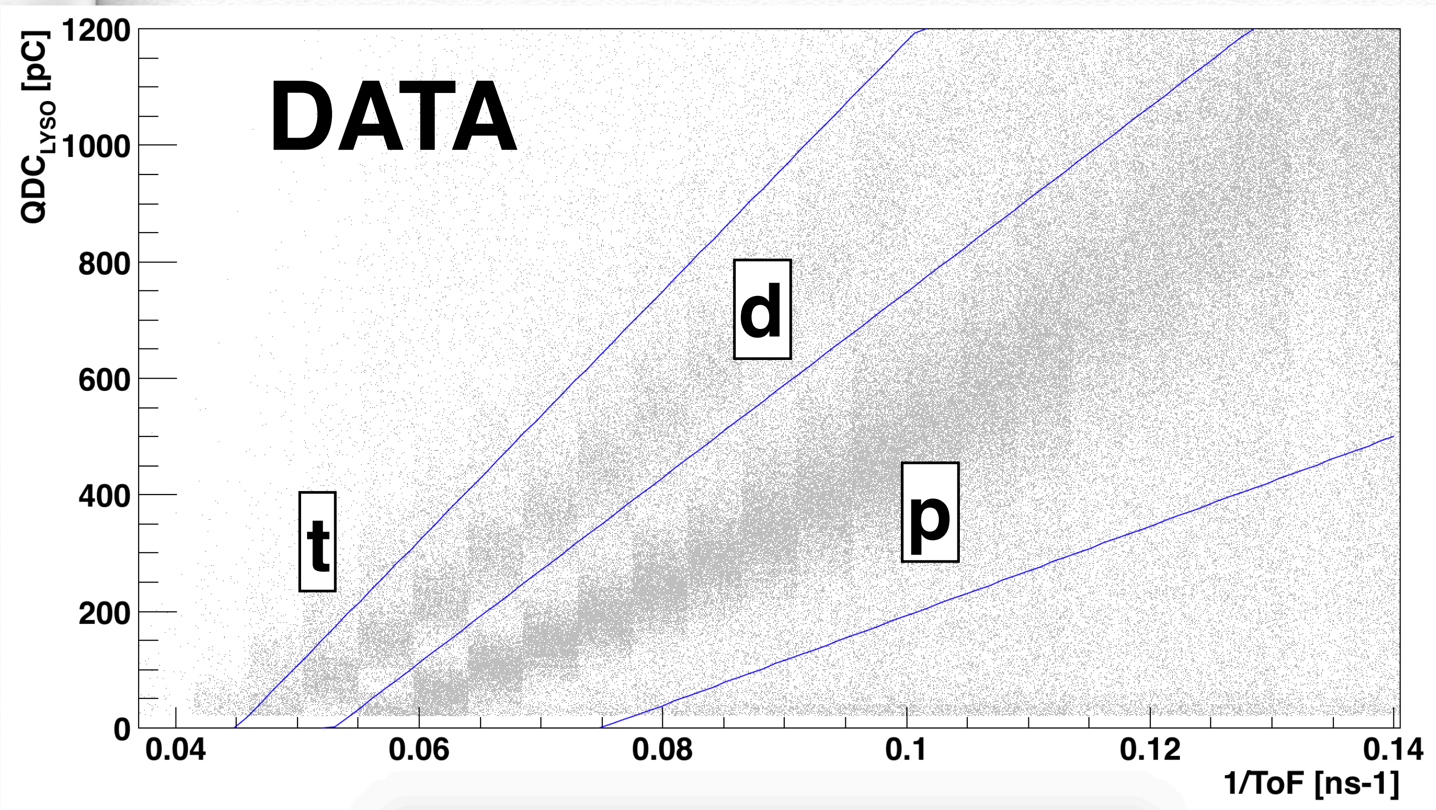

Protons and deuterons are reasonably abundant in all the specific data sets: about 80% and 20% of the fragments respectively at 32º.

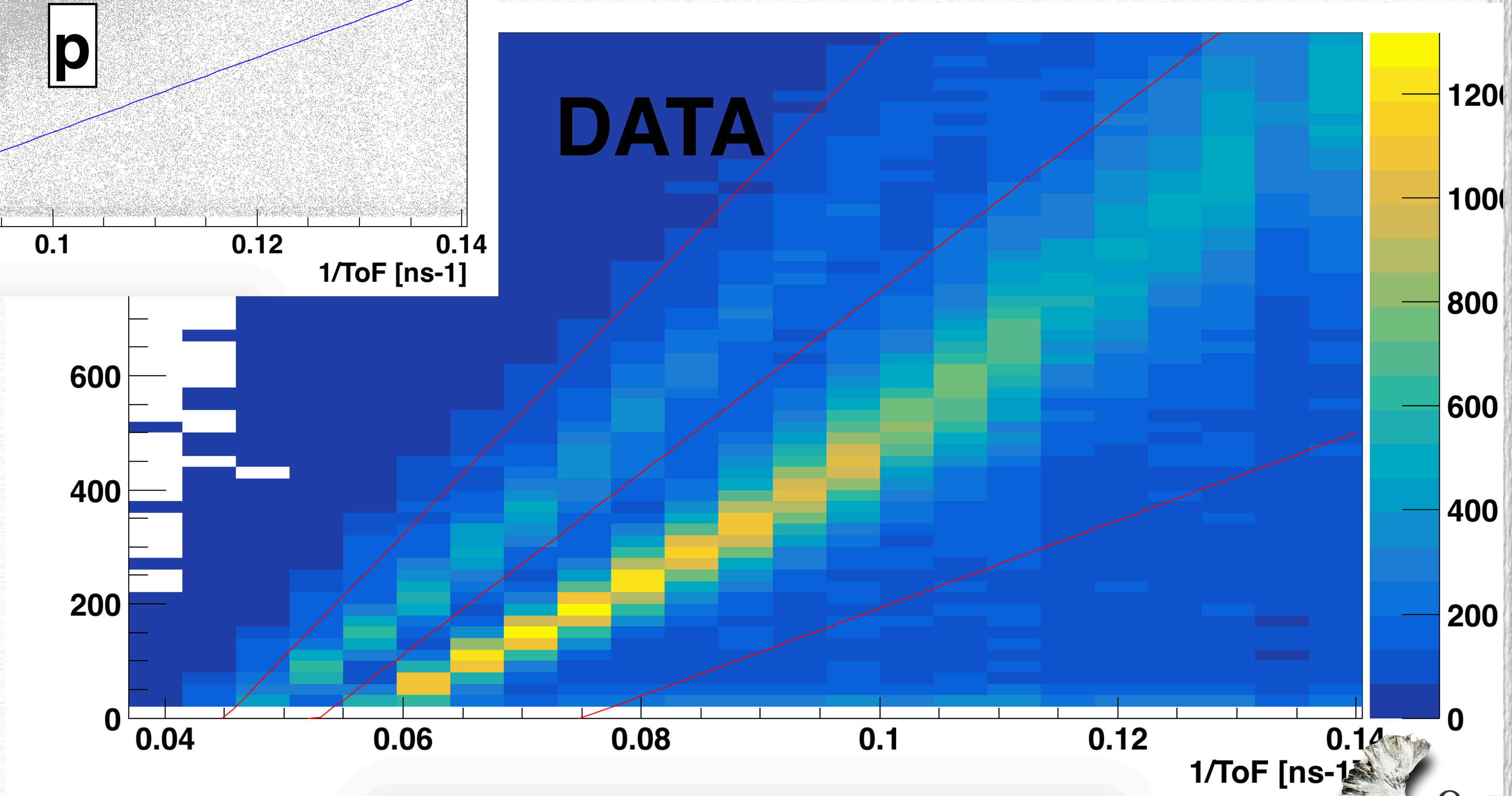

Kinetic Energy Spectra

Time of Flight distribution of protons is shown in the top plot and converted in the kinetic energy distribution as shown in the bottom plot. Data refer to Arm2, graphite target with C-ion beam at 352 MeV/u:

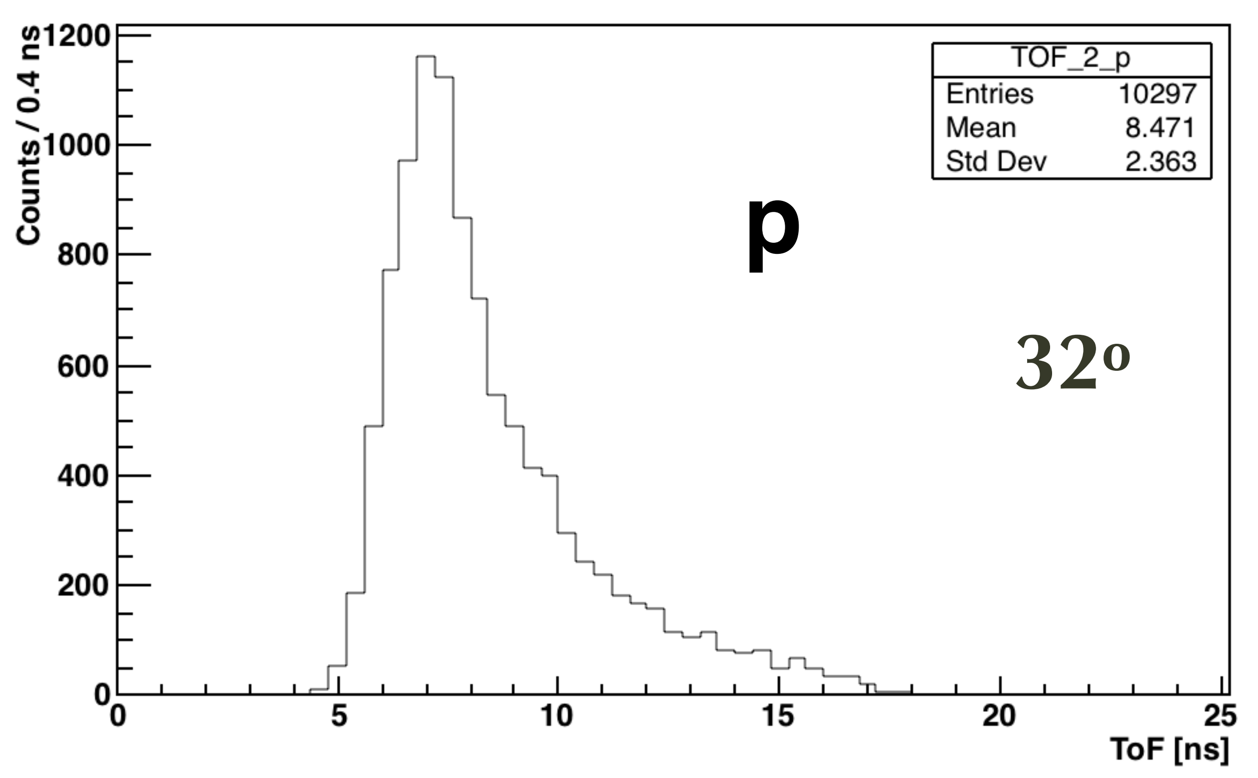

Time resolution evaluated from dedicated run:

- 50º: 720 ps
- 32º: 370 ps

$$\beta_i = L/(ToF_i \cdot c)$$

$$E_{kin} = m_i \cdot (\gamma - 1)$$

Energy resolution as a function of proton kinetic energy ranges from **12% (5%) up to 35% (20%)** for 50º (32º) (worsening with increasing energy).

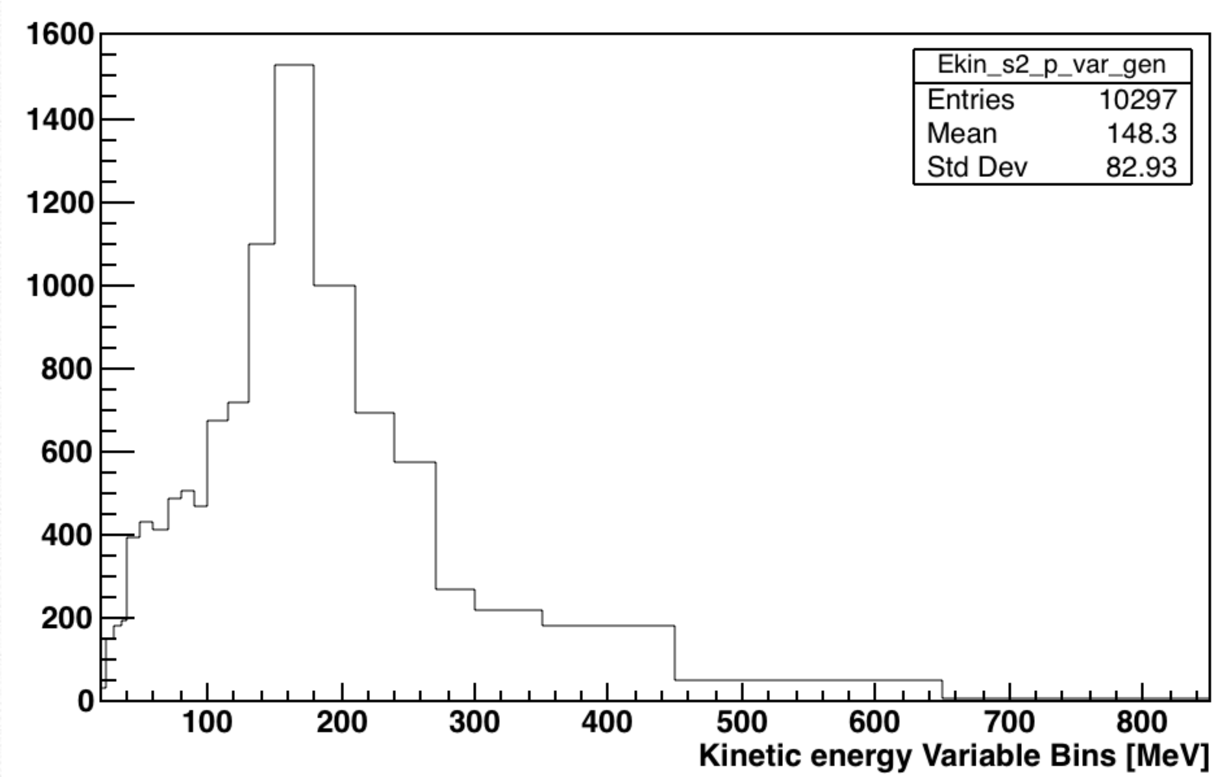

The kinetic energy has been reconstructed in variable size bins that have been chosen as a compromise between the **energy resolution and the available statistics** in each bin (in the final differential cross section evaluation).

Kinetic Energy Spectra

Time of Flight distribution of protons is shown in the top plot and converted in the kinetic energy distribution as shown in the bottom plot. Data refer to Arm2, graphite target with C-ion beam at 352 MeV/u:

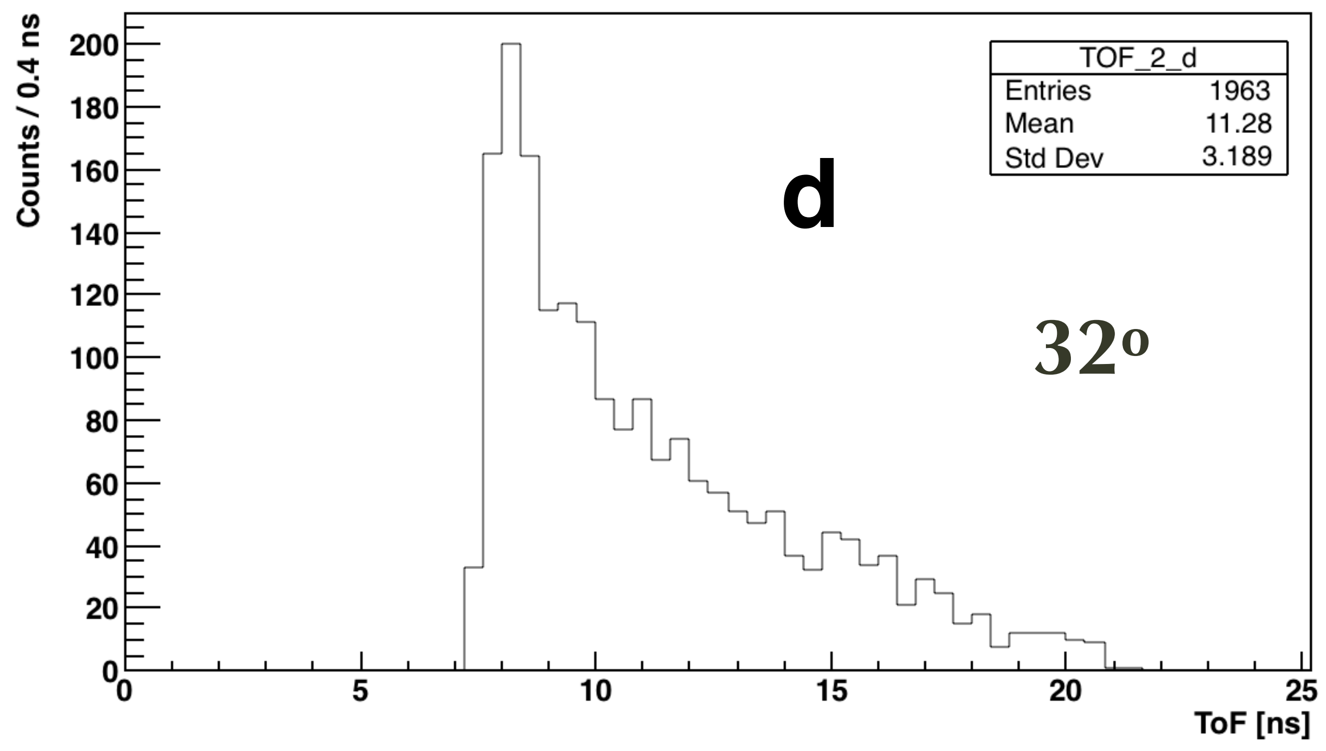

Time resolution evaluated from dedicated run:

- 50º: 720 ps
- 32º: 370 ps

$$\beta_i = L/(ToF_i \cdot c)$$

$$E_{kin} = m_i \cdot (\gamma - 1)$$

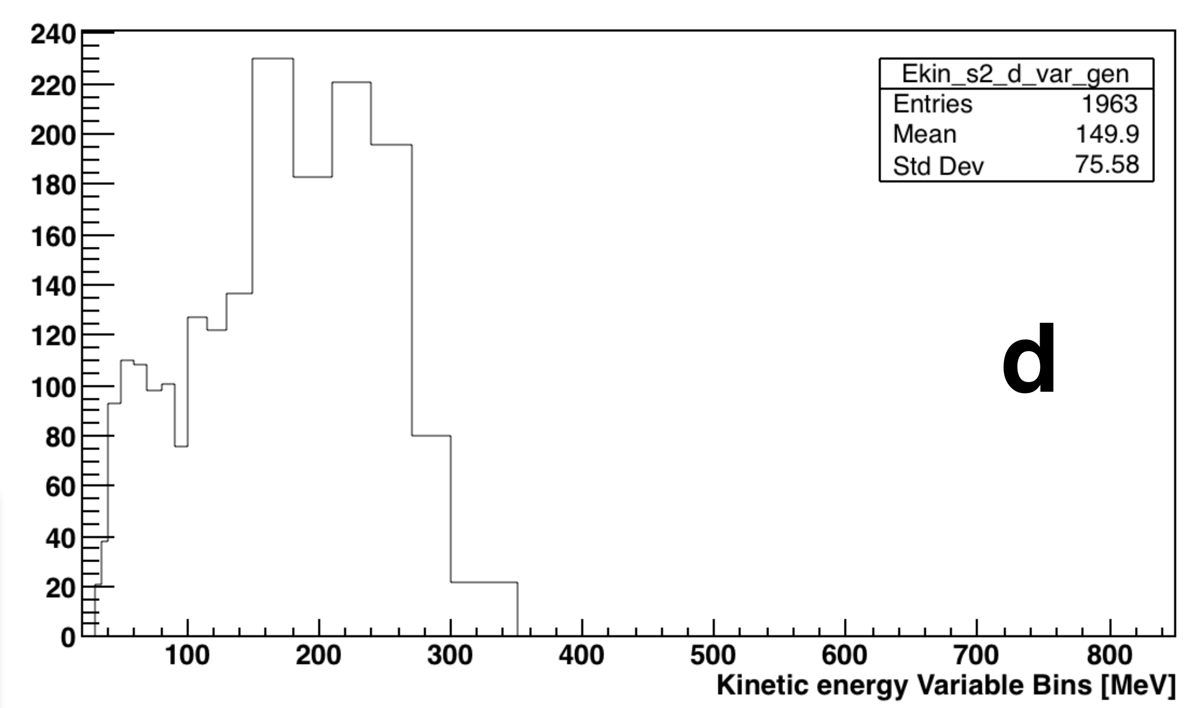

Energy resolution as a function of deuteron kinetic energy ranges from **8% (4%) up to 28% (11%)** for 50º (32º) (worsening with increasing energy).

The kinetic energy has been reconstructed in variable size bins that have been chosen as a compromise between the **energy resolution and the available statistics** in each bin (in the final differential cross section evaluation).

Efficiency evaluation:

$$\epsilon = \epsilon_{Det} \cdot \epsilon_{Sel} \cdot \epsilon_{DT}$$

The efficiency $\epsilon_{Det}(E_{kin})$ and ϵ_{Sel} have been evaluated using dedicated Monte Carlo simulations developed with the FLUKA code.

- To evaluate $\epsilon_{Det}(E_{kin})$: detector, angular, trigger, signal selection efficiency = > MC FLAT (no triggered MC: all events recorded): p, d, t sources, 4π production

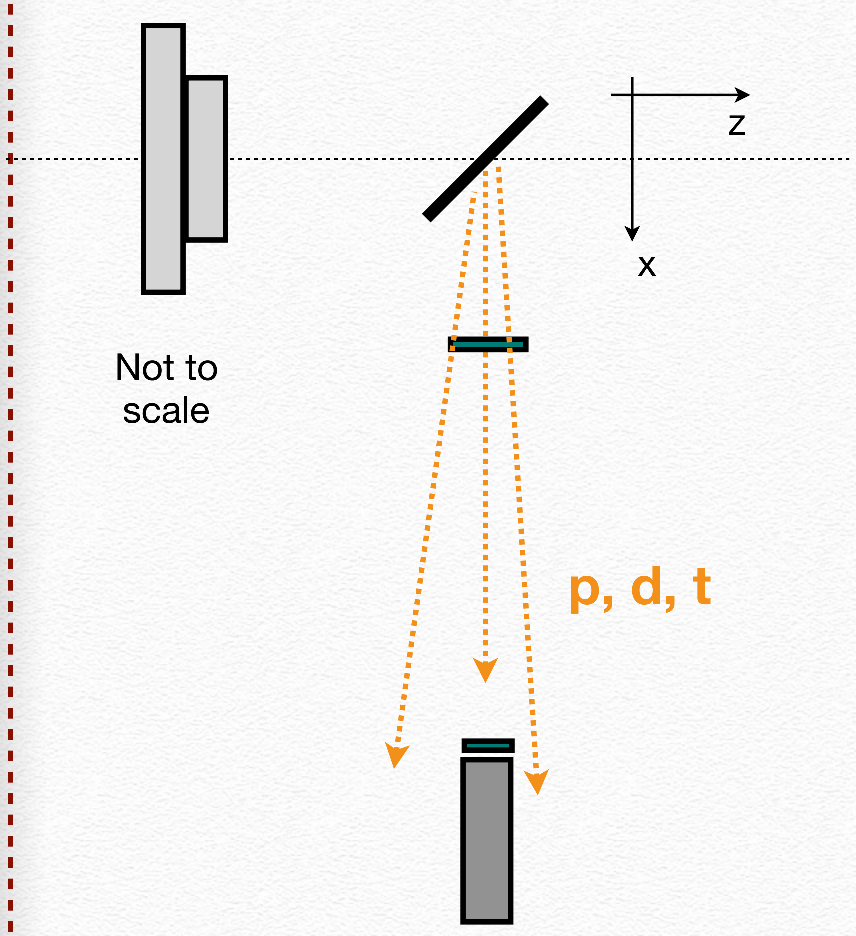

Efficiency evaluation:

$$\epsilon = \epsilon_{Det} \cdot \epsilon_{Sel} \cdot \epsilon_{DT}$$

The efficiency $\epsilon_{Det}(E_{kin})$ and ϵ_{Sel} have been evaluated using dedicated Monte Carlo simulations developed with the FLUKA code.

- To evaluate $\epsilon_{Det}(E_{kin})$: detector, angular, trigger, signal selection efficiency = > MC FLAT (no triggered MC: all events recorded): p, d, t sources, 4π production

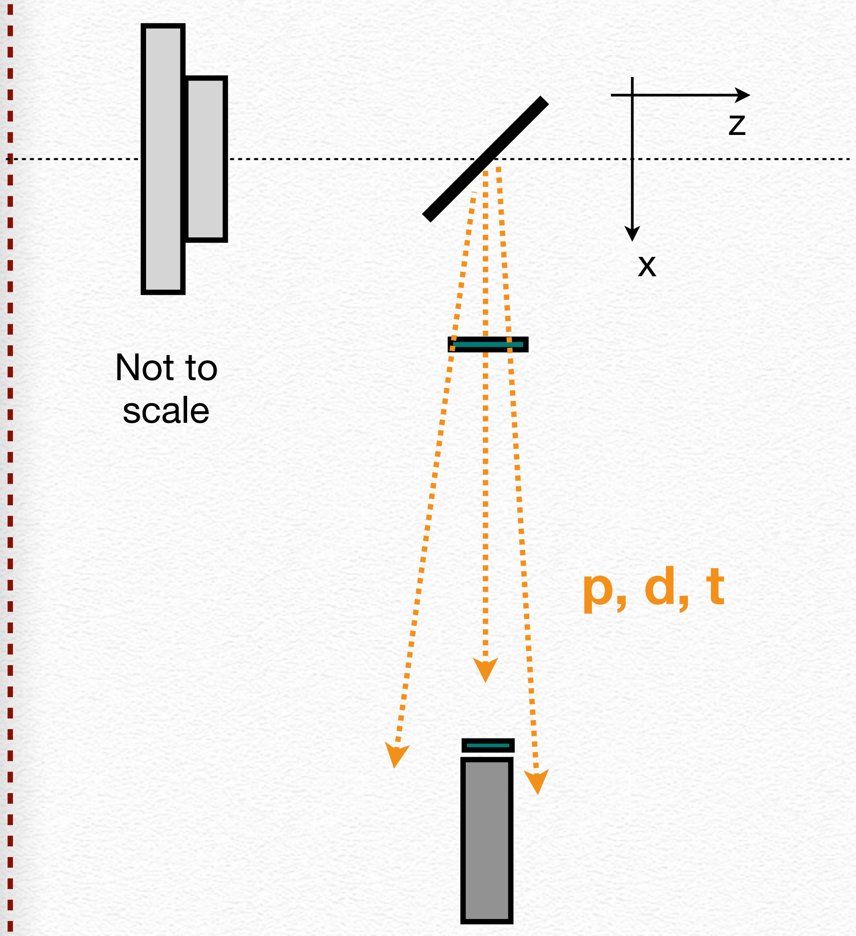

- To evaluate ϵ_{Sel}: p, d, t identification efficiency using the PID bands = > MC FULL (target, beam, etc..)

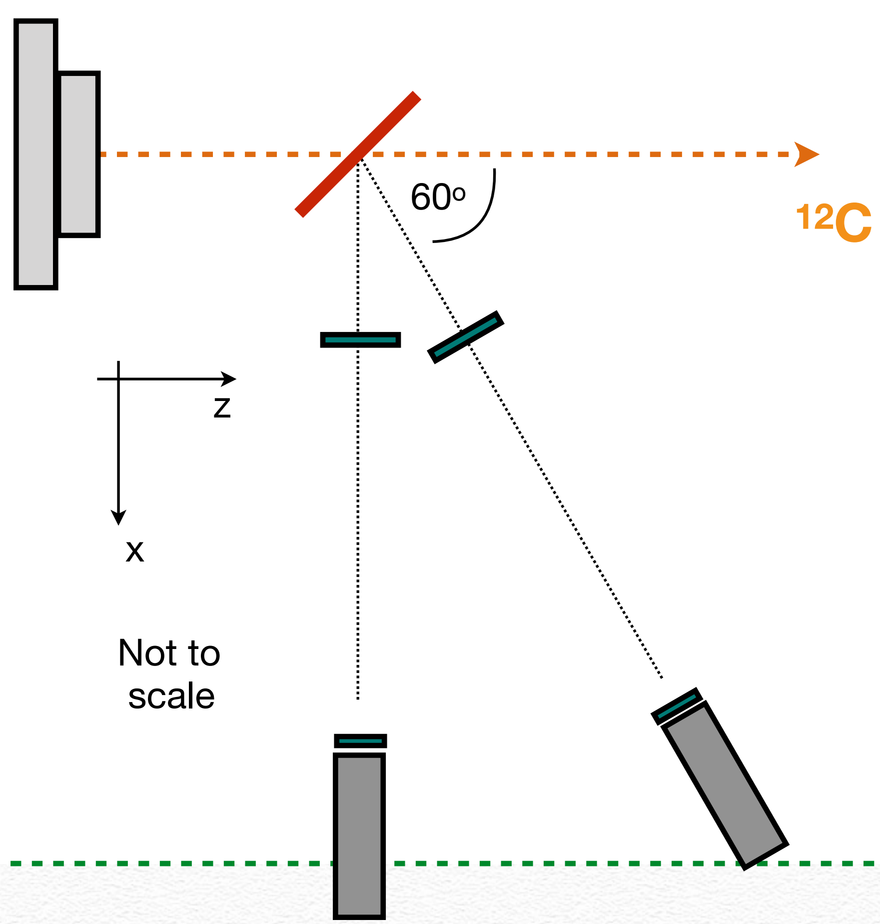

Det Efficiency: Trig + Det + Geo

Probability that a fragment of type *u* is measured by our detectors (*u = p, d, t*)

$$\epsilon^u_{Det}(E_{kin})_i = \left(\frac{N^u_{meas}}{N^u_{gen}}\right)_i$$

Simulation no trig of p (d, t) produced 4π with FLAT Ekin = [5 MeV - 1 GeV] (x2 if d) (x3 if t)

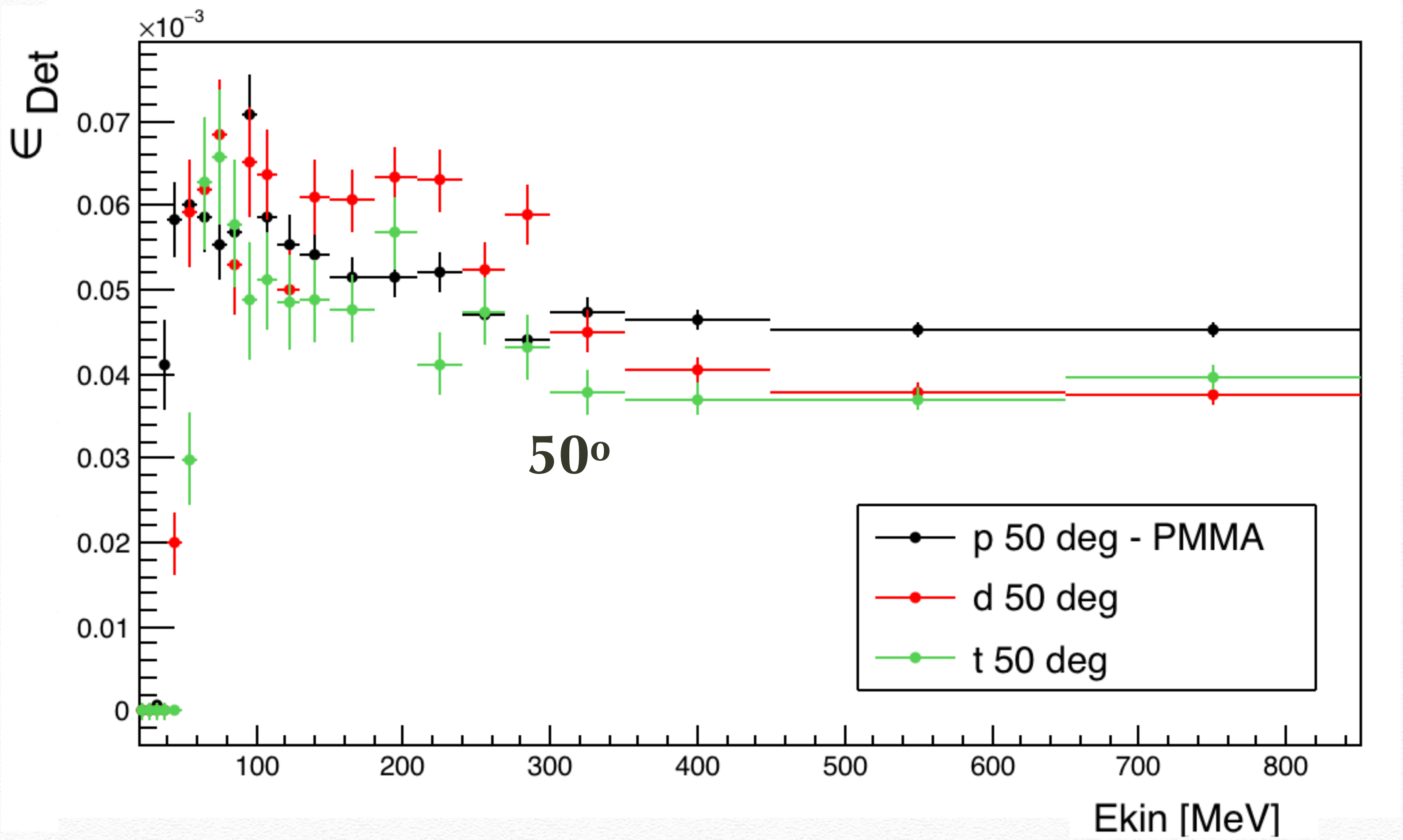

Det Efficiency: Trig + Det + Geo

Probability that a fragment of type *u* is measured by our detectors (*u* = *p, d, t*)

$$\epsilon^{u}_{Det}(E_{kin})_i = \left(\frac{N^{u}_{meas}}{N^{u}_{gen}}\right)_i$$

Simulation no trig of p (d, t) produced 4π with FLAT Ekin = [5 MeV - 1 GeV] (x2 if d) (x3 if t)

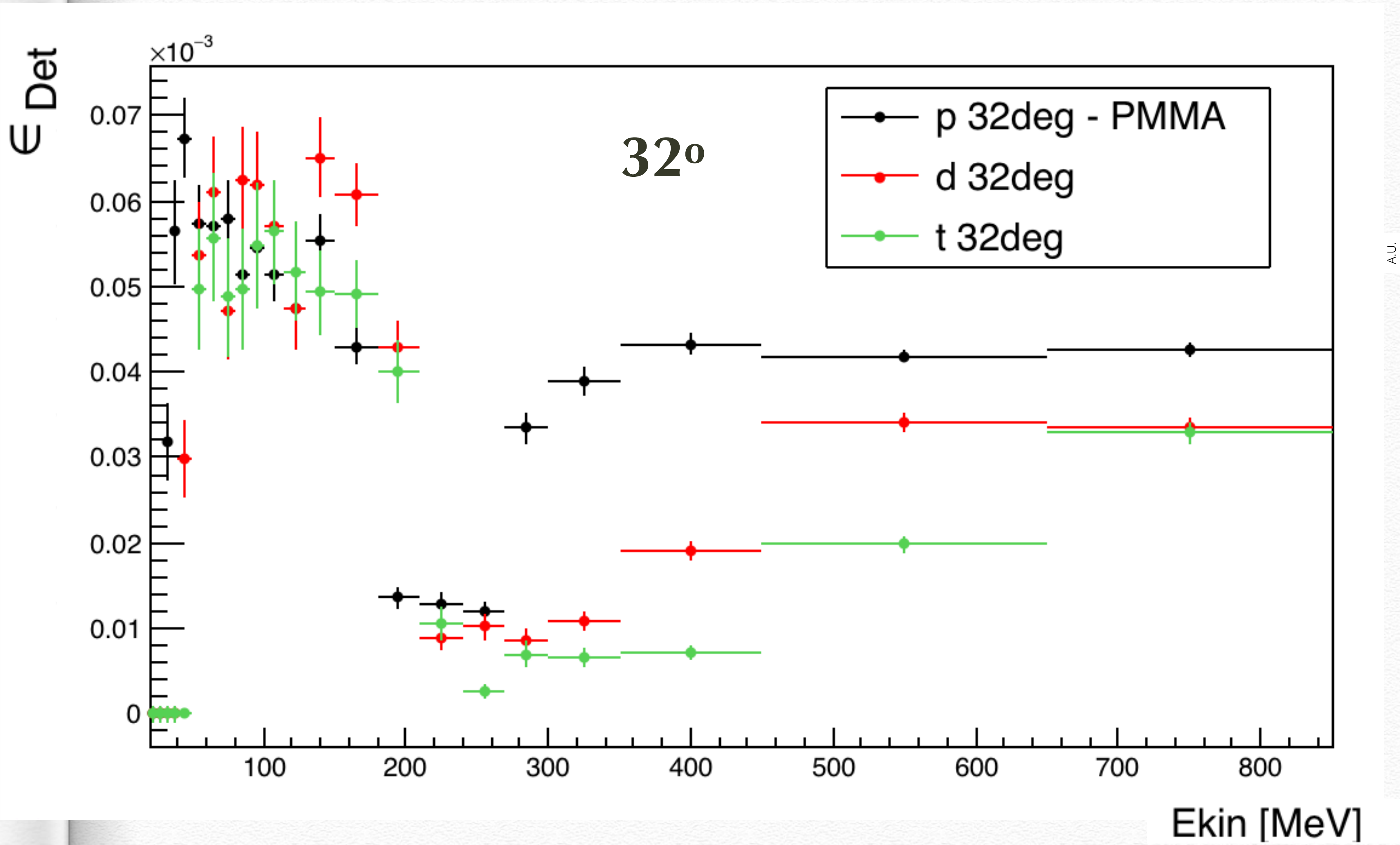

Det Efficiency: Trig + Det + Geo

Probability that a fragment of type *u* is measured by our detectors (*u = p, d, t*)

$$\epsilon^{u}_{Det}(E_{kin})_i = \left(\frac{N^u_{meas}}{N^u_{gen}}\right)_i$$

Simulation no trig of p (d, t) produced 4π with FLAT Ekin = [5 MeV - 1 GeV] (x2 if d) (x3 if t)

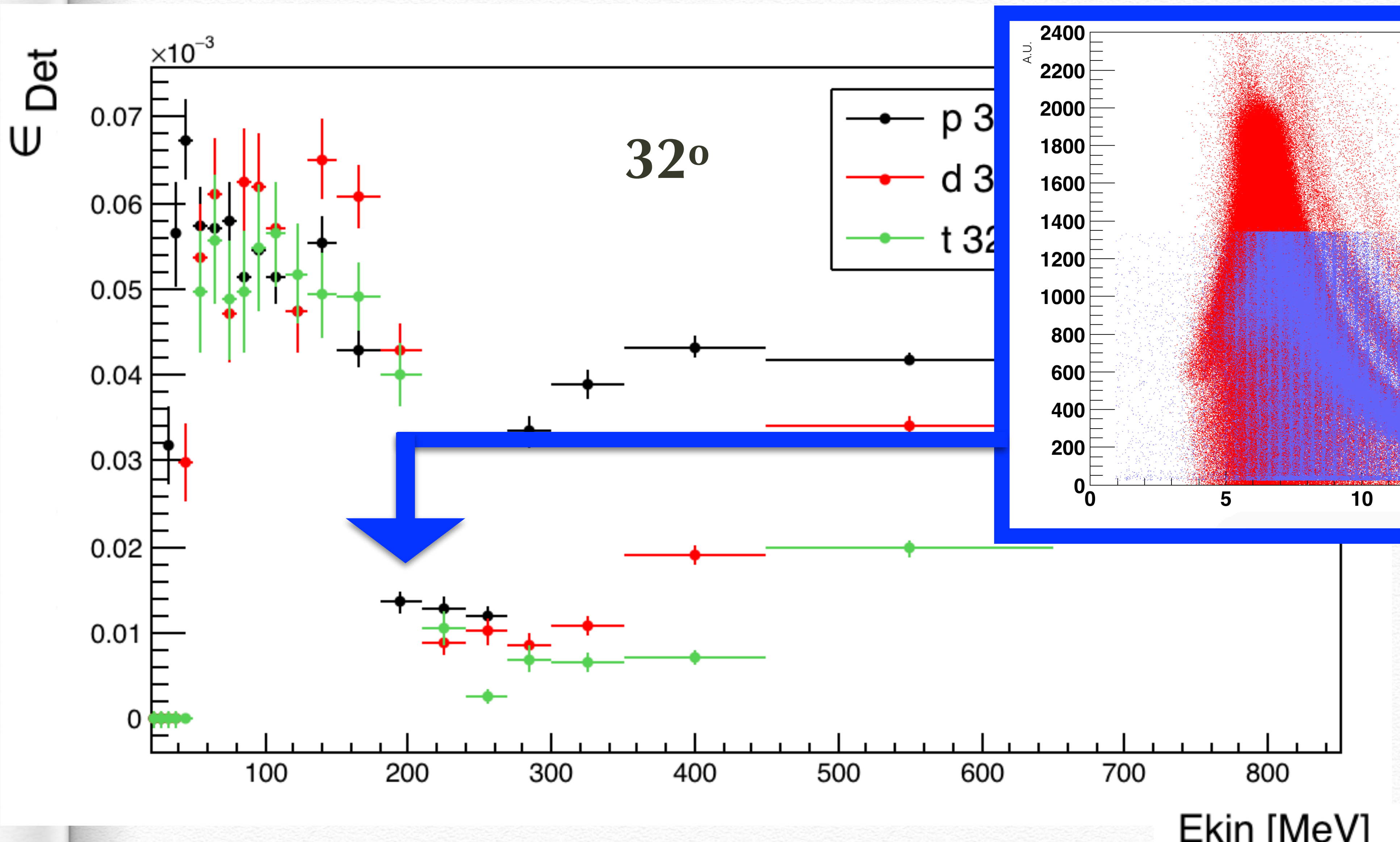

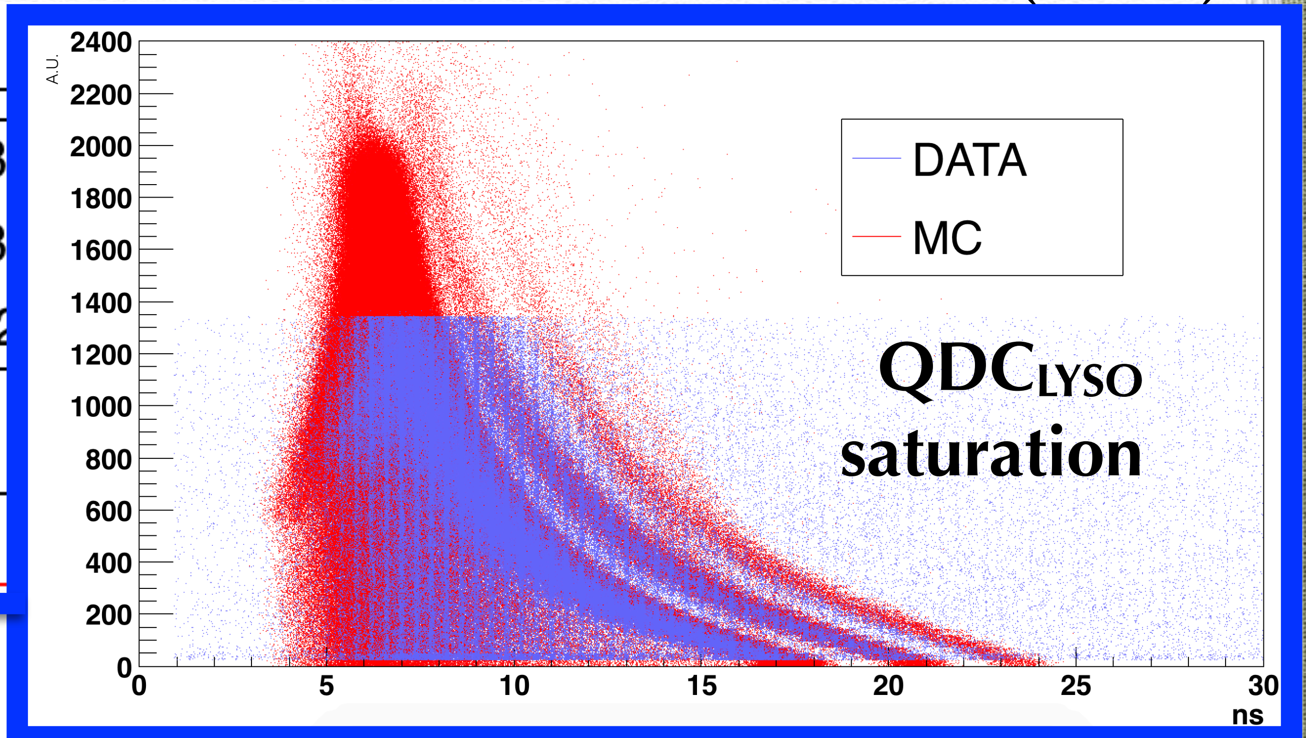

Det Efficiency: Trig + Det + Geo

Probability that a fragment of type *u* is measured by our detectors (*u* = *p*, *d*, *t*)

$$\epsilon^{u}_{Det}(E_{kin})_i = \left(\frac{N^{u}_{meas}}{N^{u}_{gen}}\right)_i$$

Simulation no trig of p (d, t) produced 4π with FLAT Ekin = [5 MeV - 1 GeV] (x2 if d) (x3 if t)

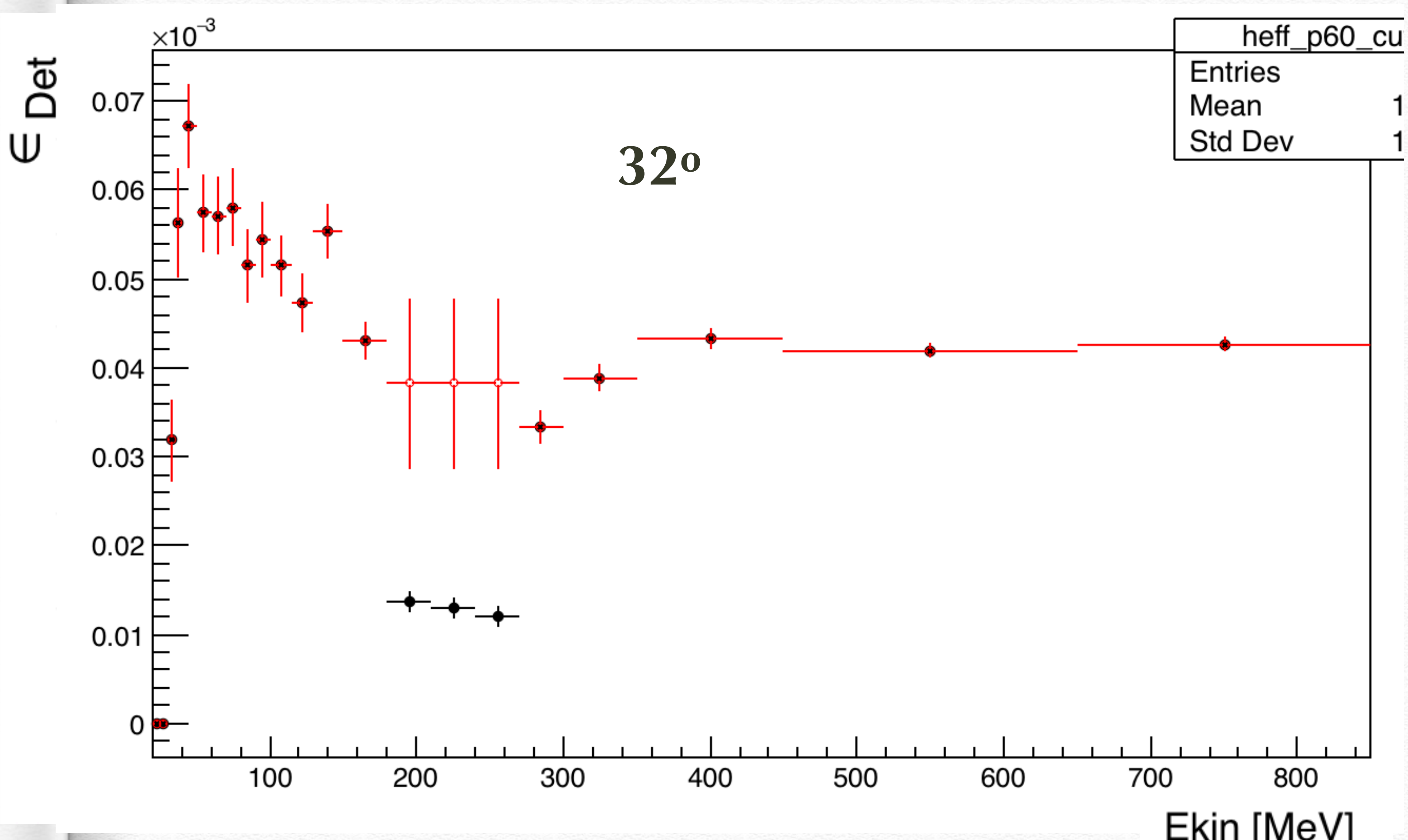

Mixing Efficiency

Probability that a fragment of type *u* is measured in the region *v* (*u, v = p, d, t*)

$$\epsilon_{mix}^{uv} = \frac{N^{uv}}{N^{u}}$$

FULL simulation of 12C ion beam impinging over a PMMA target.

$$\epsilon_{mix} = \begin{pmatrix} \epsilon^{pp} & \epsilon^{pd} & \epsilon^{pt} \\ \epsilon^{dp} & \epsilon^{dd} & \epsilon^{dt} \\ \epsilon^{tp} & \epsilon^{td} & \epsilon^{tt} \end{pmatrix}$$

ϵ_{Sel}

E_{kin}^{C} $[MeV/u]$	ϵ^{pp} [%]	ϵ^{dd} [%]	ϵ^{tt} [%]
50º			
115	95 ± 5	89 ± 9	85 ± 12
153	95 ± 5	85 ± 14	91 ± 6
221	94 ± 5	85 ± 12	86 ± 10
281	94 ± 5	84 ± 12	71 ± 31
353	94 ± 5	84 ± 14	81 ± 15
32º			
115	95 ± 4	78 ± 21	76 ± 32
153	95 ± 5	77 ± 22	83 ± 17
221	95 ± 5	75 ± 23	73 ± 32
281	95 ± 5	75 ± 24	76 ± 26
353	94 ± 5	75 ± 24	69 ± 37

E_{kin}^{C} $[MeV/u]$	ϵ^{dp} [%]	ϵ^{tp} [%]	ϵ^{pd} [%]	ϵ^{td} [%]	ϵ^{dt} [%]
50º					
115	6 ± 7	-	2 ± 2	12 ± 13	5 ± 7
153	10 ± 15	2 ± 3	1 ± 2	5 ± 4	4 ± 5
221	4 ± 4	3 ± 4	2 ± 3	11 ± 10	7 ± 6
281	5 ± 3	2 ± 2	2 ± 3	8 ± 6	8 ± 7
353	4 ± 2	1 ± 1	2 ± 2	10 ± 10	7 ± 7
32º					
115	4 ± 3	2 ± 2	1 ± 2	3 ± 4	13 ± 13
153	4 ± 2	2 ± 2	1 ± 2	2 ± 2	16 ± 16
221	4 ± 4	2 ± 2	1 ± 2	8 ± 14	17 ± 17
281	4 ± 3	3 ± 3	1 ± 2	10 ± 19	16 ± 16
353	4 ± 3	5 ± 6	2 ± 3	10 ± 14	17 ± 17

The d and t contribution to the $XSec_p$ has been subtracted and viceversa:

$$XSec_{p\_final} = XSec_p - (eps_{dp}/eps_{pp}) * XSec_d - (eps_{tp}/eps_{pp}) * XSec_t$$

Ekin Spectra (Data - FLUKA) Protons :: 50 - 32 :: PMMA

Absolute Normalization

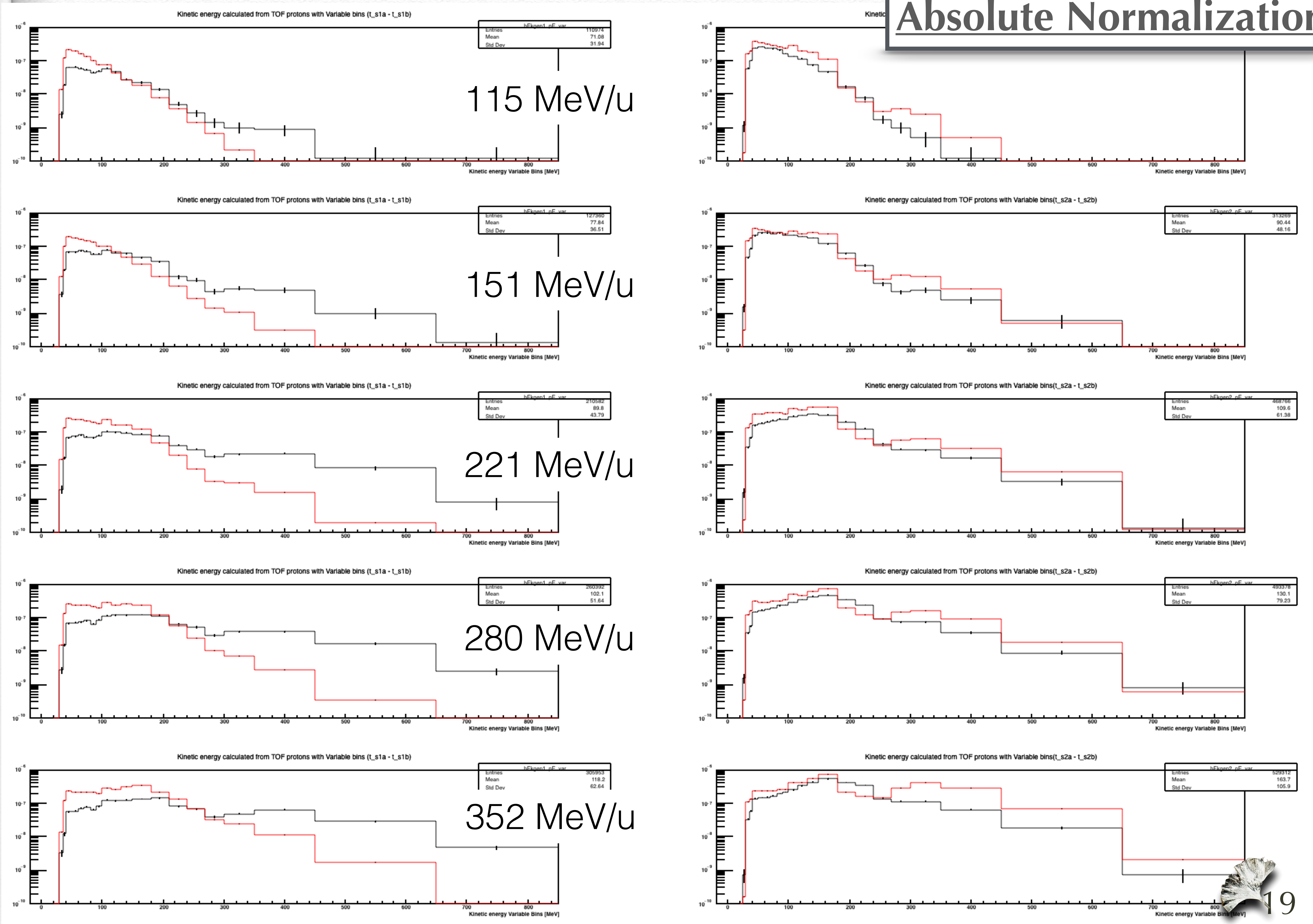

Ekin Spectra (Data - FLUKA) Protons :: 50 - 32 :: PMMA

Absolute Normalization

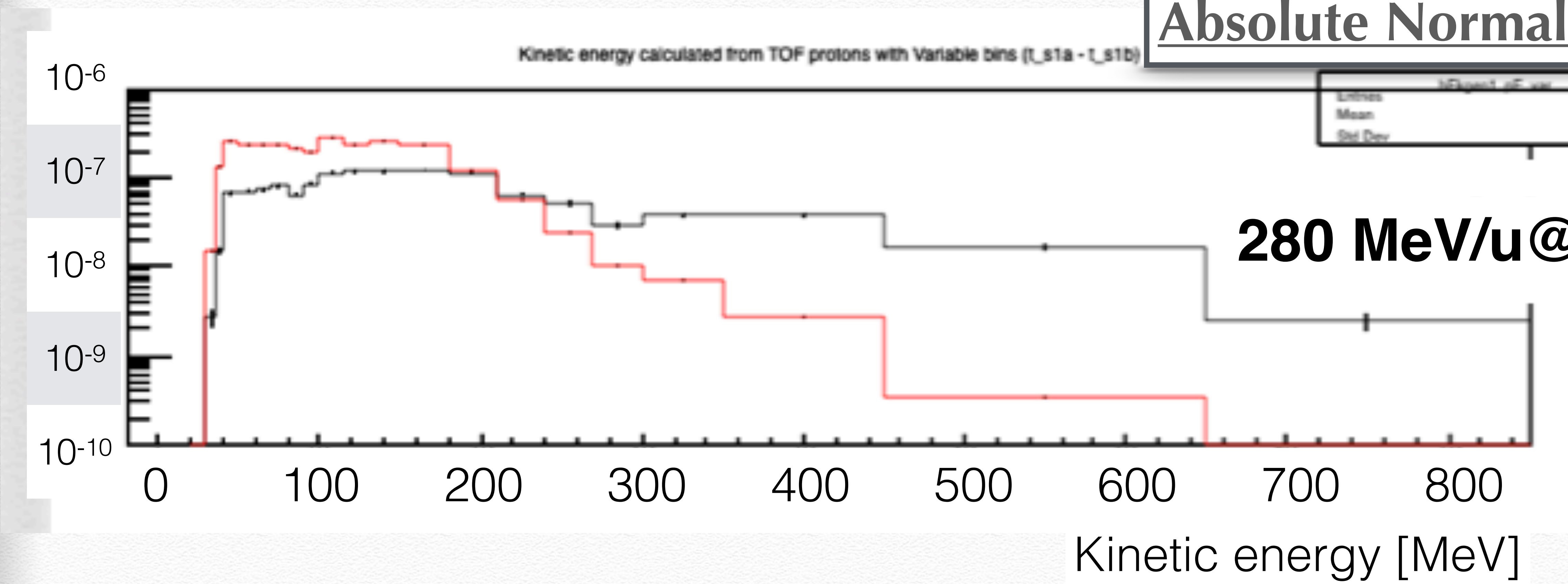

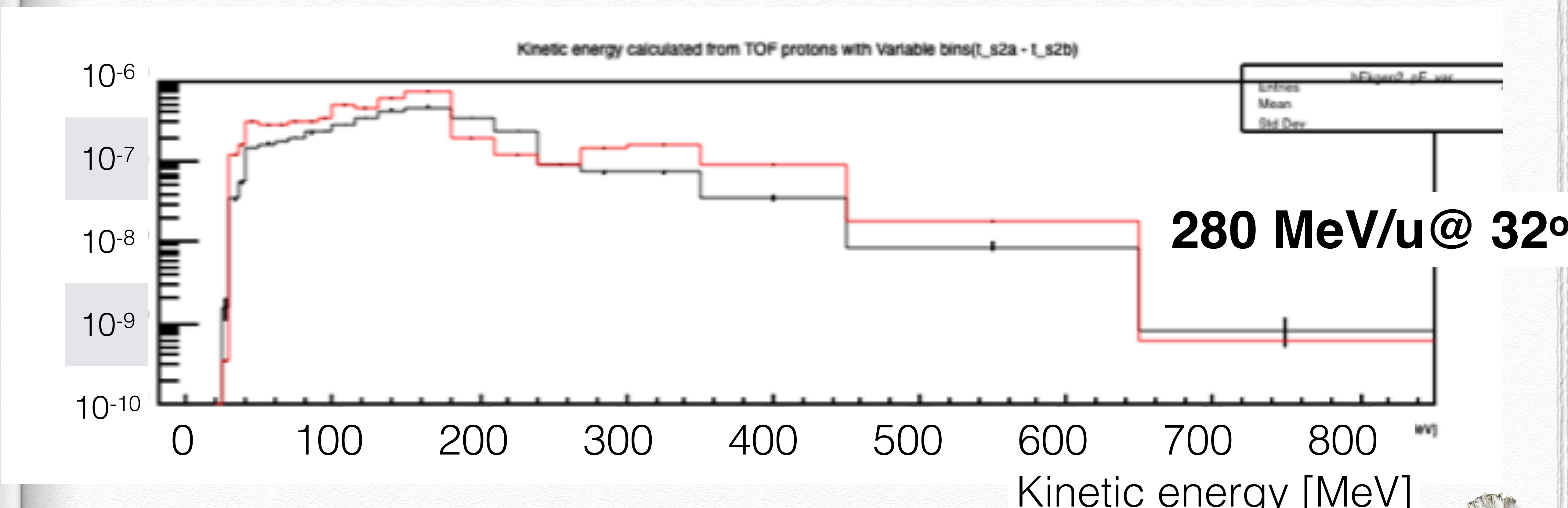

Ekin Spectra (Data - FLUKA) Deuterons :: 50 - 32 :: PMMA

Absolute Normalization

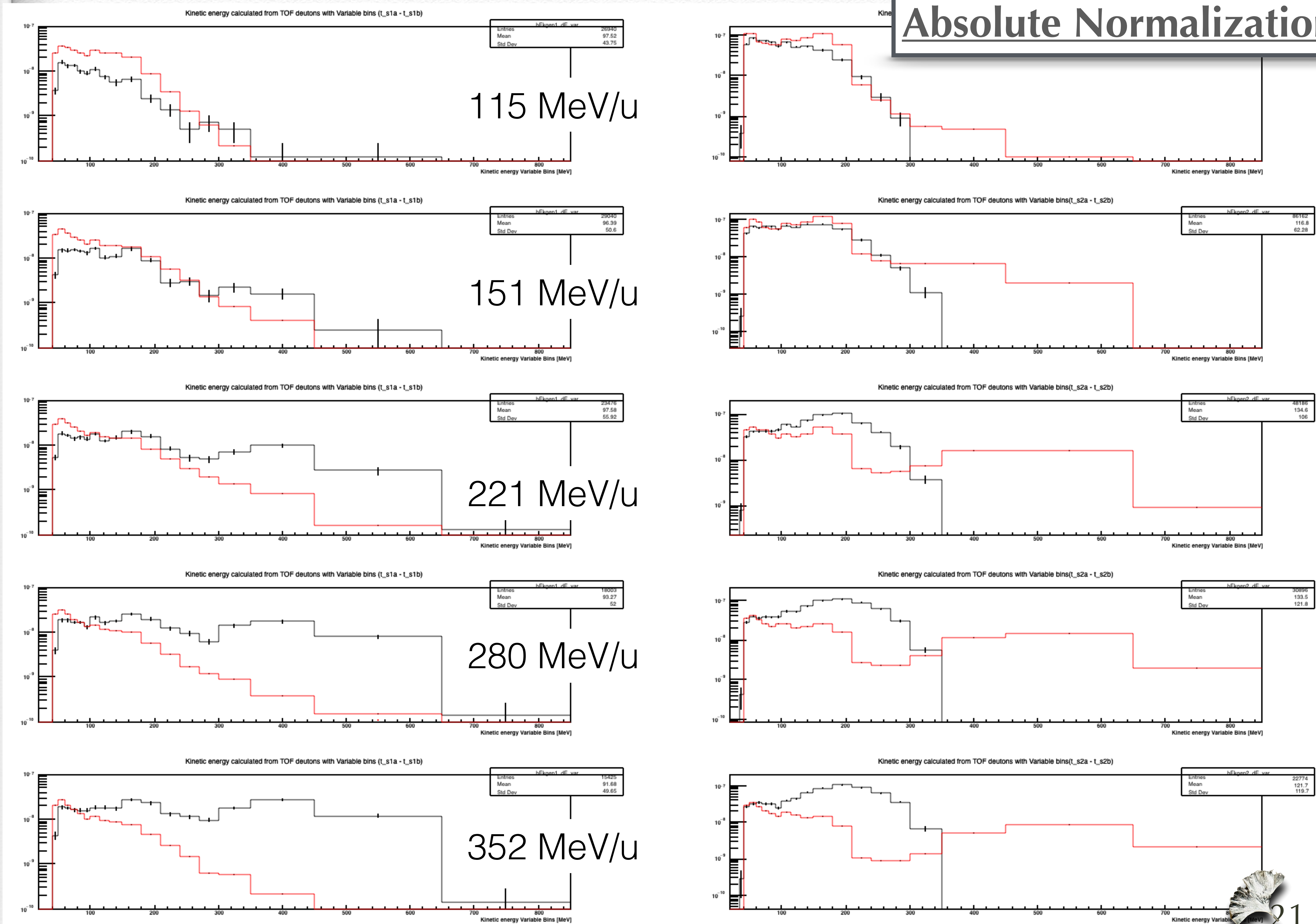

Ekin Spectra (Data - FLUKA) Protons :: 50 - 32 :: Grafite

Absolute Normalization

115 MeV/u

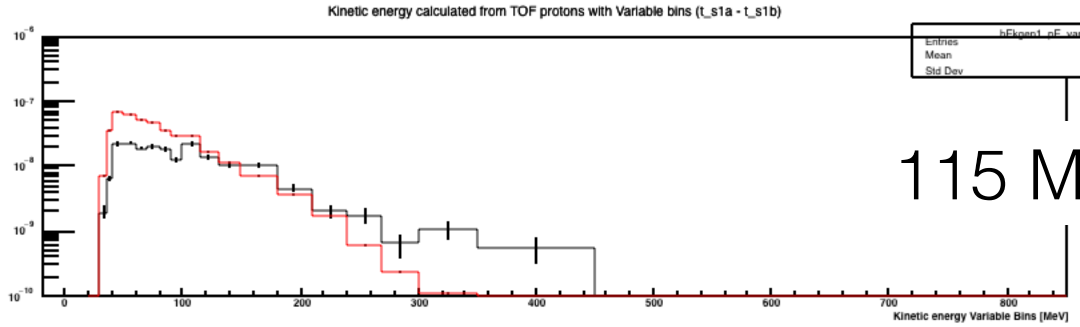

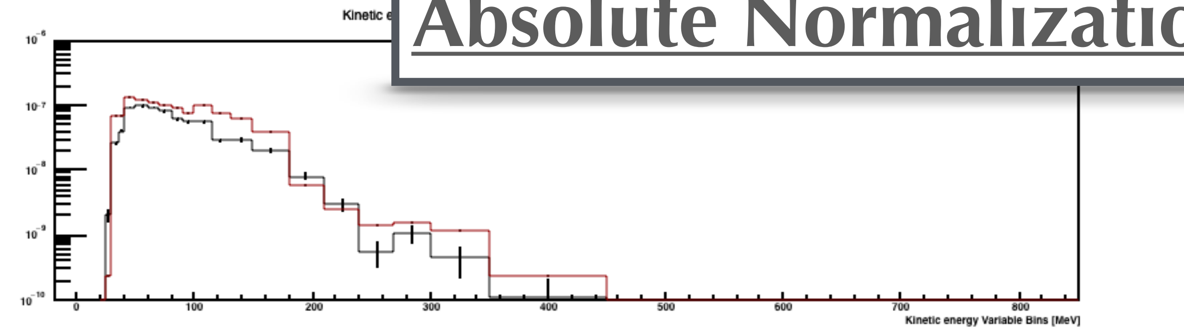

151 MeV/u

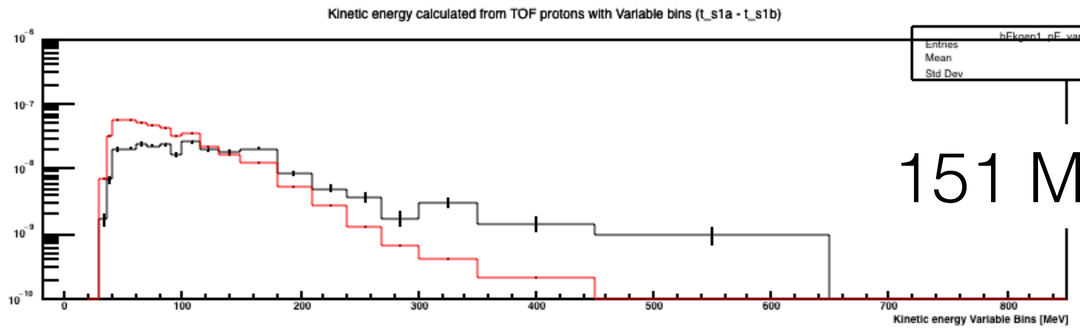

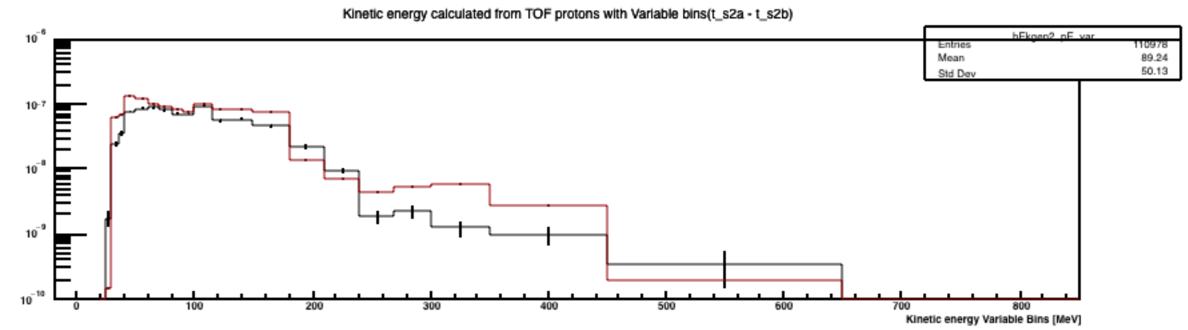

280 MeV/u

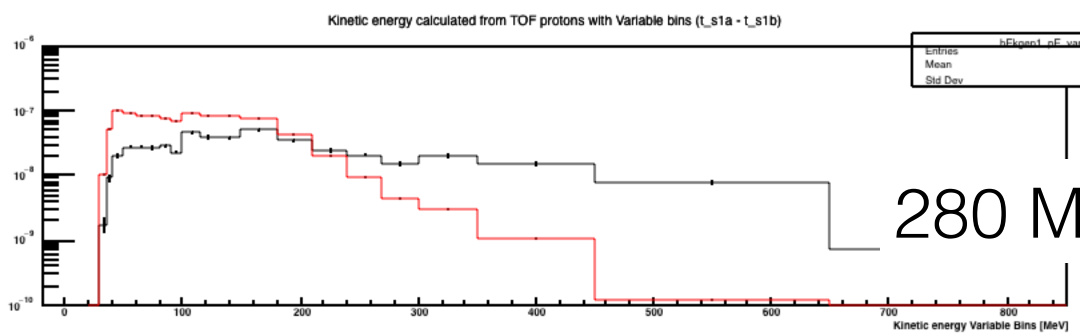

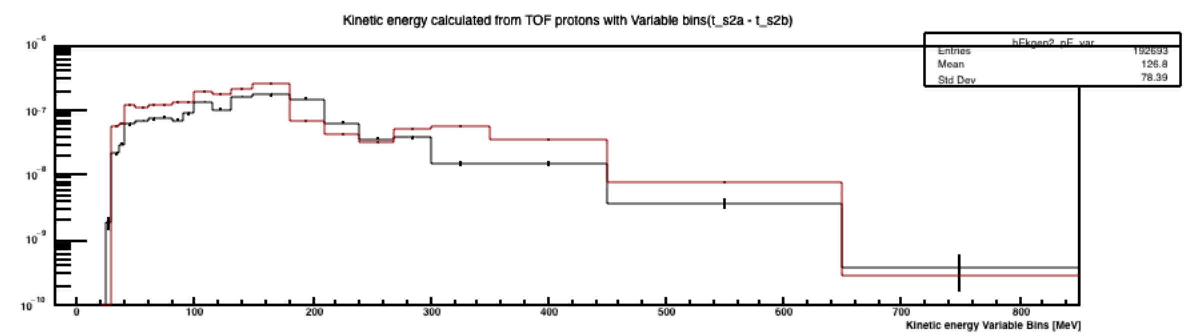

352 MeV/u

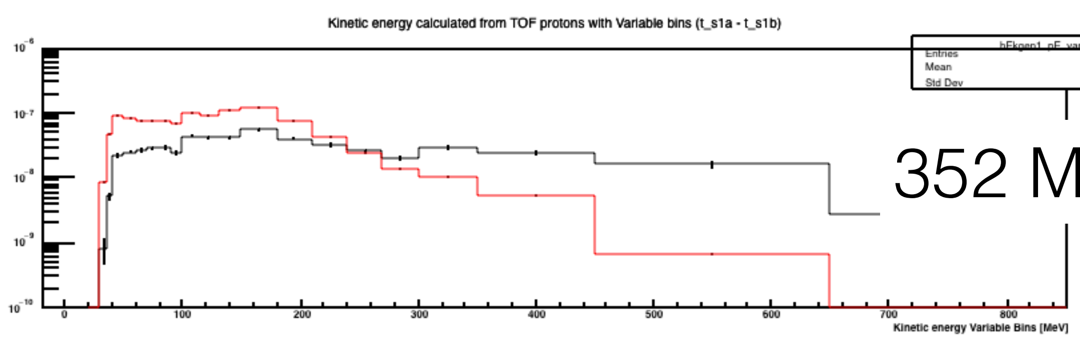

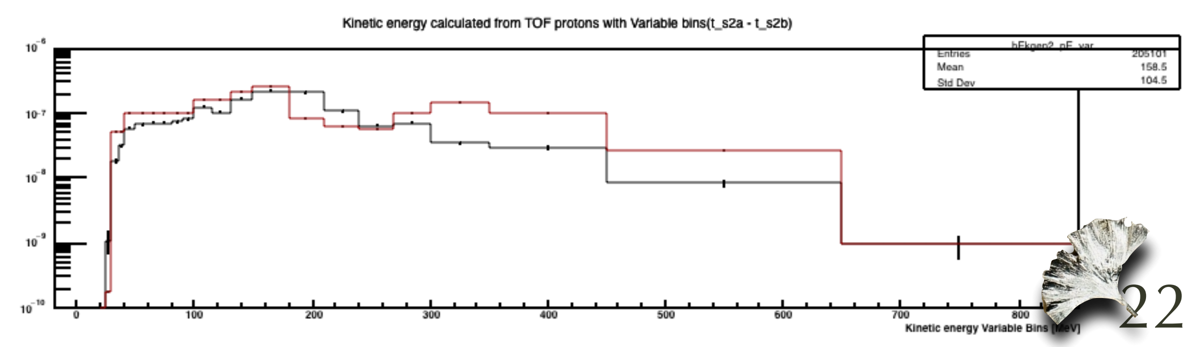

Ekin Spectra (Data - FLUKA)Deuterons :: 50 - 32 :: Grafite

Absolute Normalization

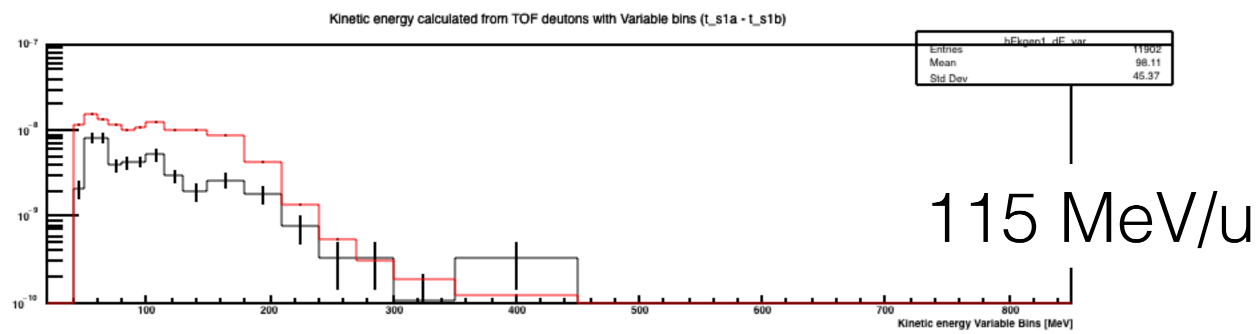

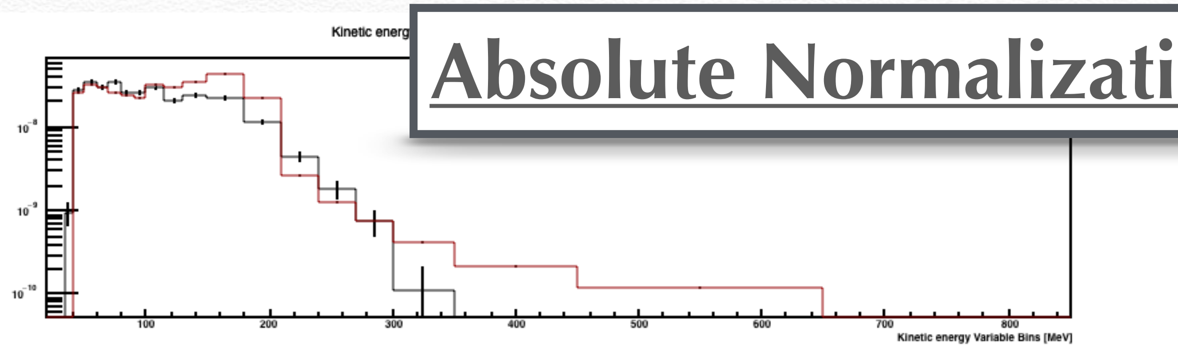

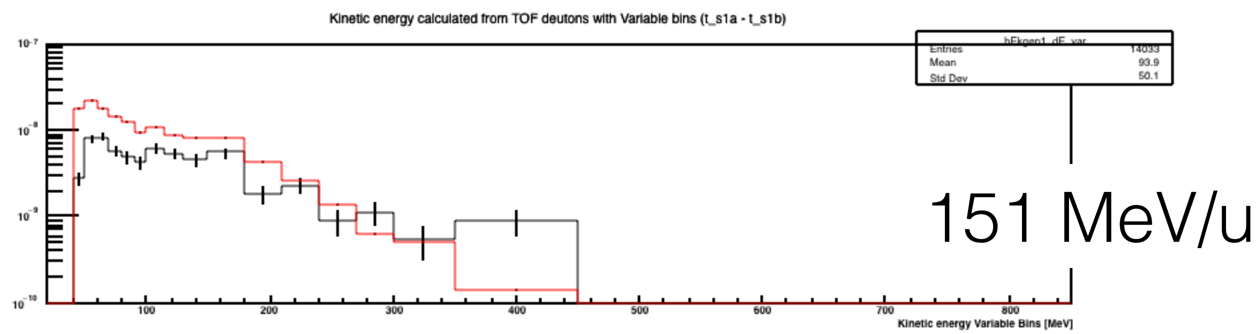

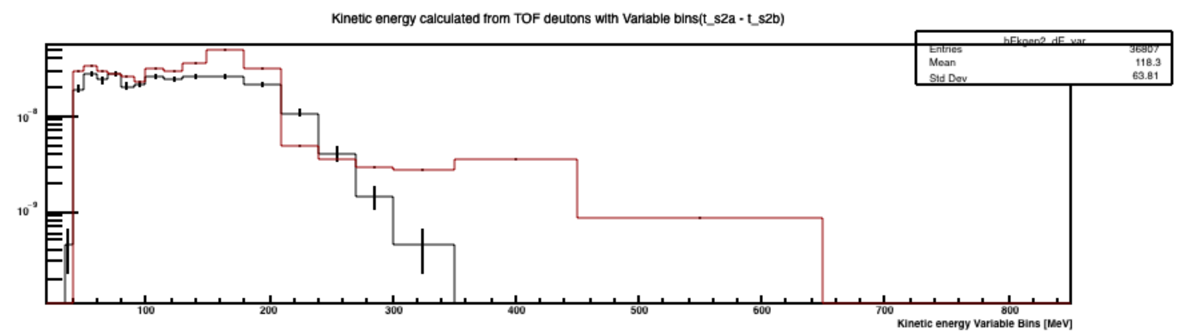

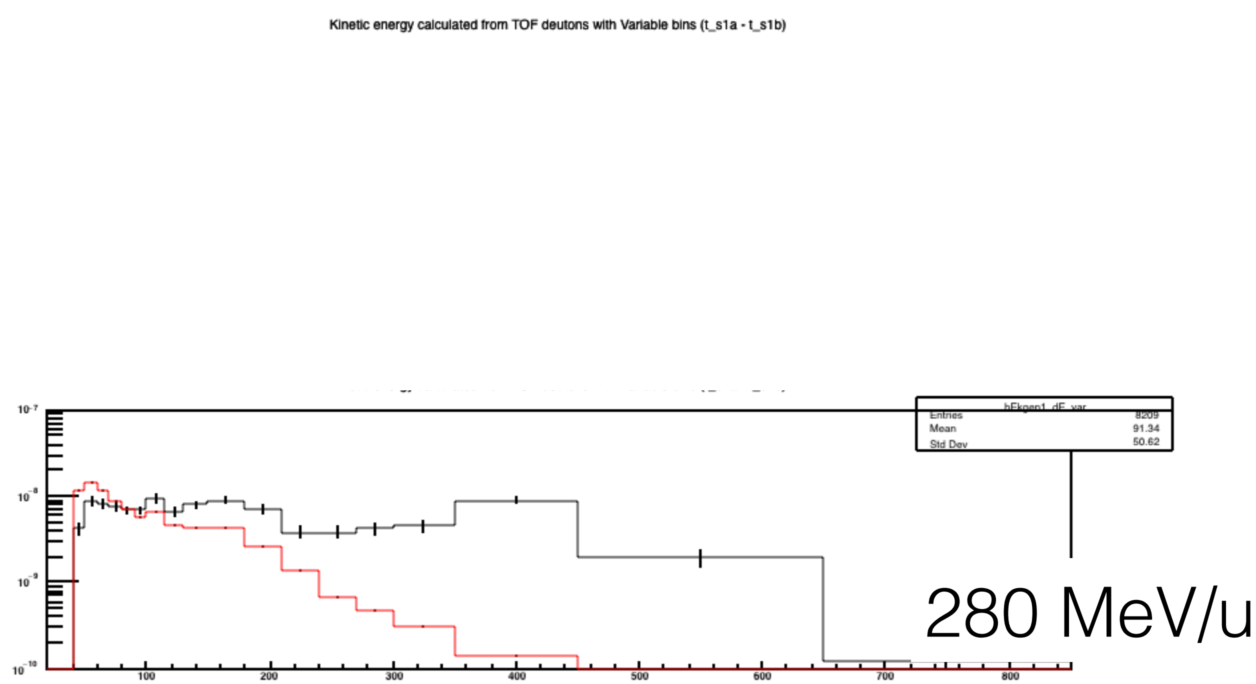

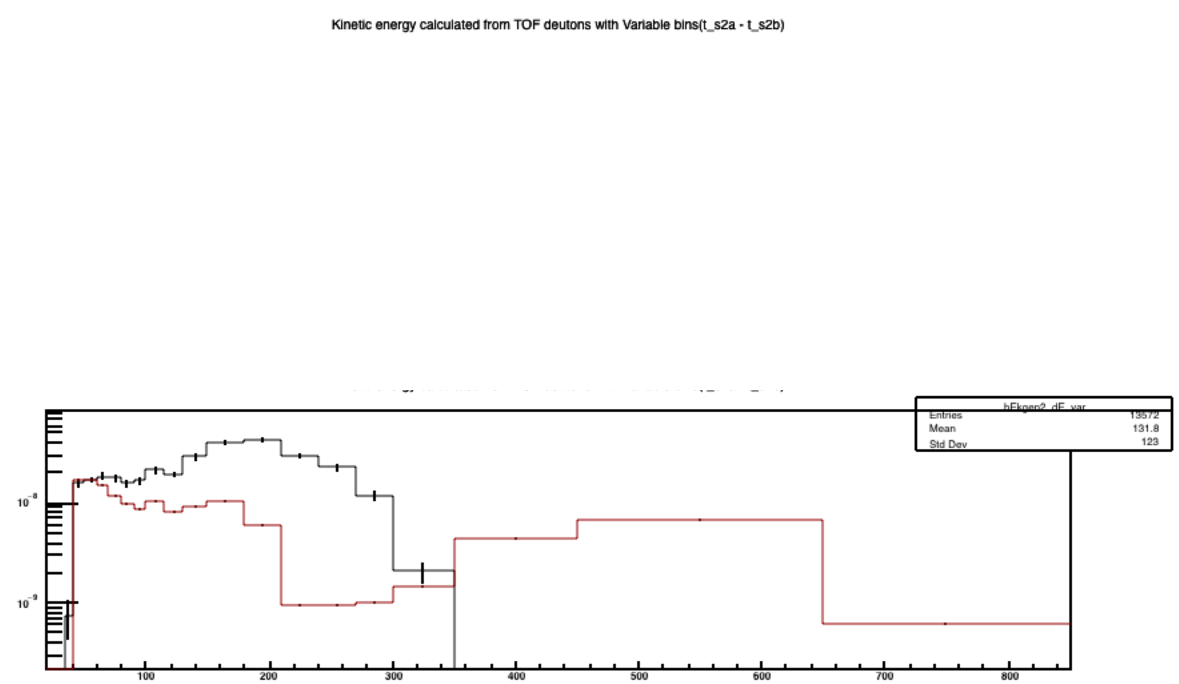

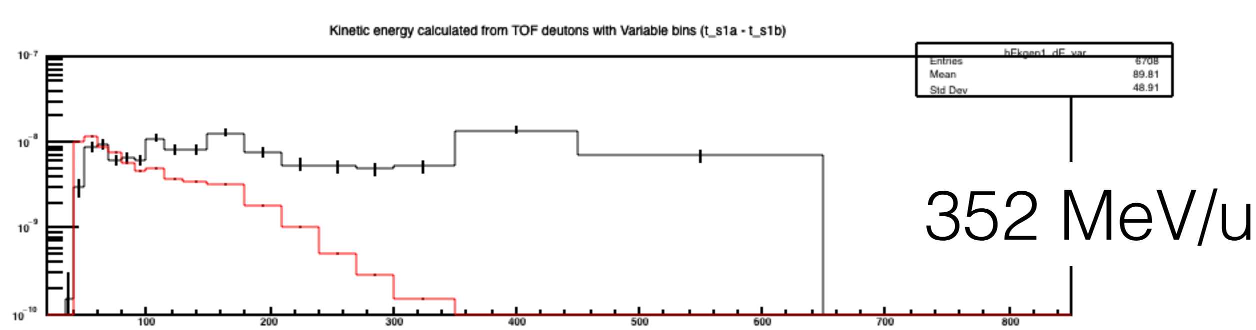

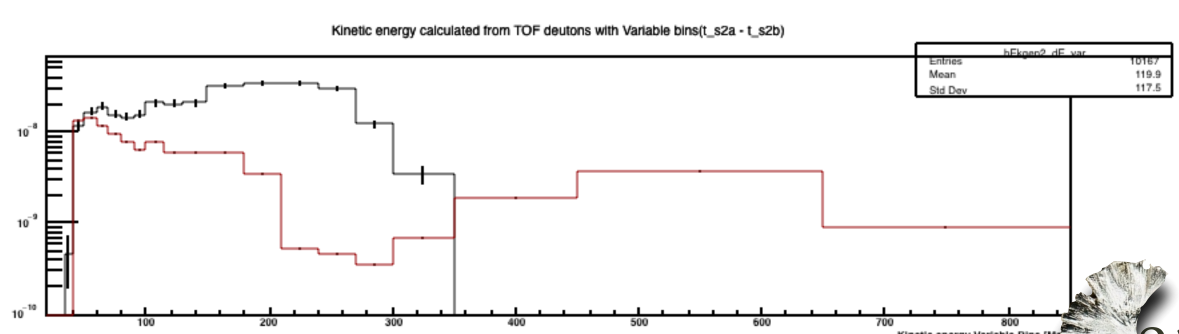

Ekin Spectra (Data - FLUKA) Protons :: 50 - 32 :: Scint

Absolute Normalization

115 MeV/u

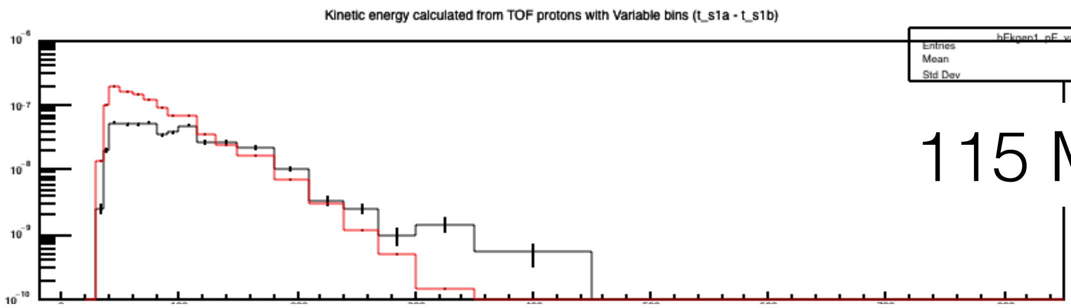

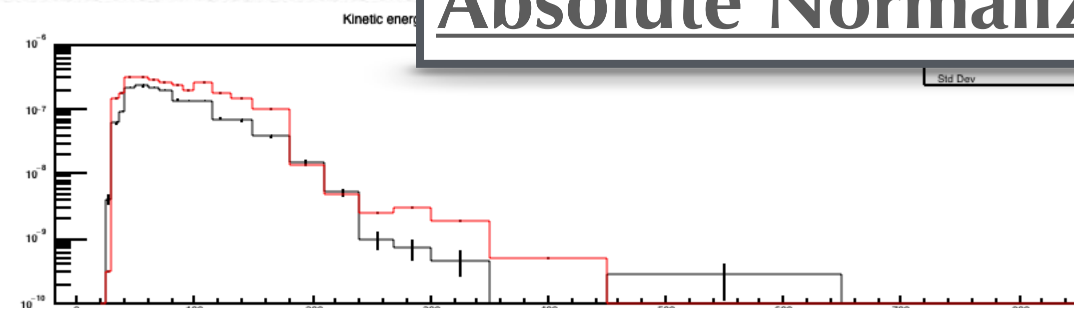

280 MeV/u

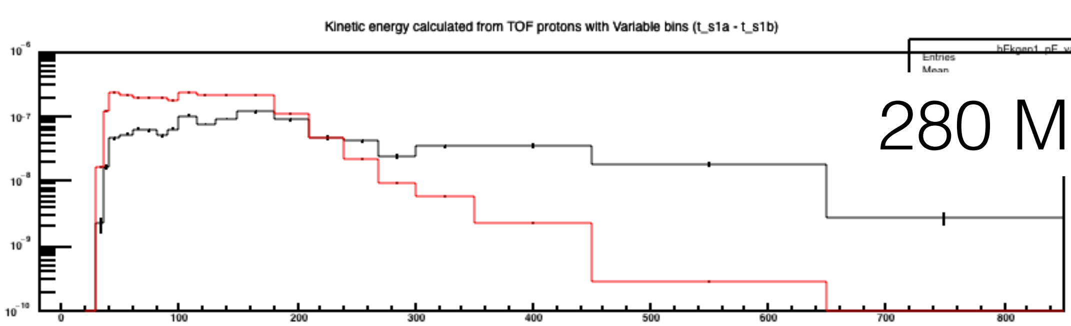

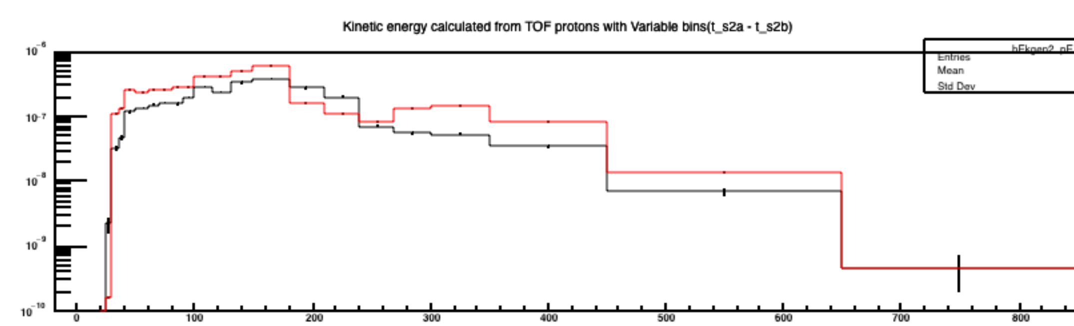

352 MeV/u

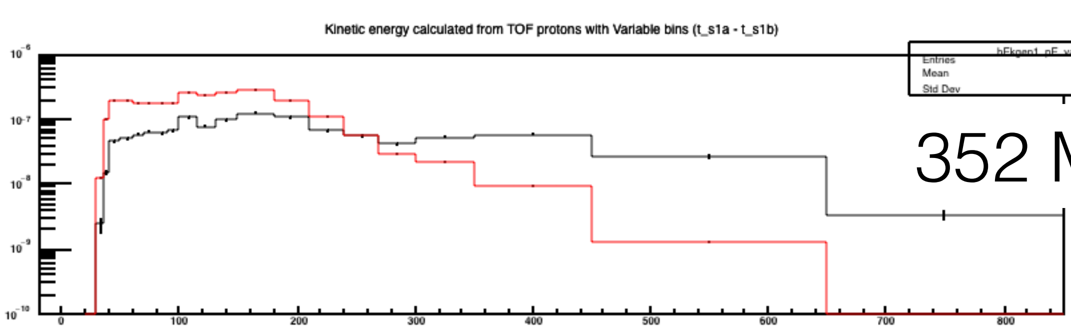

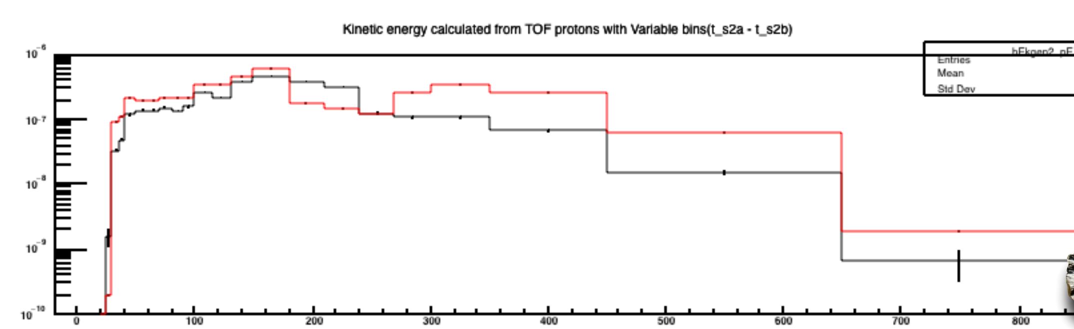

Ekin Spectra (Data - FLUKA) Deuterons :: 50 - 32 :: Scint

Absolute Normalization

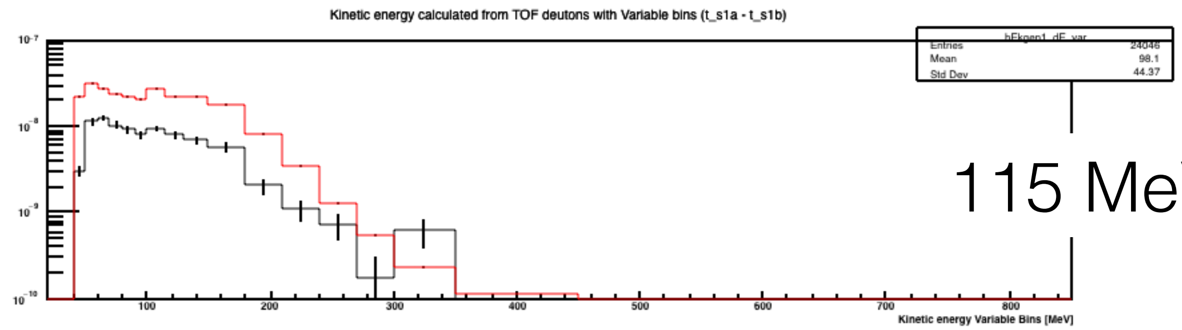

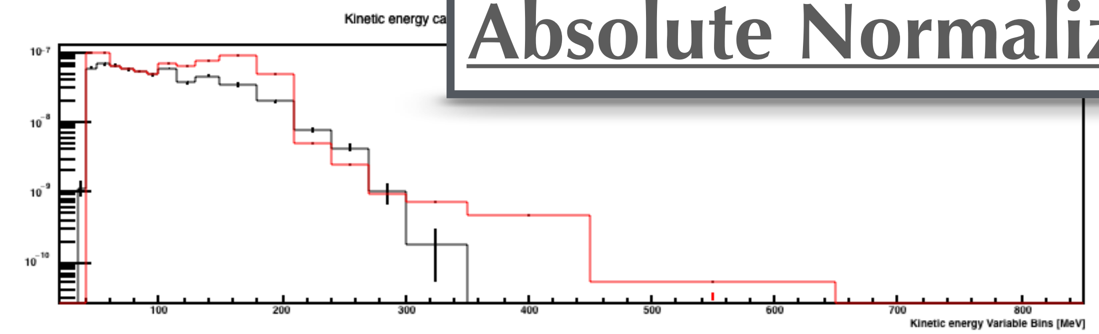

115 MeV/u

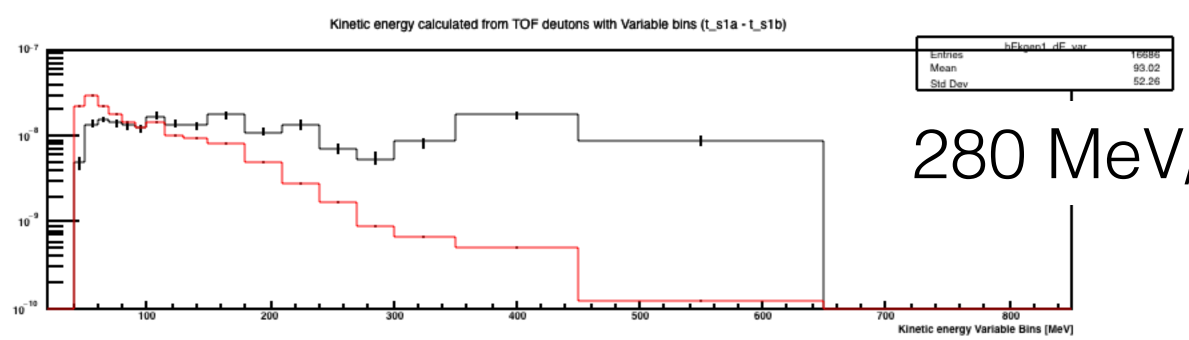

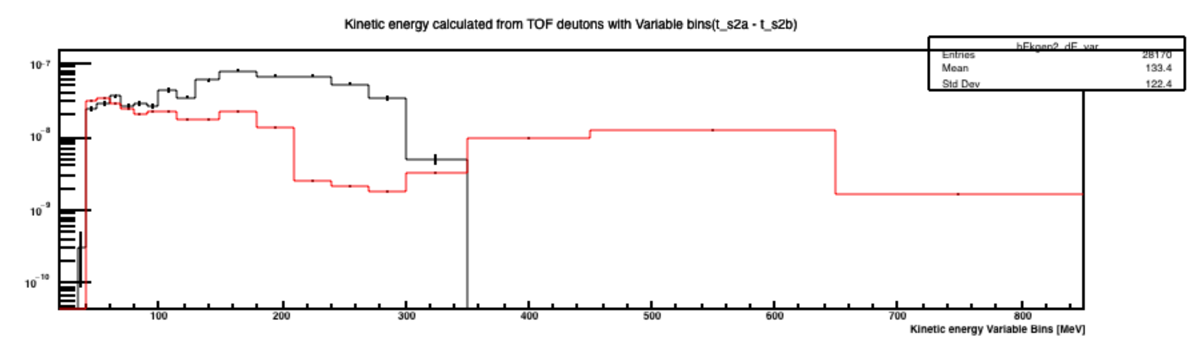

280 MeV/u

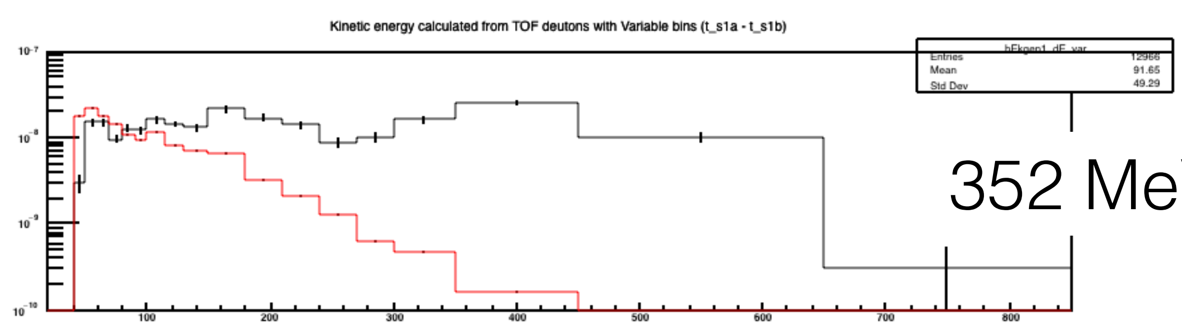

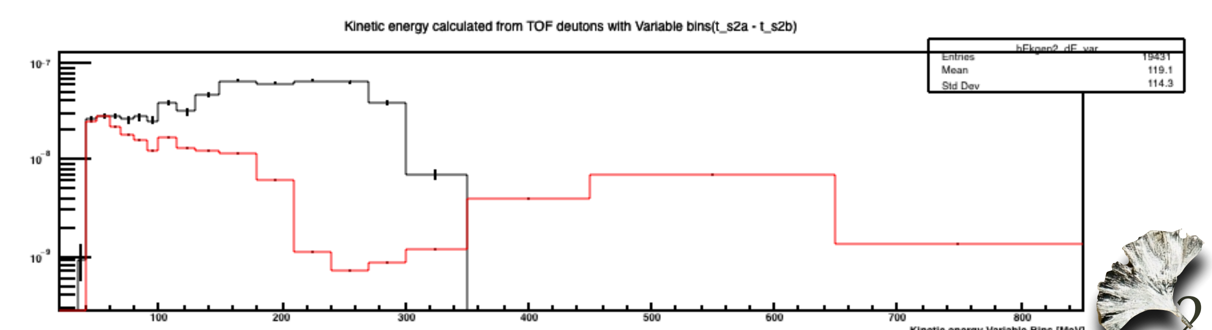

352 MeV/u

Cross section on TARGET

*Only statistical uncertainties

PMMA, Graphite and Plastic scintillator. All efficiencies included.

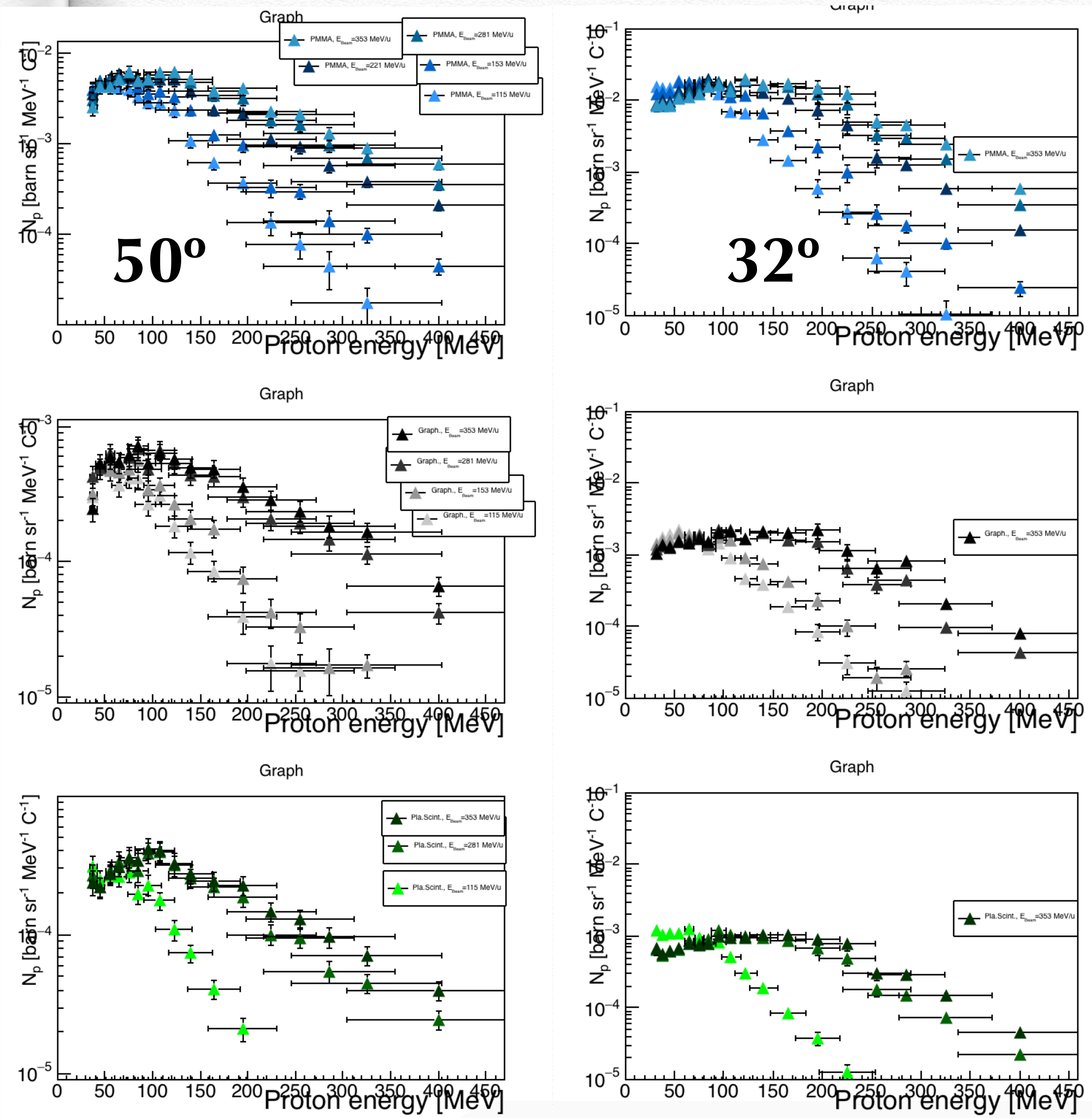

PROTONS

N_p [barn sr^{-1} MeV^{-1} C^{-1}]
vs Proton Energy [MeV]
(10^{-5}÷10^{-1}) / (0 ÷ 400)

- PMMA = $C_5O_2H_8$
- Graphite = C
- EJ-212 = C_bH_a

Beam Energy
C 115
C 150
C 220
C 279
C 351

Cross section on TARGET

*Only statistical uncertainties

PMMA, Graphite and Plastic scintillator. All efficiencies included.

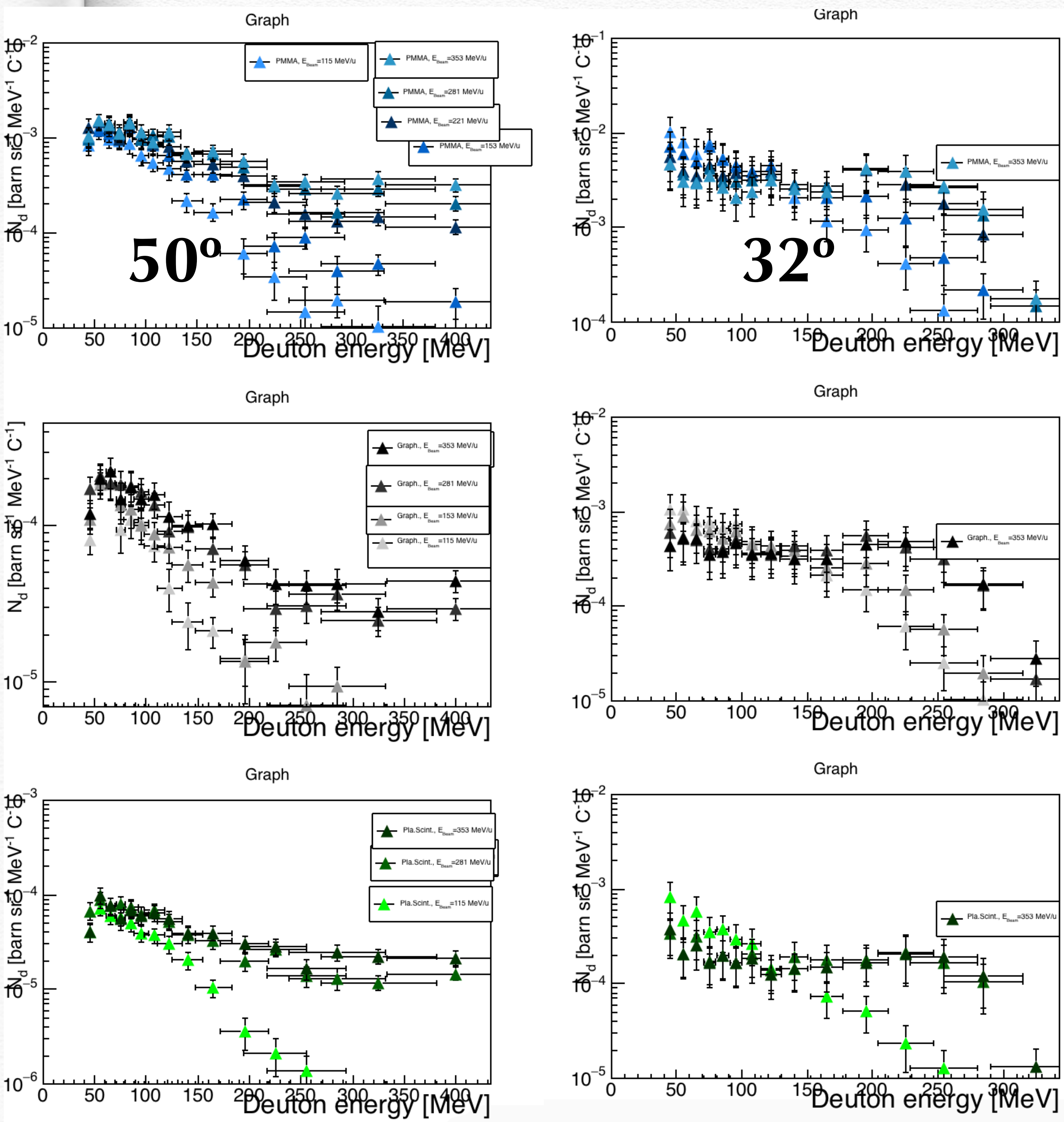

DEUTERONS

N_d [barn sr^{-1} MeV^{-1} C^{-1}]
vs Deuteron Energy [MeV]
($10^{-5} \div 10^{-1}$) / ($0 \div 400$)

- PMMA = $C_5O_2H_8$
- Graphite = C
- EJ-212 = C_bH_a

Beam Energy
C 115
C 150
C 220
C 279
C 351

XSec: From the combination of the different targets (subtraction of C from C2H4 and of C and H from C5O2H8) we obtain the C, O, H proton production cross-sections as a function of the kinetic energy, at 90º and 60º.

PROTONS

• Graphite = **C**

$$\frac{d\sigma_C}{dE_k} = \frac{d\sigma^{Graphite}}{dE_k}$$

• EJ-212 = C_b**H**$_a$

$$\frac{d\sigma_H}{dE_k} = \frac{1}{0.524} \cdot [\frac{d\sigma^{PS}}{dE_k} - 0.476 \cdot \frac{d\sigma_C}{dE_k}]$$

• PMMA = C_5**O**$_2H_8$

$$\frac{d\sigma_O}{dE_k} = \frac{1}{2} \cdot [\frac{d\sigma^{PMMA}}{dE_k} - 8 \cdot \frac{d\sigma_H}{dE_k} - 5 \cdot \frac{d\sigma_C}{dE_k}]$$

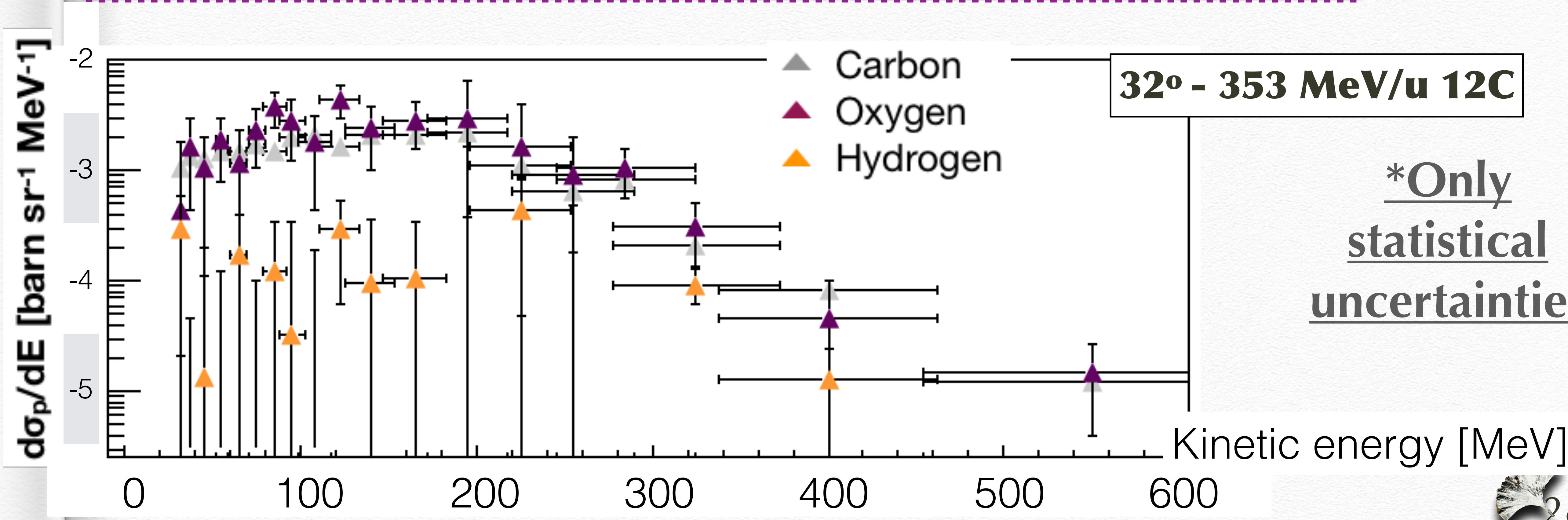

32º - 353 MeV/u 12C

***Only statistical uncertainties**

XSec: From the combination of the different targets (subtraction of C from C2H4 and of C and H from C5O2H8) we obtain the C, O, H proton production cross-sections as a function of the kinetic energy, at 90º and 60º.

DEUTERONS

- Graphite = **C**

$$\frac{d\sigma_C}{dE_k} = \frac{d\sigma^{Graphite}}{dE_k}$$

- EJ-212 = C_b**H_a**

$$\frac{d\sigma_H}{dE_k} = \frac{1}{0.524} \cdot [\frac{d\sigma^{PS}}{dE_k} - 0.476 \cdot \frac{d\sigma_C}{dE_k}]$$

- PMMA = C_5**O_2**H_8

$$\frac{d\sigma_O}{dE_k} = \frac{1}{2} \cdot [\frac{d\sigma^{PMMA}}{dE_k} - 8 \cdot \frac{d\sigma_H}{dE_k} - 5 \cdot \frac{d\sigma_C}{dE_k}]$$

32º - 353 MeV/u 12C

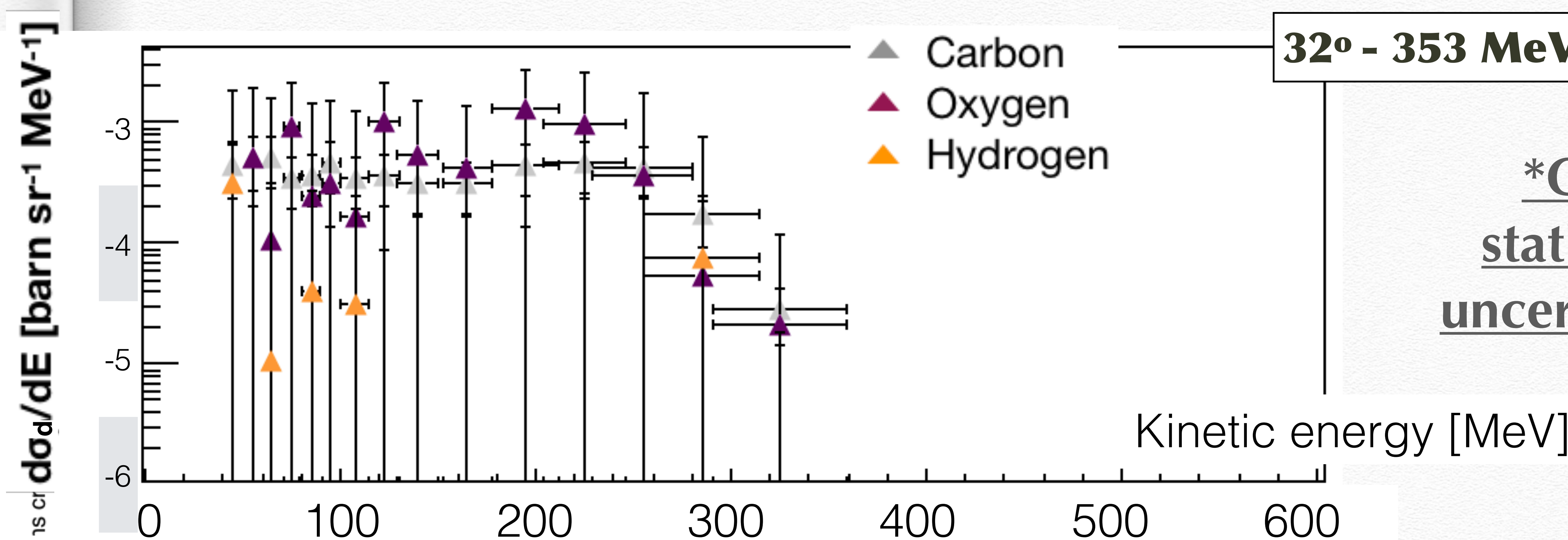

***Only statistical uncertainties**

Comparison with GANIL & FLUKA

*Only statistical uncertainties

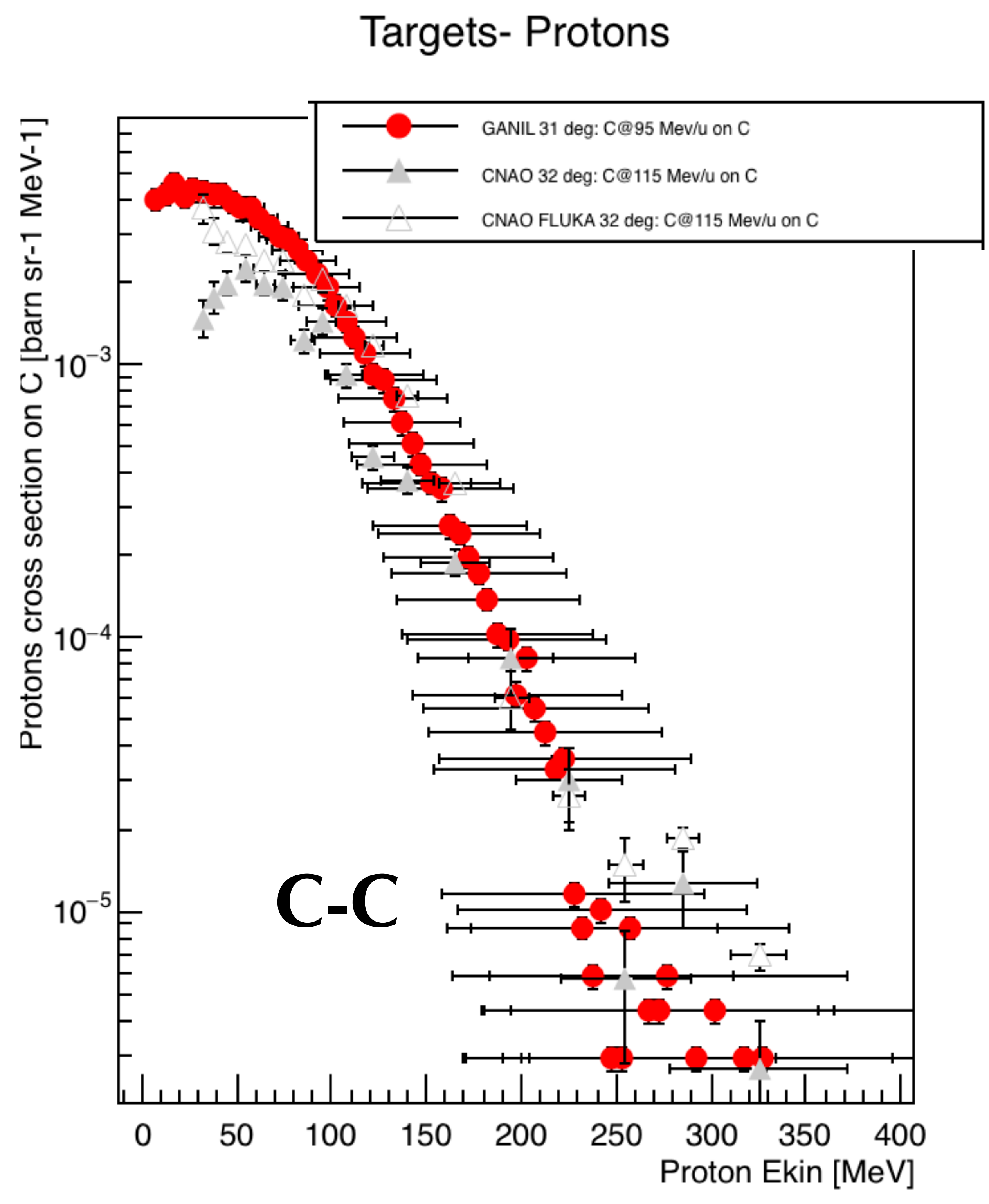

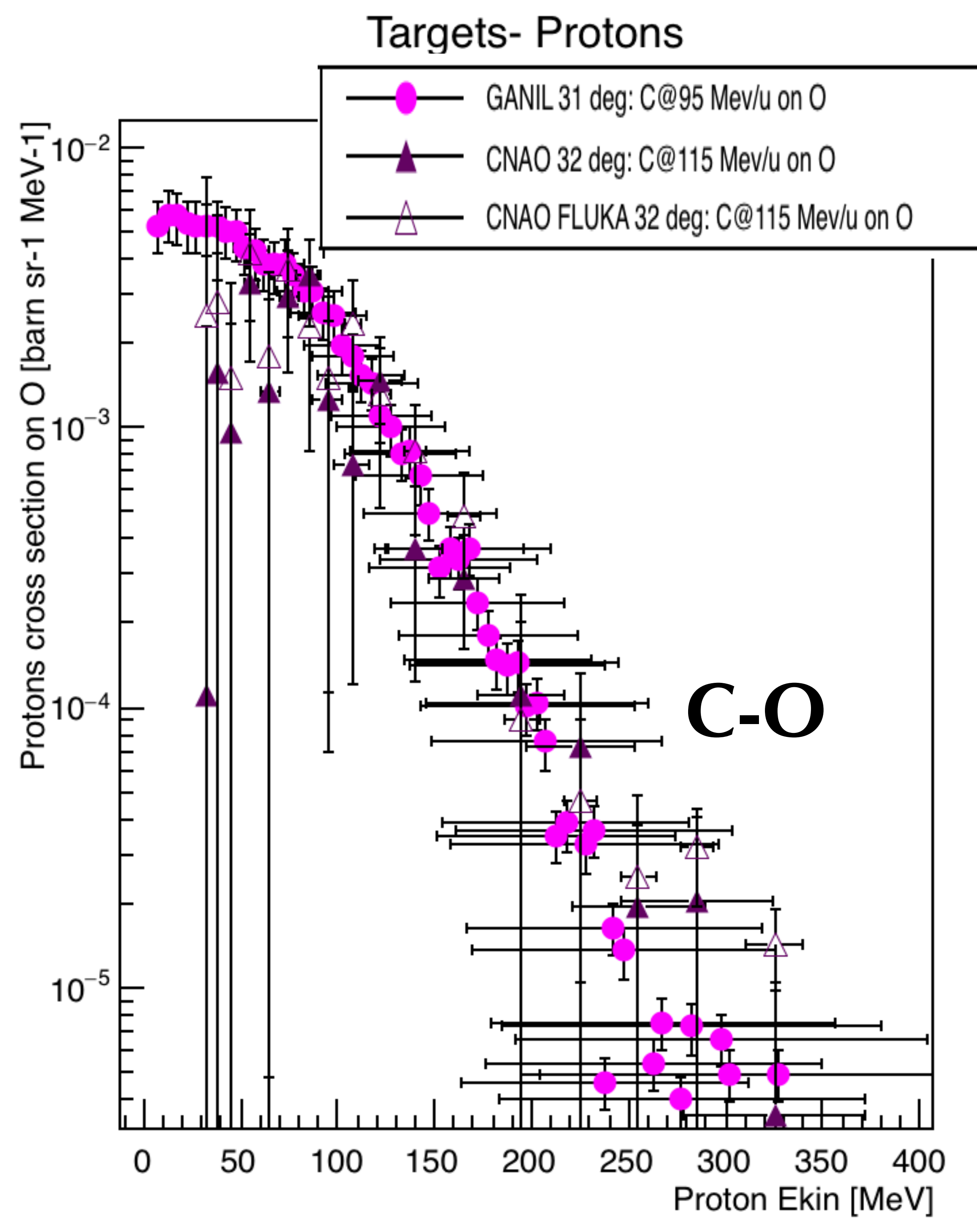

Comparison with GANIL & FLUKA

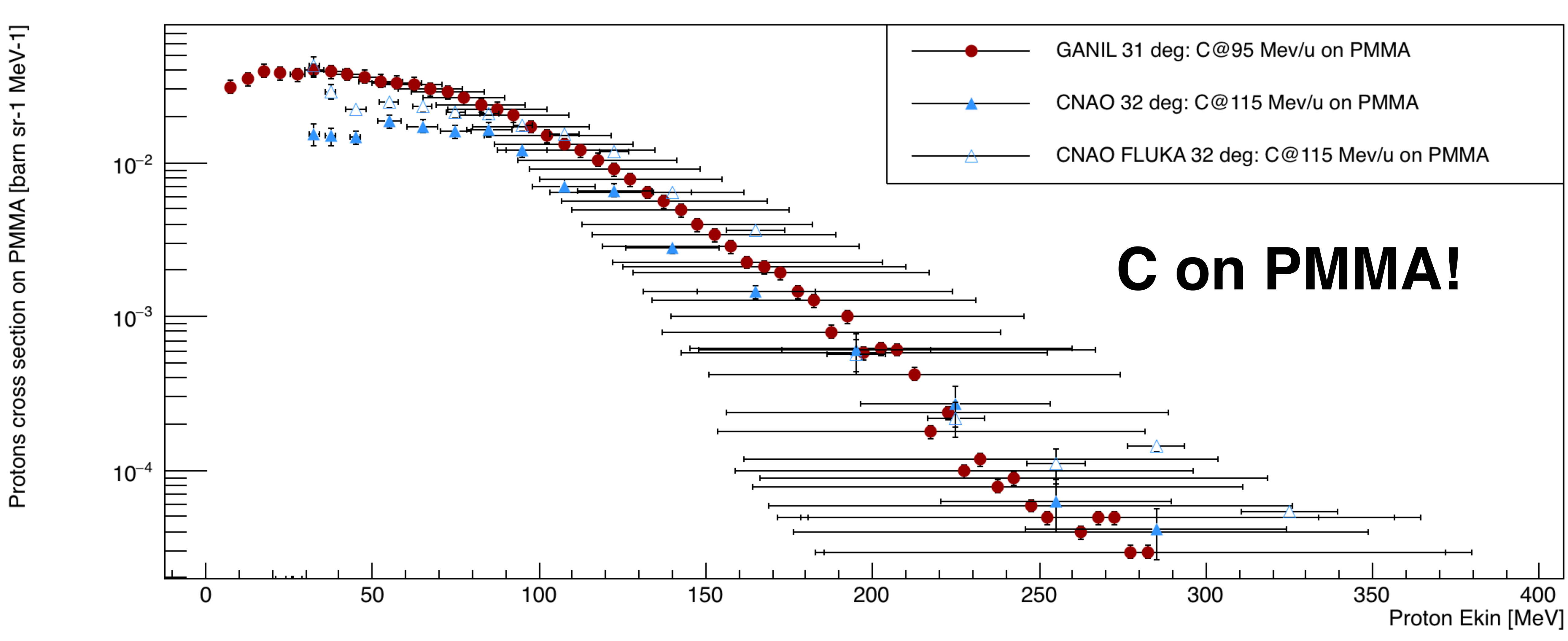

*Only statistical uncertainties

TOTAL XSec vs Beam Energy

*Stat+Sys err

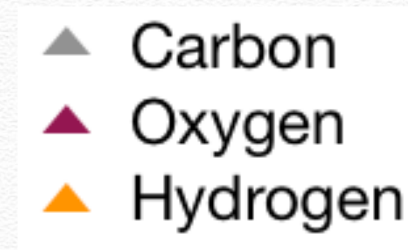

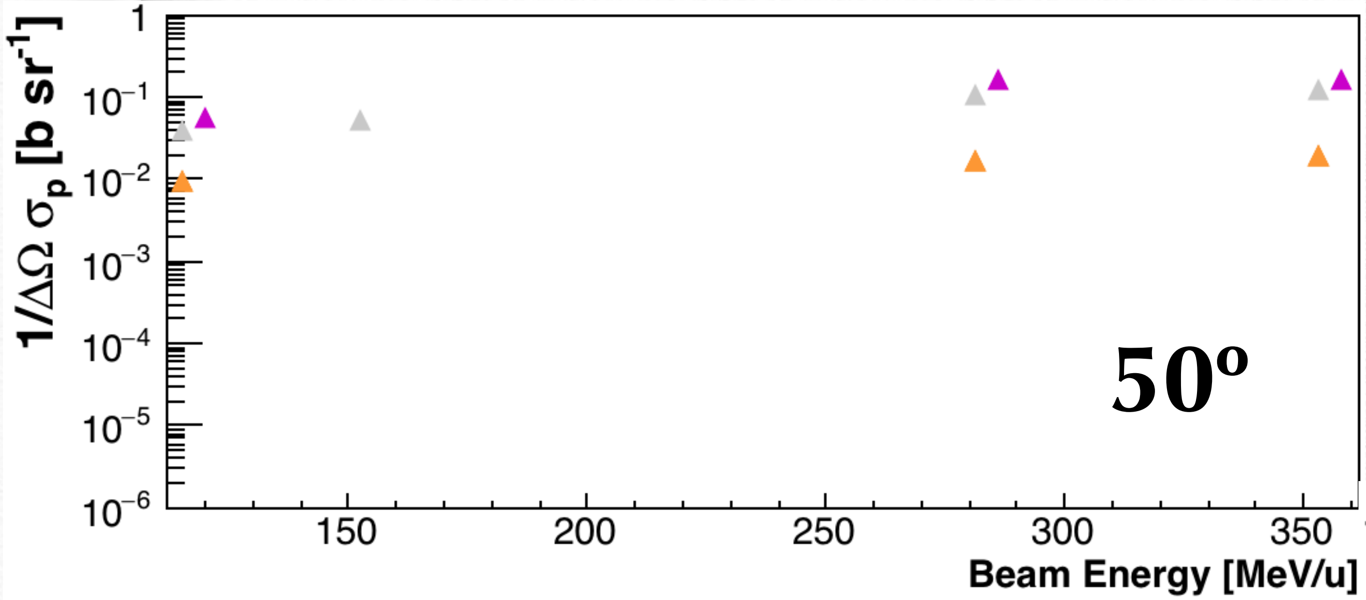

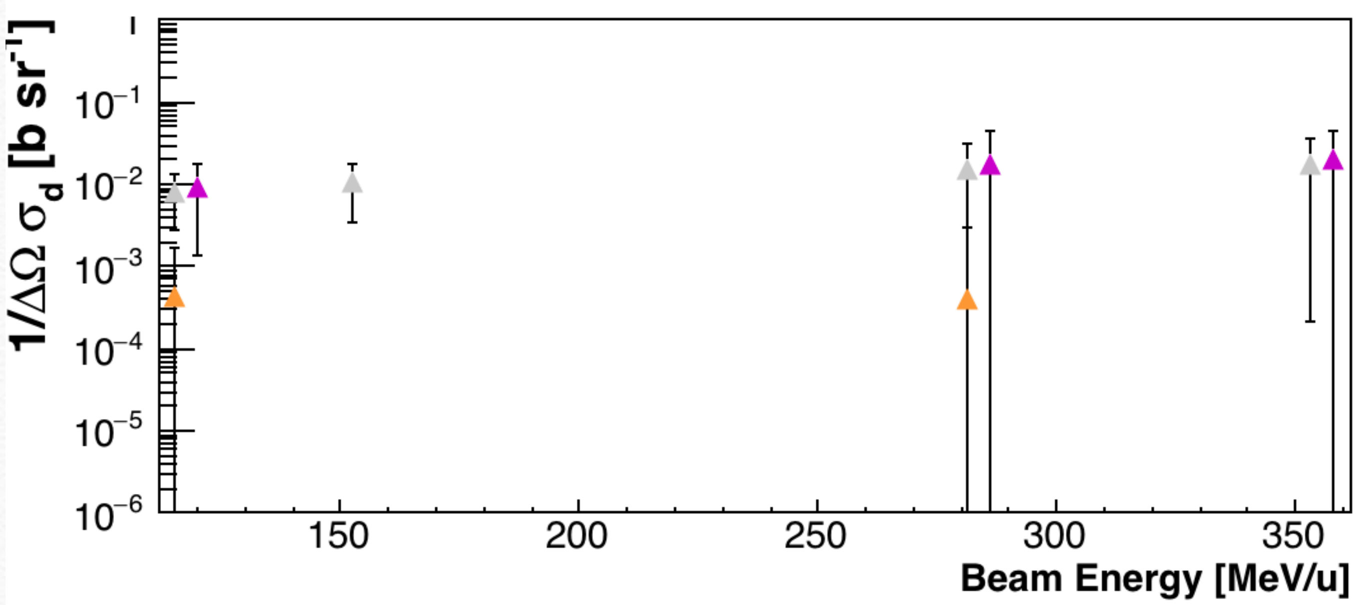

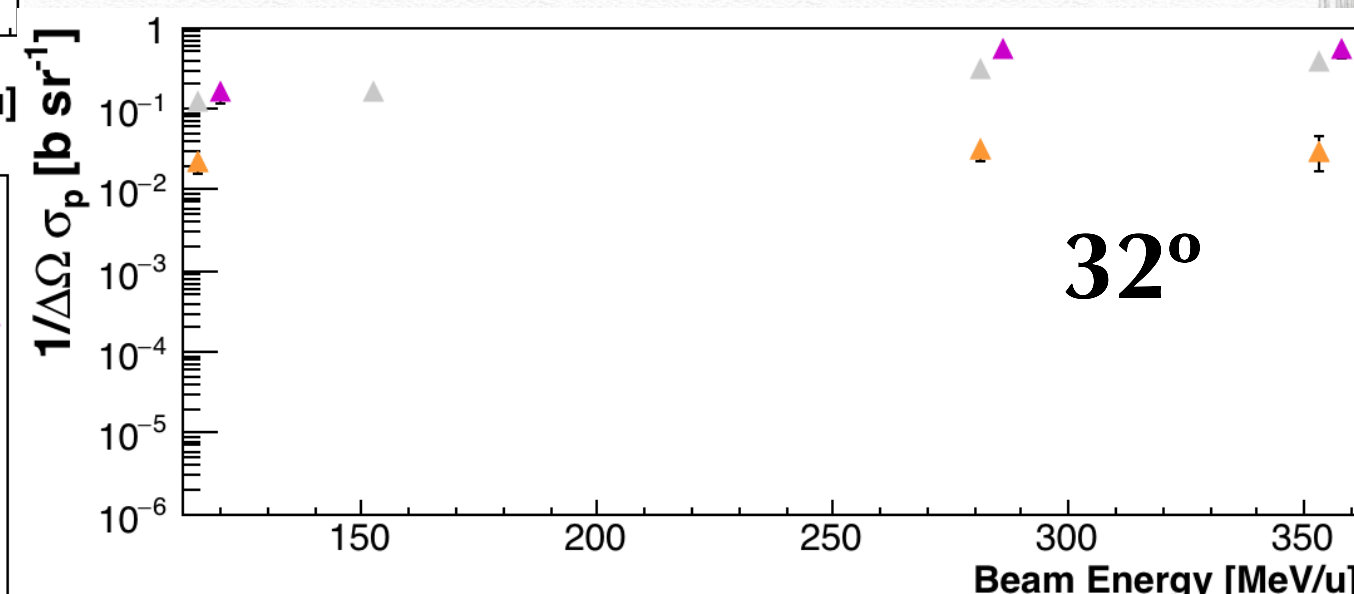

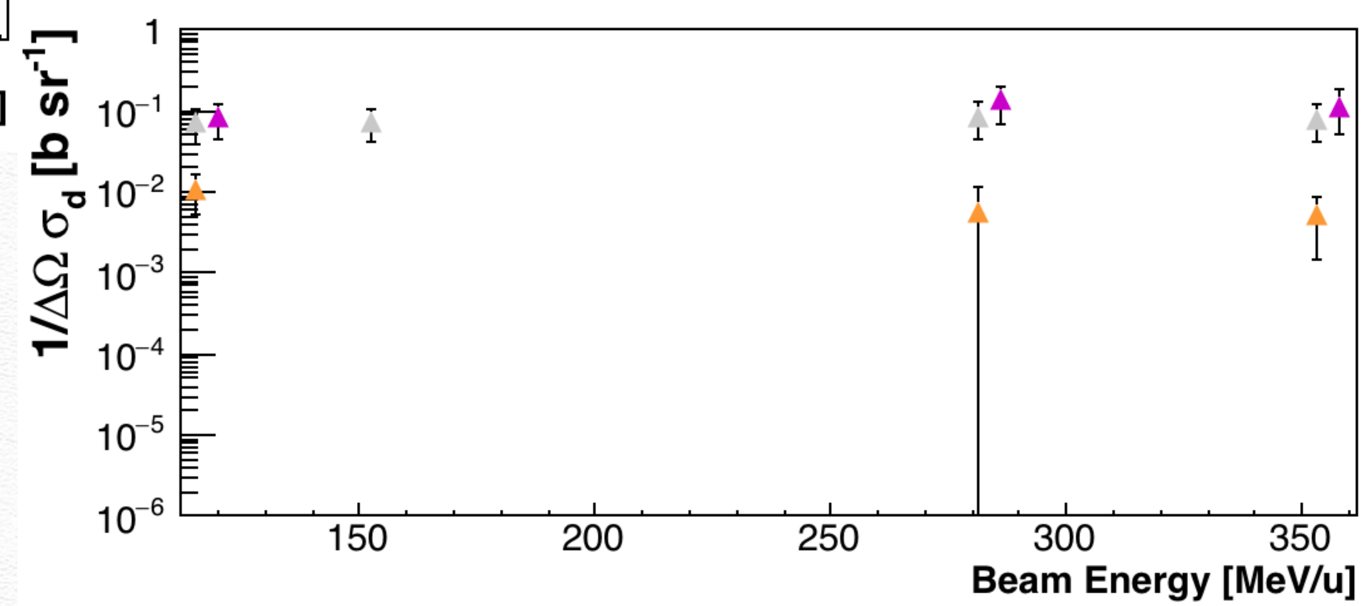

In the TOTAL Xsec, DATA are corrected for the contamination of deuterons in the proton signal

TOTAL XSec vs Angle

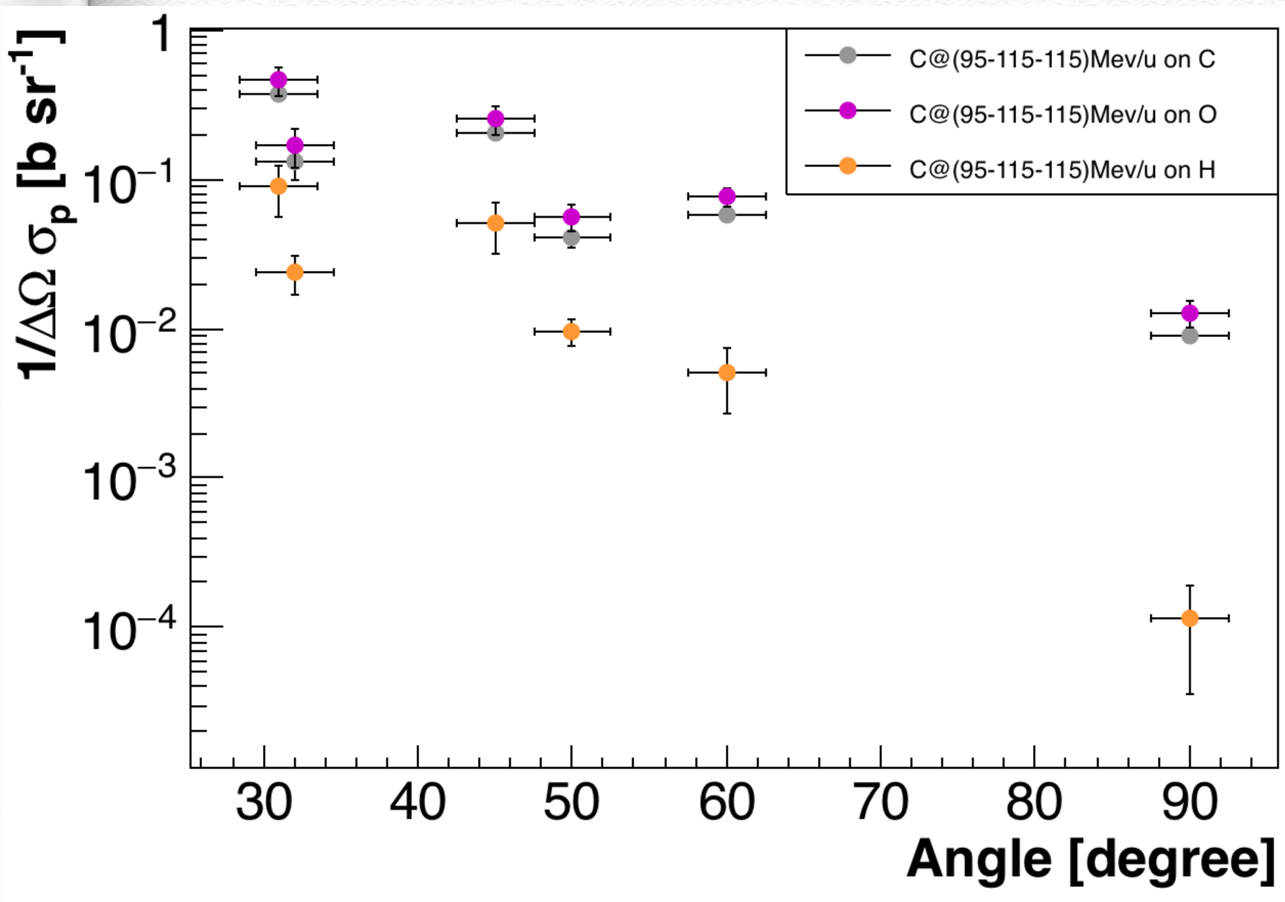

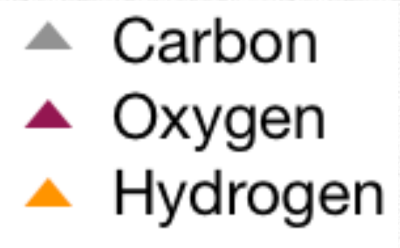

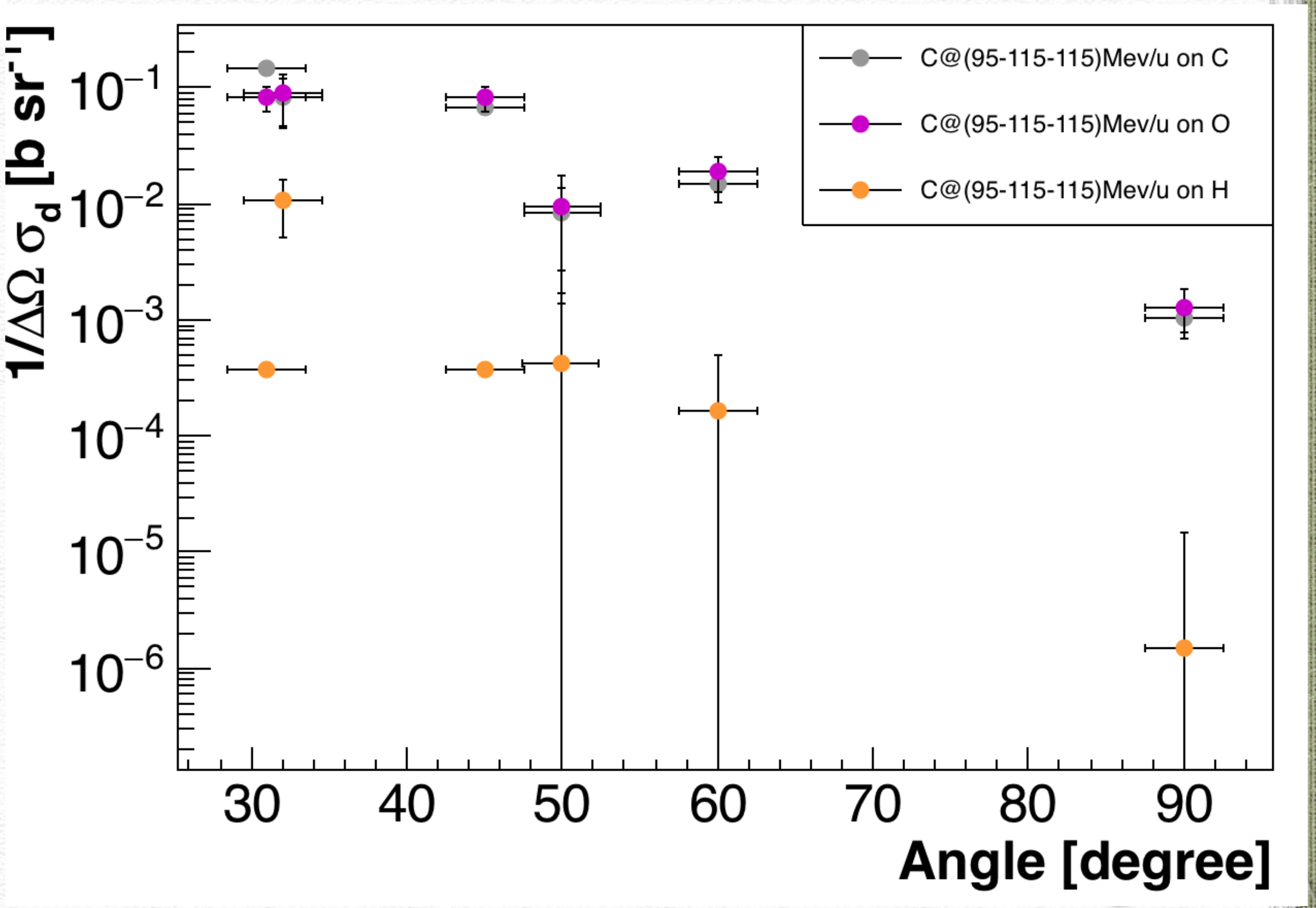

Conclusions

- The experimental data analysis is at its conclusion
- Tritons are not included since the statistics is too poor
- The DATA-FLUKA comparison has been studied at 90º and 60º and it is encouraging regarding the models status (see backup slides).
  The analysis strategy has to be changed in order to take into account the mixing efficiency dependency to the fragment kinetic energy.
- Our aim is to publish also the DATA-FLUKA comparison at all 4 angles as a FOOT collaboration paper.

backup

Particle Identification

Protons and Deutons have been selected from all other particles exploiting **deposited Energy vs ToF,** Edep vs 1/ToF, dE vs E and dE vs ToF information.

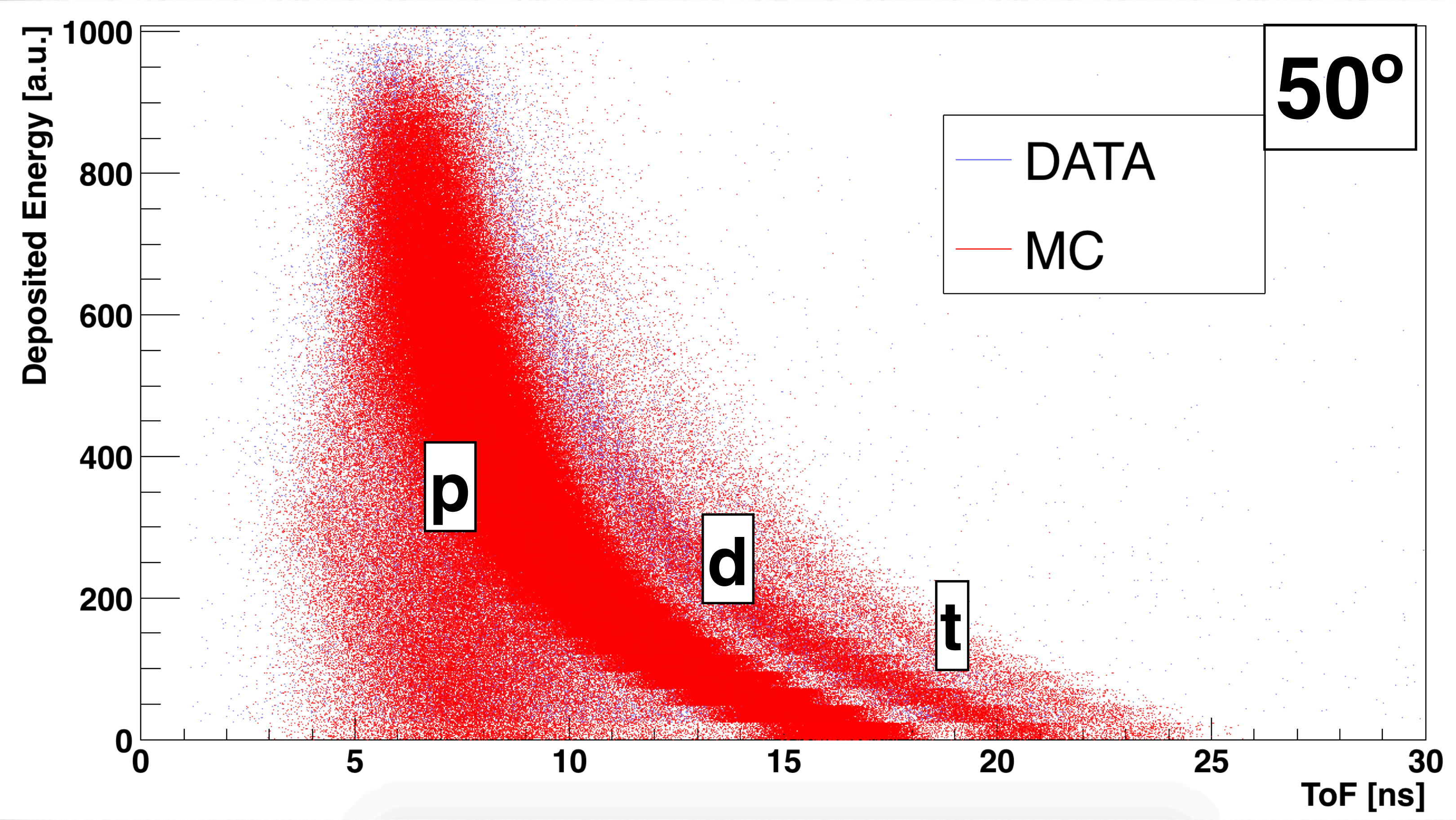

The use of MC allows to clearly identify the fragments and define our identification strategy.
In the plot the separation lines that are applied on data to separate in mass the fragments are reported.

The deposited energy in the LYSO crystal is shown as a function of the time of flight of the measured particles for data and MC-data. For the data and the MC, the deposited energy is in arbitrary units. The fragments identity is shown in order to confirm the described data selection strategy.

Particle Identification

50°

Protons Deutons and tritons have been selected from all other particles exploiting deposited Energy vs ToF, **Edep vs 1/ToF**, dE vs E and **dE vs ToF** information.

Protons and deuterons are reasonably abundant in all the specific data sets: about 80% and 20% of the fragments respectively at 32°.

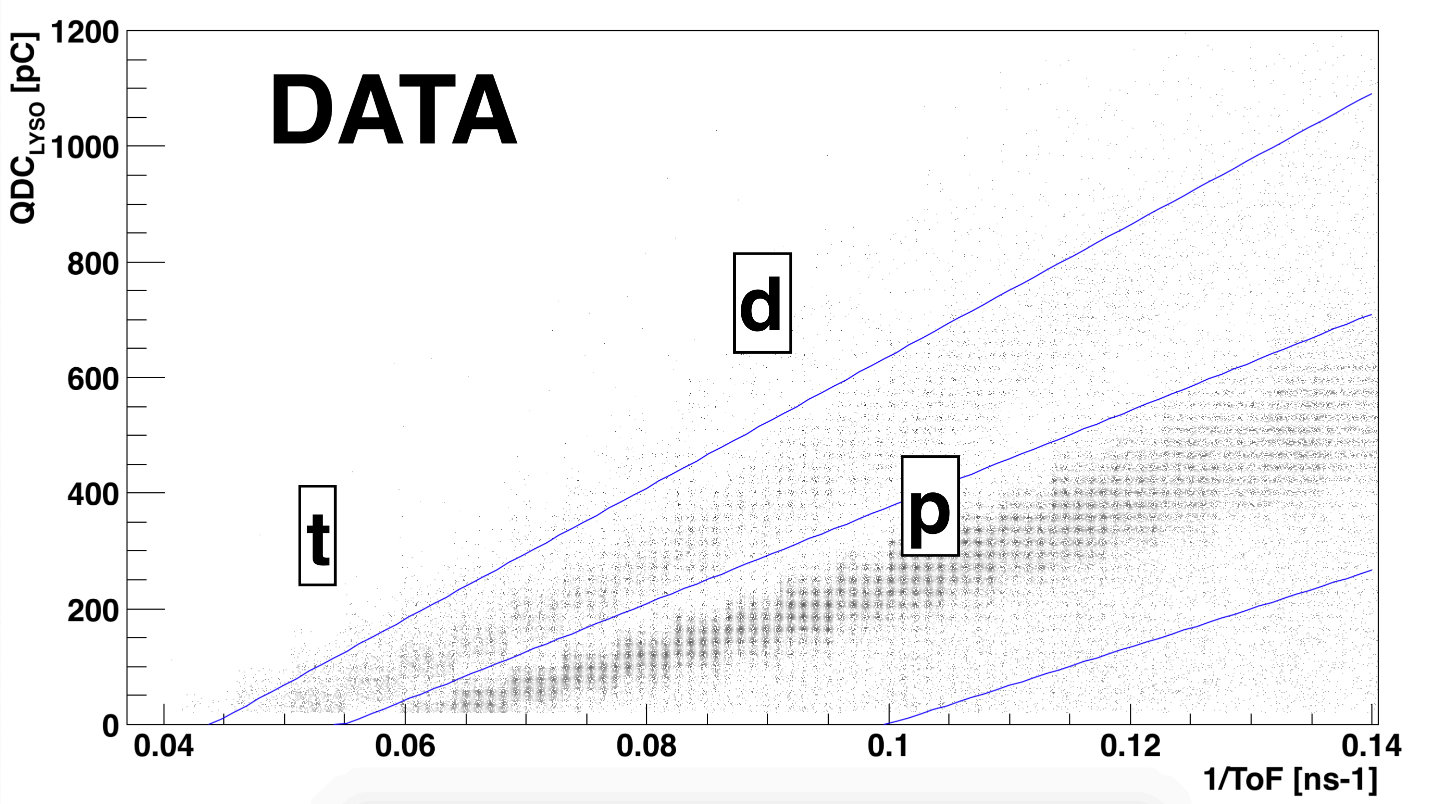

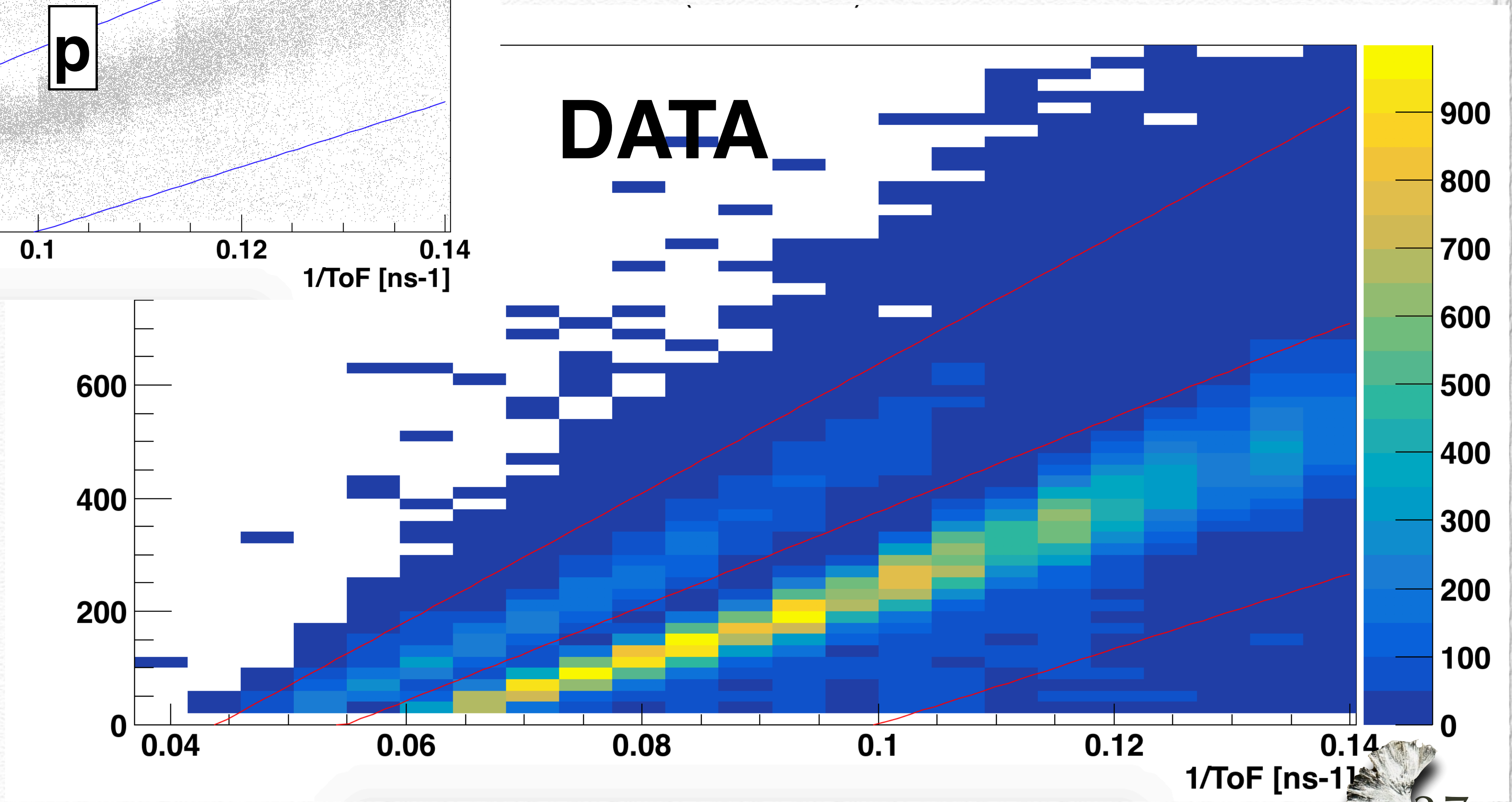

In this presentation we show the proton analysis

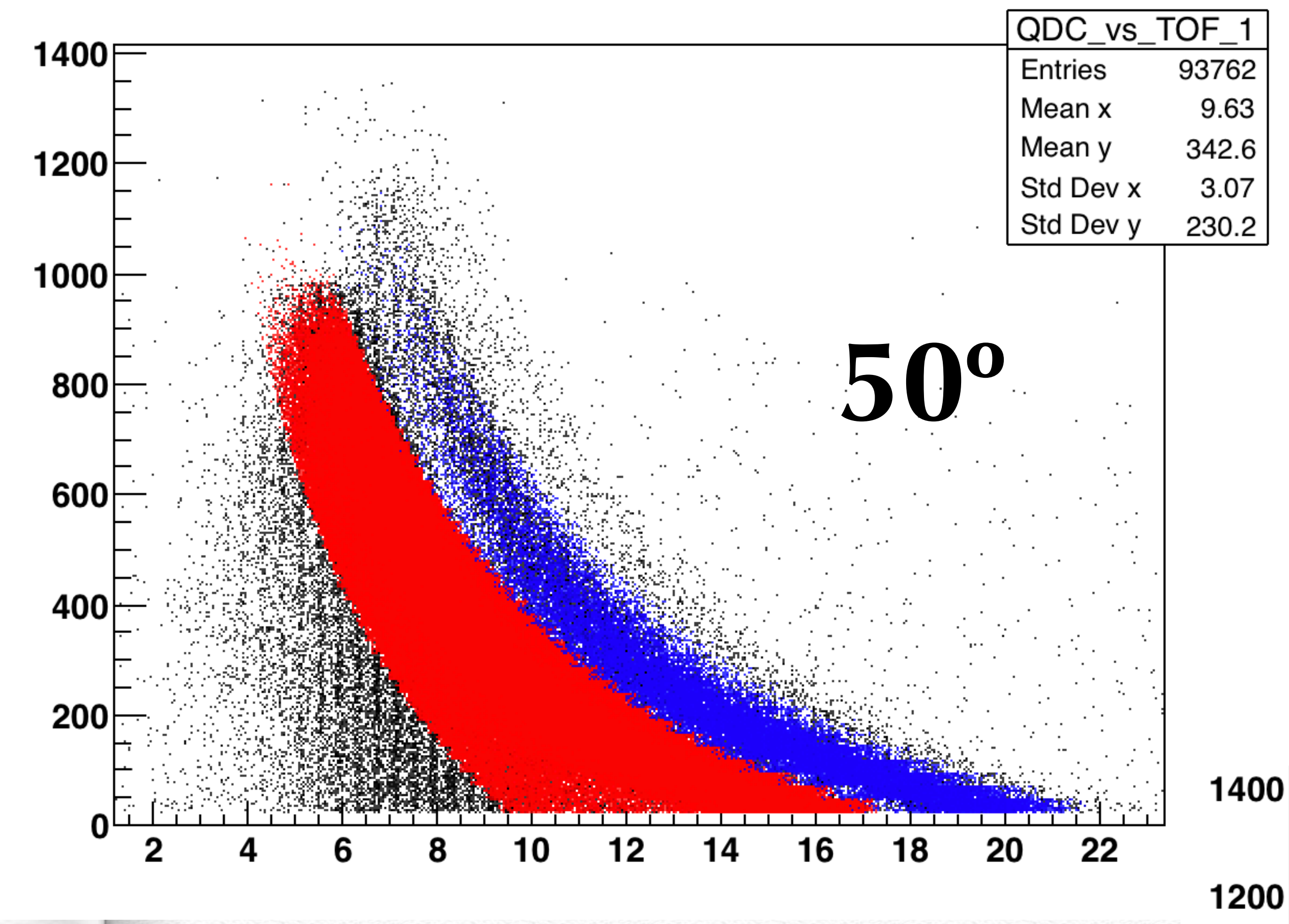
QDC_vs_TOF_1
Entries 93762
Mean x 9.63
Mean y 342.6
Std Dev x 3.07
Std Dev y 230.2
50°
1400
1200
1000
800
600
400
200
0
2 4 6 8 10 12 14 16 18 20 22

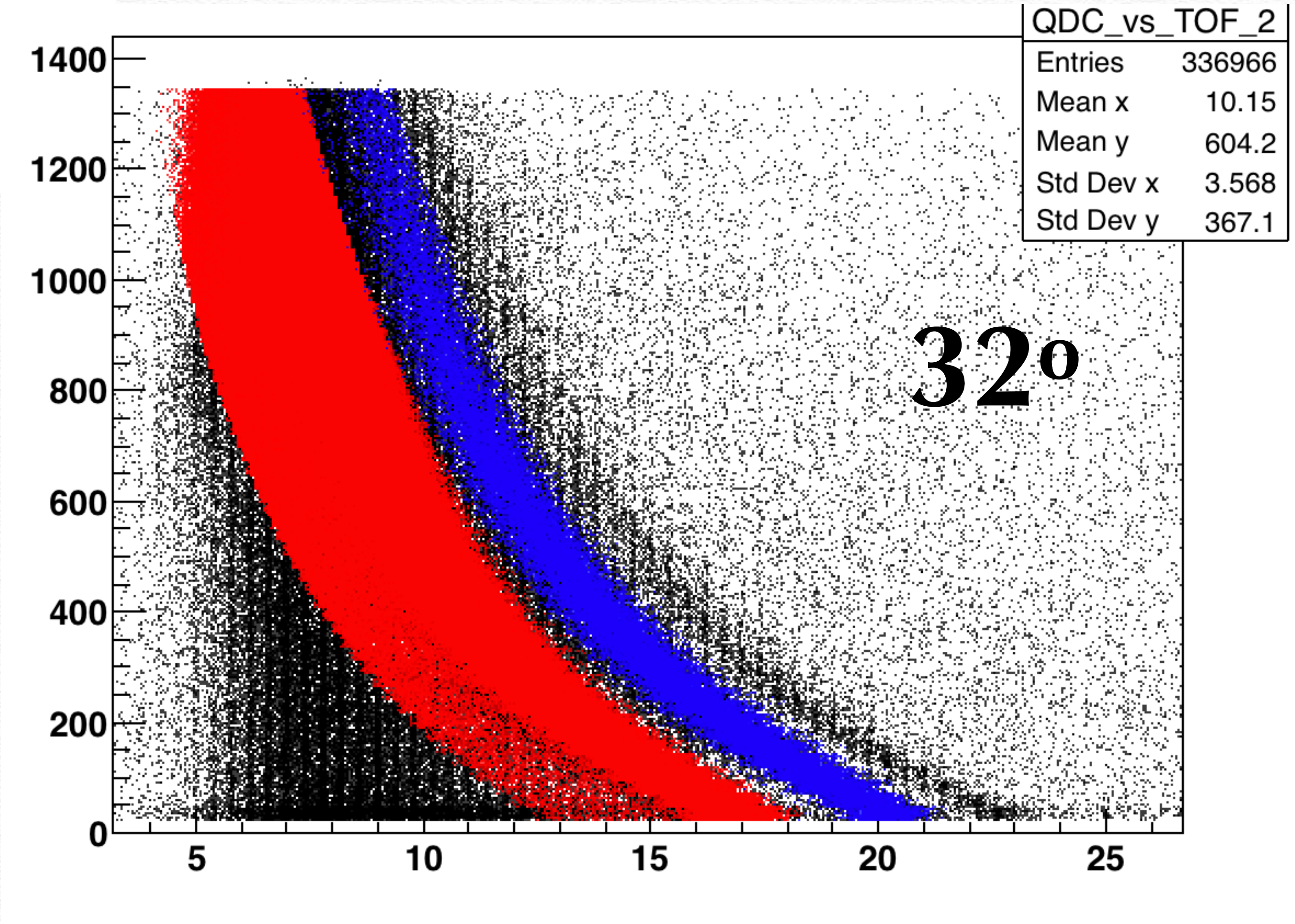
QDC_vs_TOF_2
Entries 336966
Mean x 10.15
Mean y 604.2
Std Dev x 3.568
Std Dev y 367.1
32°
1400
1200
1000
800
600
400
200
0
5 10 15 20 25

Cr

C350

The 12 … e obtained as:

$$\ldots k) \cdot \frac{1}{N_Y} \cdot \frac{1}{\epsilon}$$

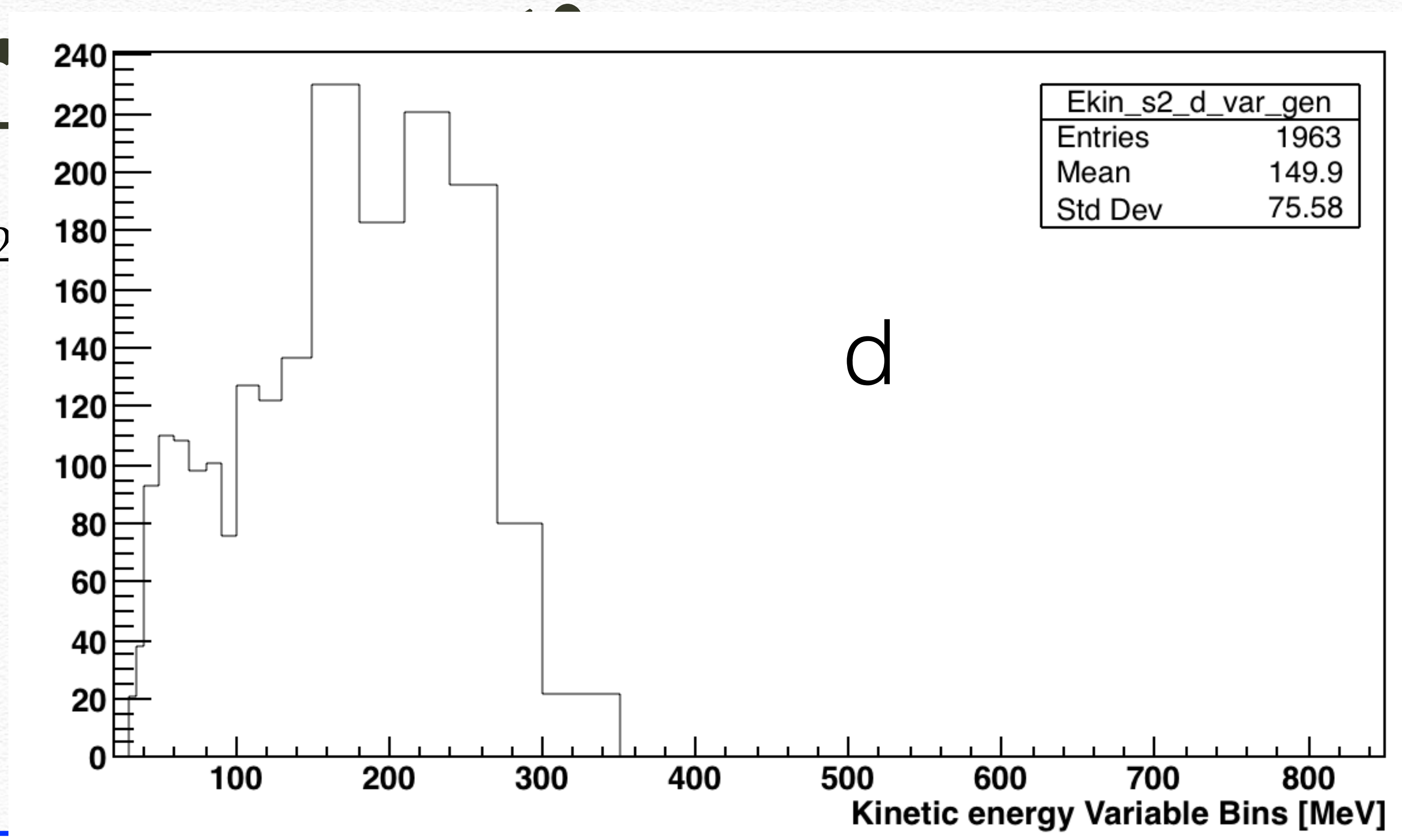

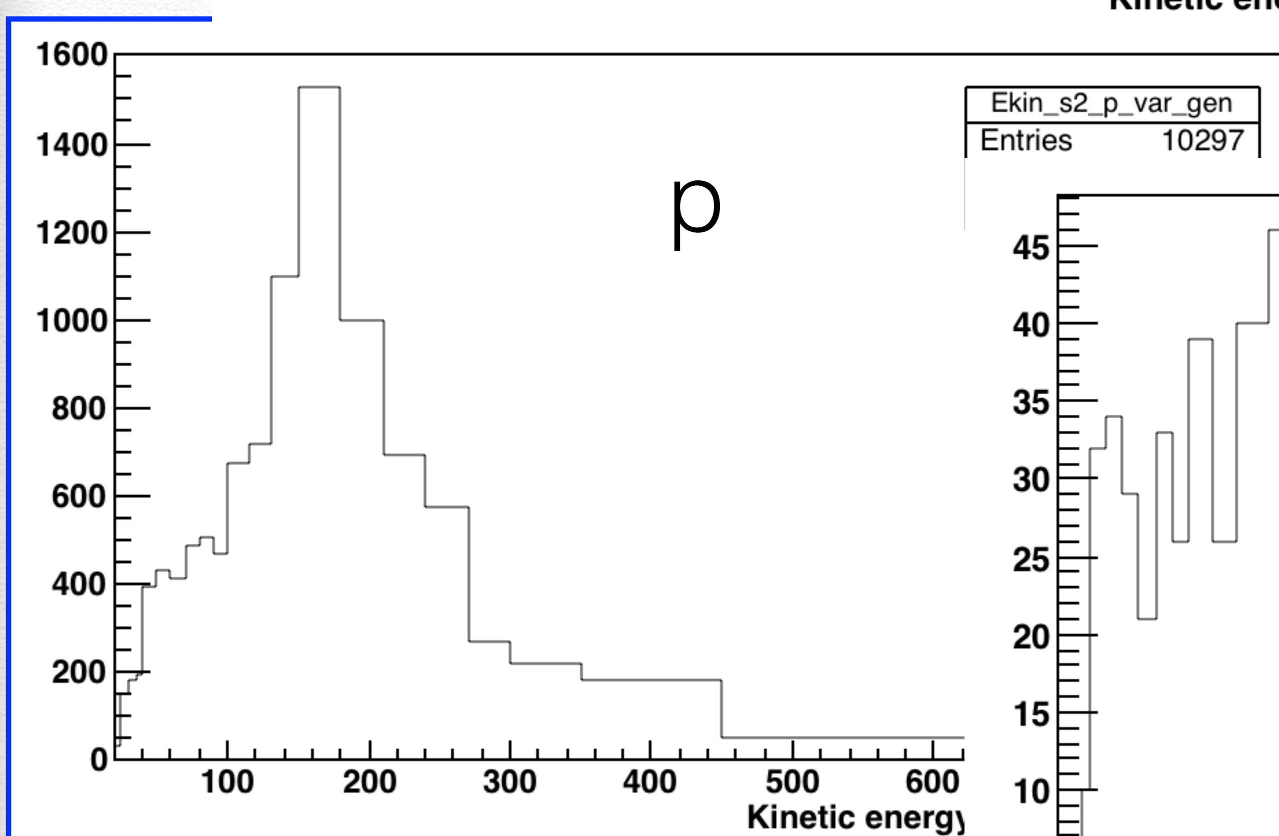

The energy loss by the

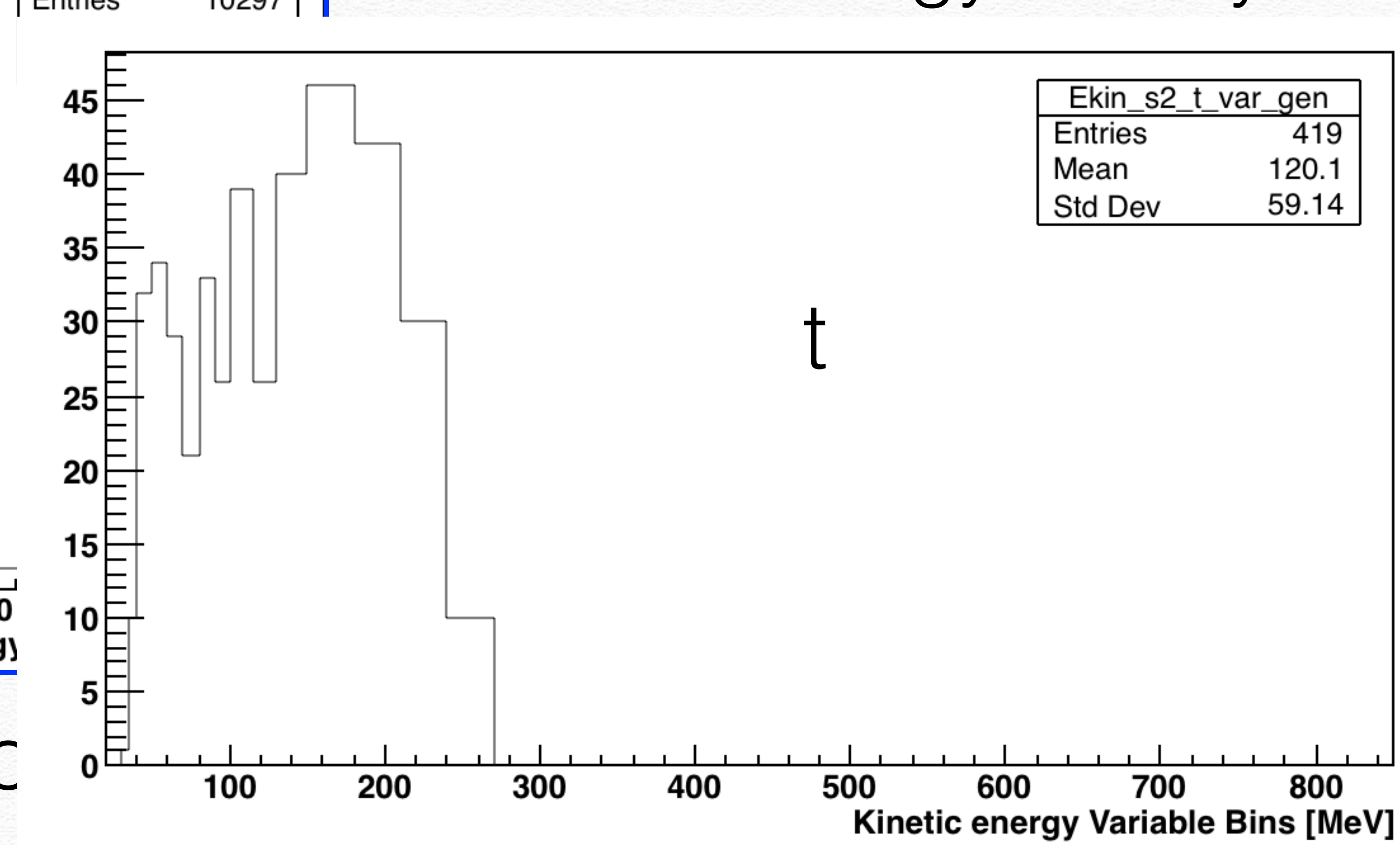

Ekin at generatio

C350

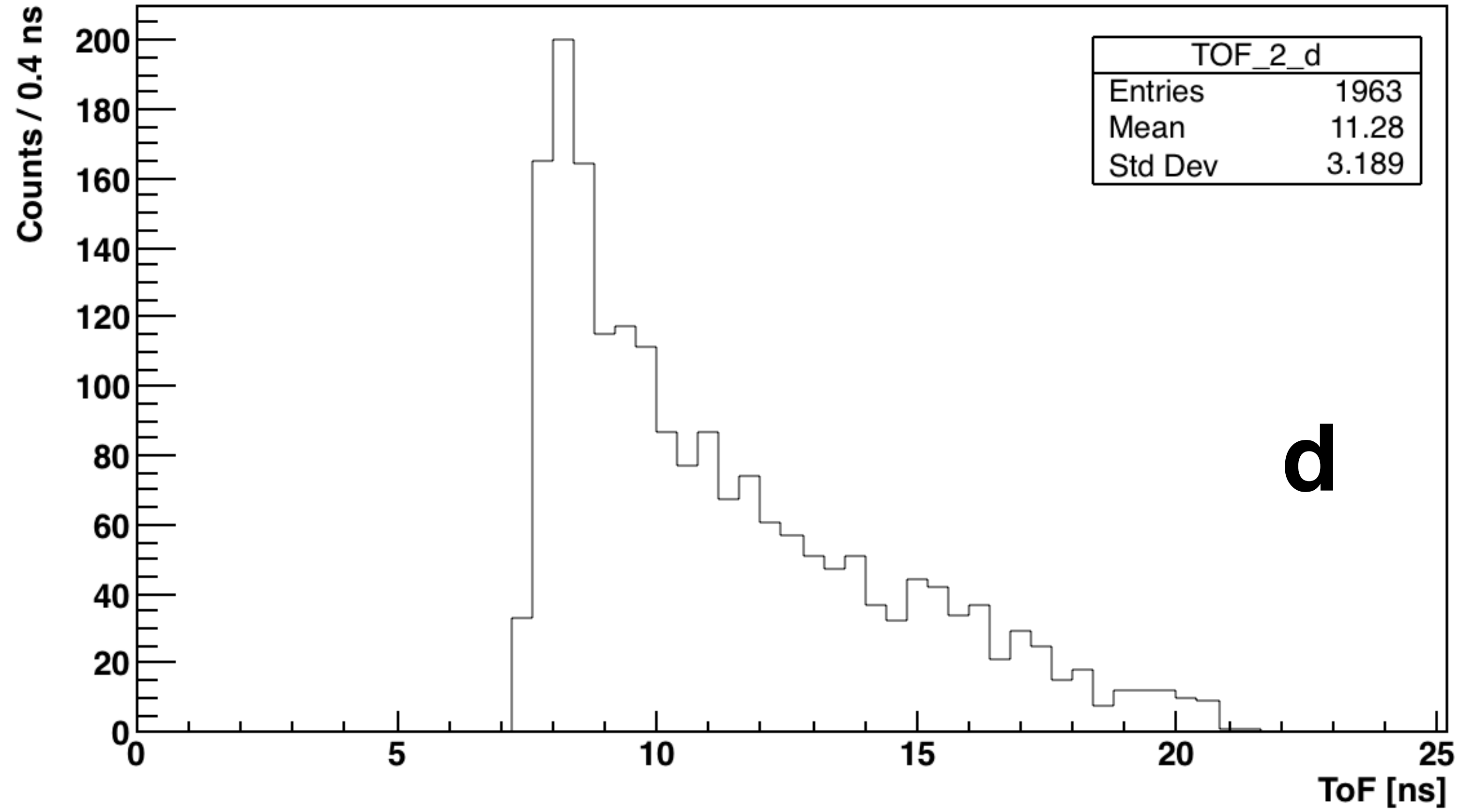

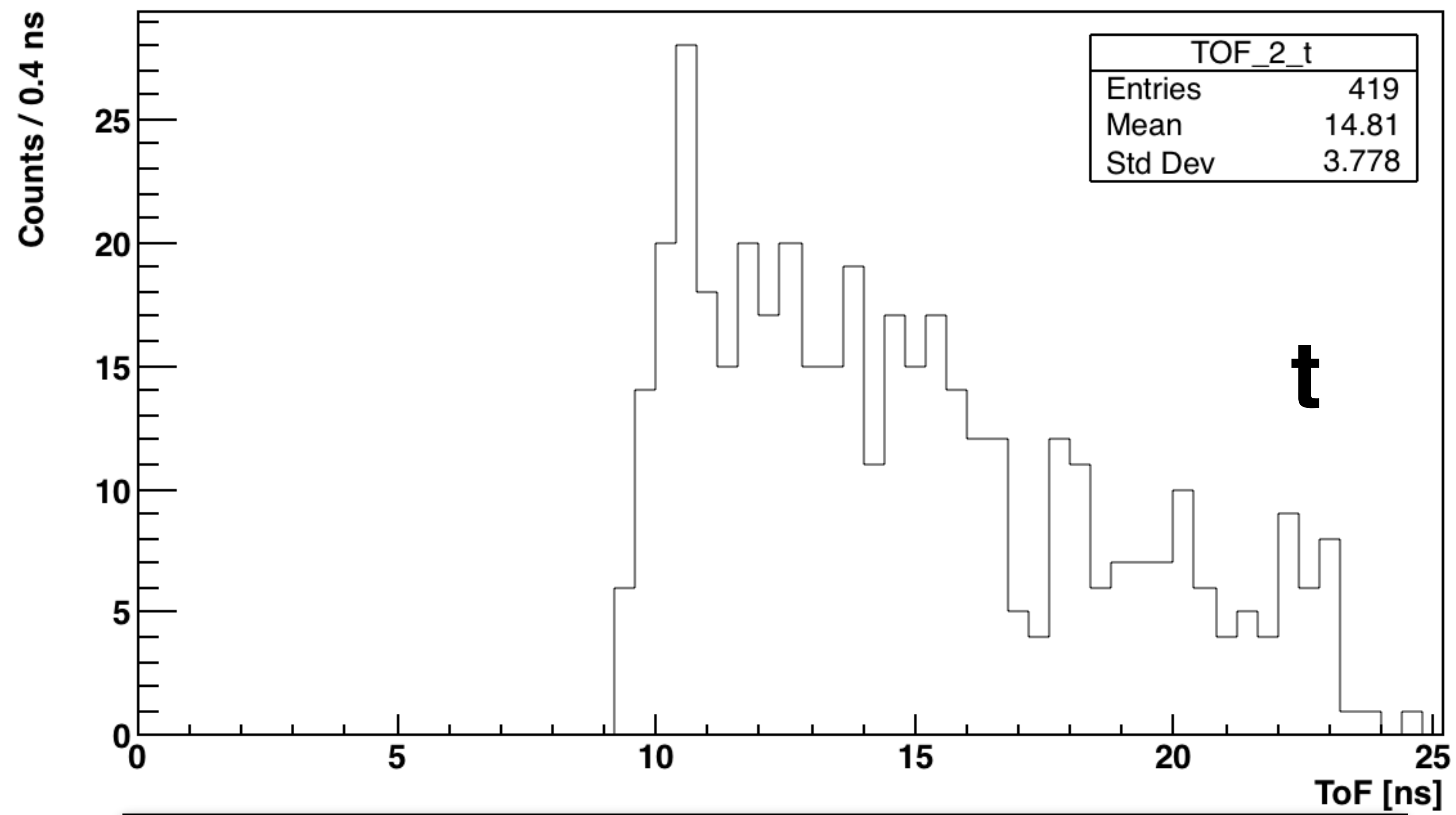

e top plot and converted in the kinetic
ta refer to Arm2, graphite target with C-ion

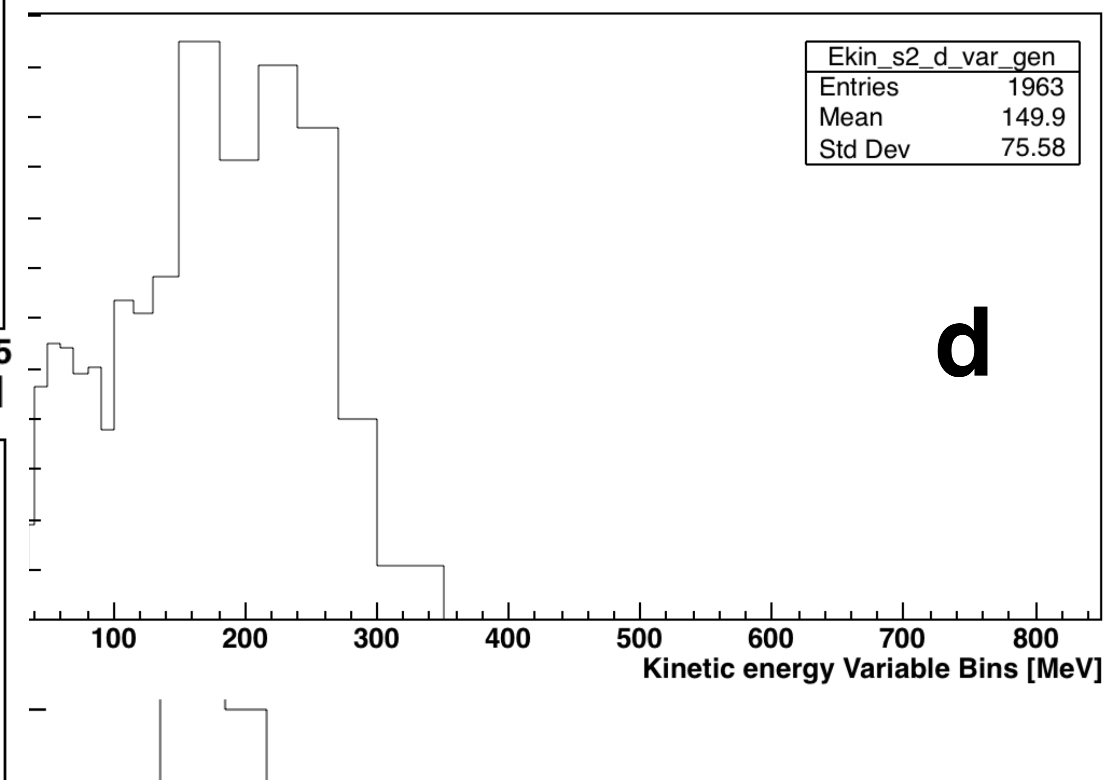

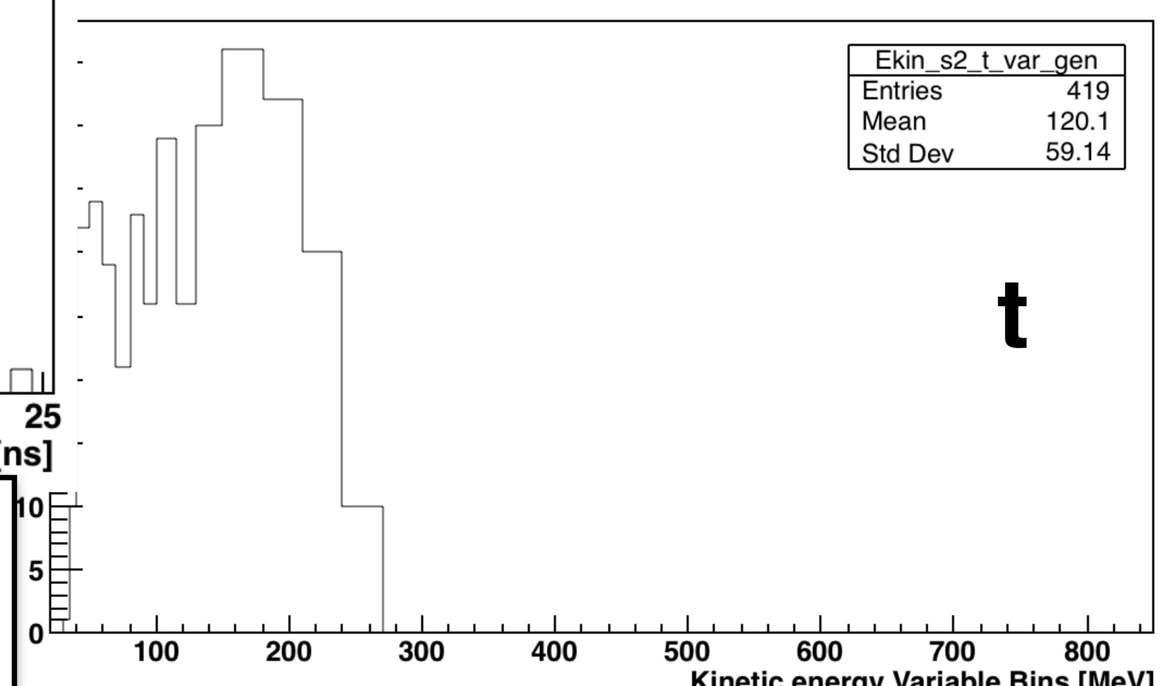

Energy resolution as a function of deuteron kinetic energy ranges from **8% (4%) up to 28% (11%)** for 50° (32°) (worsening with increasing energy).

OLD FLUKA vs NEW FLUKA

@90°,60°

OLD

Table III

PARTICLE IDENTIFICATION EFFICIENCY: SELECTION EFFICIENCIES EVALUATED FOR BOTH 90° AND 60° DETECTION CONFIGURATIONS.

E^C_{kin} $[MeV/u]$	ϵ^{pp} [%]	ϵ^{dd} [%]	ϵ^{tt} [%]
90^o			
115	95 ± 5	89 ± 9	85 ± 12
153	95 ± 5	85 ± 14	91 ± 6
221	94 ± 5	85 ± 12	86 ± 10
281	94 ± 5	84 ± 12	71 ± 31
353	94 ± 5	84 ± 14	81 ± 15
60^o			
115	95 ± 4	78 ± 21	76 ± 32
153	95 ± 5	77 ± 22	83 ± 17
221	95 ± 5	75 ± 23	73 ± 32
281	95 ± 5	75 ± 24	76 ± 26
353	94 ± 5	75 ± 24	69 ± 37

Table IV

PARTICLE IDENTIFICATION EFFICIENCY: OFF DIAGONAL ELEMENTS EVALUATED FOR BOTH THE 90° AND 60° DETECTION CONFIGURATIONS.

E^C_{kin} $[MeV/u]$	ϵ^{dp} [%]	ϵ^{tp} [%]	ϵ^{pd} [%]	ϵ^{td} [%]	ϵ^{dt} [%]
90^o					
115	6 ± 7	-	2 ± 2	12 ± 13	5 ± 7
153	10 ± 15	2 ± 3	1 ± 2	5 ± 4	4 ± 5
221	4 ± 4	3 ± 4	2 ± 3	11 ± 10	7 ± 6
281	5 ± 3	2 ± 2	2 ± 3	8 ± 6	8 ± 7
353	4 ± 2	1 ± 1	2 ± 2	10 ± 10	7 ± 7
60^o					
115	4 ± 3	2 ± 2	1 ± 2	3 ± 4	13 ± 13
153	4 ± 2	2 ± 2	1 ± 2	2 ± 2	16 ± 16
221	4 ± 4	2 ± 2	1 ± 2	8 ± 14	17 ± 17
281	4 ± 3	3 ± 3	1 ± 2	10 ± 19	16 ± 16
353	4 ± 3	5 ± 6	2 ± 3	10 ± 14	17 ± 17

NEW

Table III

PARTICLE IDENTIFICATION EFFICIENCY: SELECTION EFFICIENCIES EVALUATED FOR BOTH 90° AND 60° DETECTION CONFIGURATIONS.

E^C_{kin} $[MeV/u]$	ϵ^{pp} [%]	ϵ^{dd} [%]	ϵ^{tt} [%]
50^o			
115	95 ± 5	88 ± 12	86 ± 19
150	95 ± 5	81 ± 21	89 ± 7
221	94 ± 5	86 ± 12	91 ± 6.1
279	95 ± 5	85 ± 11	91 ± 6.3
351	95 ± 5	85 ± 13	83 ± 21
32^o			
115	95 ± 5	79 ± 20	81 ± 30
150	95 ± 4.8	78 ± 22	79 ± 30
221	95 ± 4.6	76 ± 23	86 ± 14
279	95 ± 4.7	76 ± 24	83 ± 18
351	94 ± 5.4	76 ± 23	82 ± 23

Table IV

PARTICLE IDENTIFICATION EFFICIENCY: OFF DIAGONAL ELEMENTS EVALUATED FOR BOTH THE 90° AND 60° DETECTION CONFIGURATIONS.

E^C_{kin} $[MeV/u]$	ϵ^{dp} [%]	ϵ^{tp} [%]	ϵ^{pd} [%]	ϵ^{td} [%]	ϵ^{dt} [%]
90^o					
115	4 ± 7	1 ± 2	1 ± 1	10 ± 18	6 ± 12
150	7 ± 8	0.4 ± 1	2 ± 2	9 ± 8	5 ± 6
221	4 ± 4	1 ± 2	2 ± 3	6 ± 6	7 ± 9
279	5 ± 4	0.5 ± 1	2 ± 2	6 ± 6	7 ± 7
351	5 ± 4	1 ± 2	2 ± 2	11 ± 10	8 ± 8
60^o					
115	4 ± 4	1 ± 1	1 ± 2	3 ± 3	13 ± 13
150	4 ± 3	2 ± 3	1 ± 2	3 ± 2	15 ± 16
221	4 ± 4	2 ± 2	1 ± 2	3 ± 3	16 ± 16
279	4 ± 3	2 ± 3	1 ± 2	3 ± 2	16 ± 16
351	4 ± 3	5 ± 7	2 ± 3	3 ± 3	15 ± 15

OLD FLUKA vs NEW FLUKA

@90º,60º

OLD

Table III

PARTICLE IDENTIFICATION EFFICIENCY: SELECTION EFFICIENCIES EVALUATED FOR BOTH 90° AND 60° DETECTION CONFIGURATIONS.

E^C_{kin} $[MeV/u]$	ϵ^{pp} [%]	ϵ^{dd} [%]	ϵ^{tt} [%]
90^o			
115	95 ± 5	89 ± 9	85 ± 12
153	95 ± 5	85 ± 14	91 ± 6
221	94 ± 5	85 ± 12	86 ± 10
281	94 ± 5	84 ± 12	71 ± 31
353	94 ± 5	84 ± 14	81 ± 15
60^o			
115	95 ± 4	78 ± 21	76 ± 32
153	95 ± 5	77 ± 22	83 ± 17
221	95 ± 5	75 ± 23	73 ± 32
281	95 ± 5	75 ± 24	76 ± 26
353	94 ± 5	75 ± 24	69 [illegible]

T[illegible]

PARTICLE IDENTIFICAT[illegible]
EVALUATED FOR BO[illegible] ONS.

E^C_{kin} $[MeV/u]$	[illegible]	[illegible]	[illegible]	[%]	ϵ^{dt} [%]
90^o					
115	6 ± [illegible]	[illegible]	2 ± 2	12 ± 13	5 ± 7
153	10 ± [illegible]	2 ± 3	1 ± 2	5 ± 4	4 ± 5
221	4 ± 4	3 ± 4	2 ± 3	11 ± 10	7 ± 6
281	5 ± 3	2 ± 2	2 ± 3	8 ± 6	8 ± 7
353	4 ± 2	1 ± 1	2 ± 2	10 ± 10	7 ± 7
60^o					
115	4 ± 3	2 ± 2	1 ± 2	3 ± 4	13 ± 13
153	4 ± 2	2 ± 2	1 ± 2	2 ± 2	16 ± 16
221	4 ± 4	2 ± 2	1 ± 2	8 ± 14	17 ± 17
281	4 ± 3	3 ± 3	1 ± 2	10 ± 19	16 ± 16
353	4 ± 3	5 ± 6	2 ± 3	10 ± 14	17 ± 17

NEW

Table III

PARTICLE IDENTIFICATION EFFICIENCY: SELECTION EFFICIENCIES EVALUATED FOR BOTH 90° AND 60° DETECTION CONFIGURATIONS.

E^C_{kin} $[MeV/u]$	ϵ^{pp} [%]	ϵ^{dd} [%]	ϵ^{tt} [%]
50^o			
115	95 [illegible]	[illegible] ± 12	86 ± 19
150	[illegible]	[illegible] 21	89 ± 7
22[illegible]	[illegible]	[illegible] 12	91 ± 6.1
[illegible]	[illegible]	[illegible] 11	91 ± 6.3
[illegible]	[illegible]	[illegible]	83 ± 21
[illegible]			
[illegible]	[illegible]	79 ± 20	81 ± 30
[illegible]	[illegible] ± 4.8	78 ± 22	79 ± 30
[illegible]	95 ± 4.6	76 ± 23	86 ± 14
[illegible]79	95 ± 4.7	76 ± 24	83 ± 18
351	94 ± 5.4	76 ± 23	82 ± 23

Table IV

PARTICLE IDENTIFICATION EFFICIENCY: OFF DIAGONAL ELEMENTS EVALUATED FOR BOTH THE 90° AND 60° DETECTION CONFIGURATIONS.

E^C_{kin} $[MeV/u]$	ϵ^{dp} [%]	ϵ^{tp} [%]	ϵ^{pd} [%]	ϵ^{td} [%]	ϵ^{dt} [%]
90^o					
115	4 ± 7	1 ± 2	1 ± 1	10 ± 18	6 ± 12
150	7 ± 8	0.4 ± 1	2 ± 2	9 ± 8	5 ± 6
221	4 ± 4	1 ± 2	2 ± 3	6 ± 6	7 ± 9
279	5 ± 4	0.5 ± 1	2 ± 2	6 ± 6	7 ± 7
351	5 ± 4	1 ± 2	2 ± 2	11 ± 10	8 ± 8
60^o					
115	4 ± 4	1 ± 1	1 ± 2	3 ± 3	13 ± 13
150	4 ± 3	2 ± 3	1 ± 2	3 ± 2	15 ± 16
221	4 ± 4	2 ± 2	1 ± 2	3 ± 3	16 ± 16
279	4 ± 3	2 ± 3	1 ± 2	3 ± 2	16 ± 16
351	4 ± 3	5 ± 7	2 ± 3	3 ± 3	15 ± 15

Nothing has changed in view of the published PAPER results

Differential cross section for proton production from C on PMMA, CH, C vs Eprotons

- FLUKA (open) vs DATA (filled) -

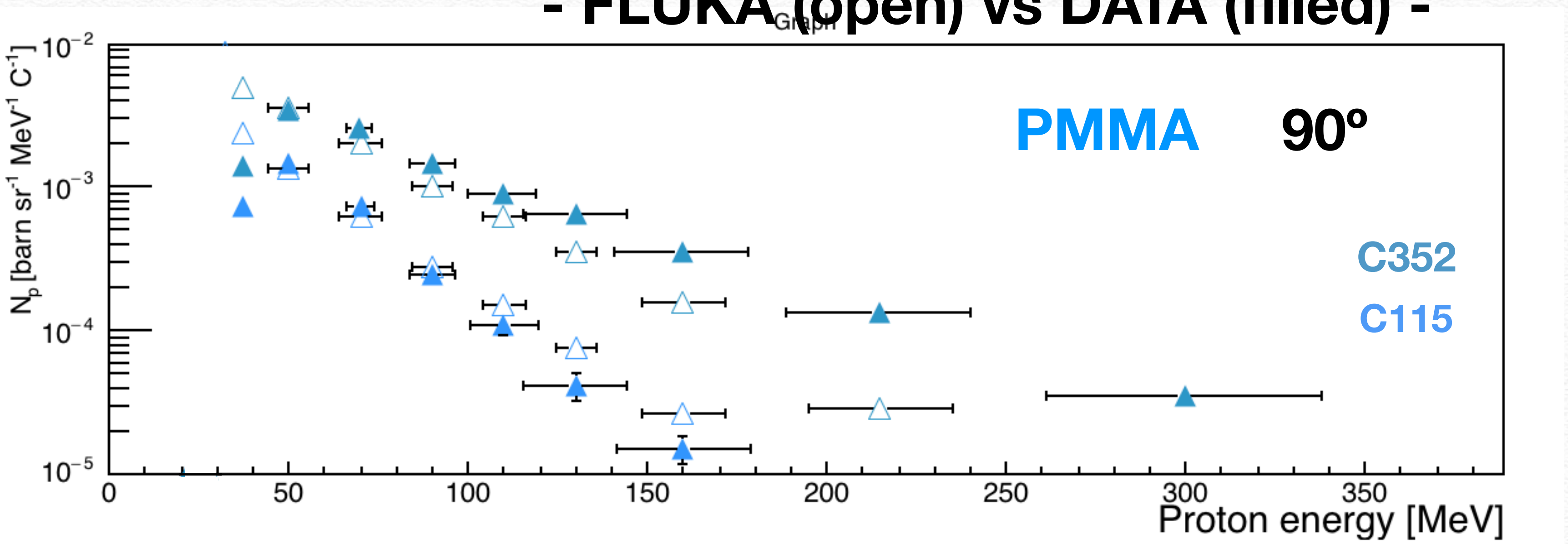

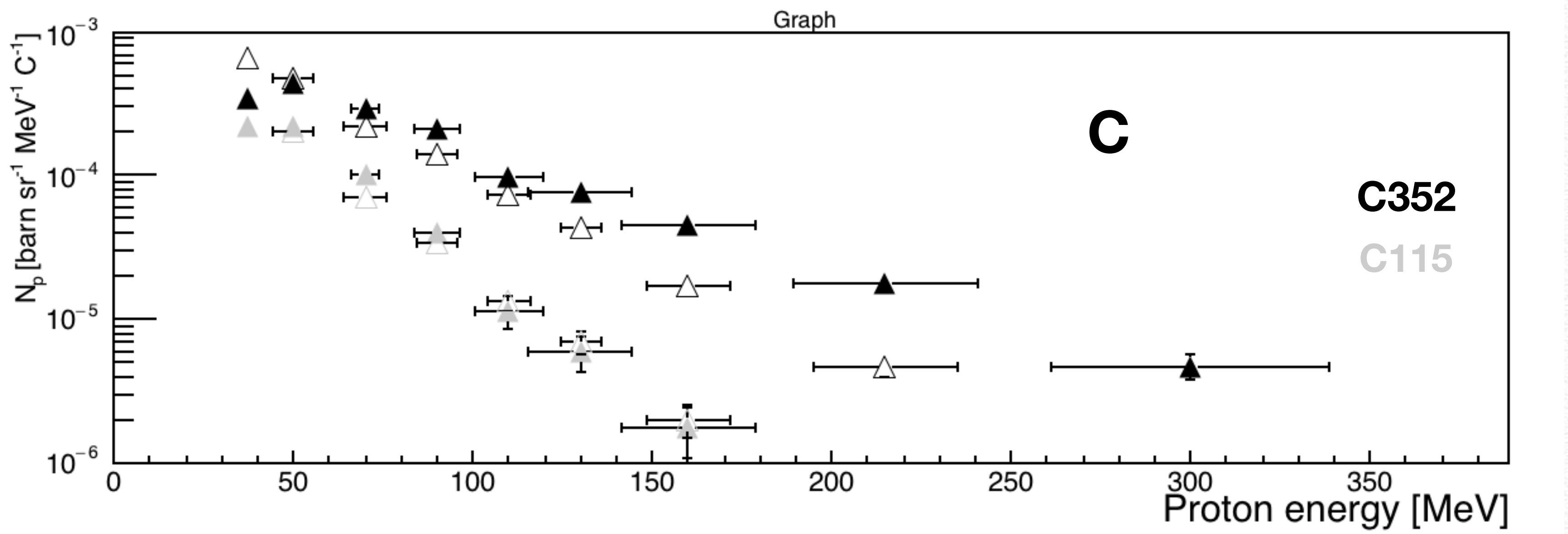

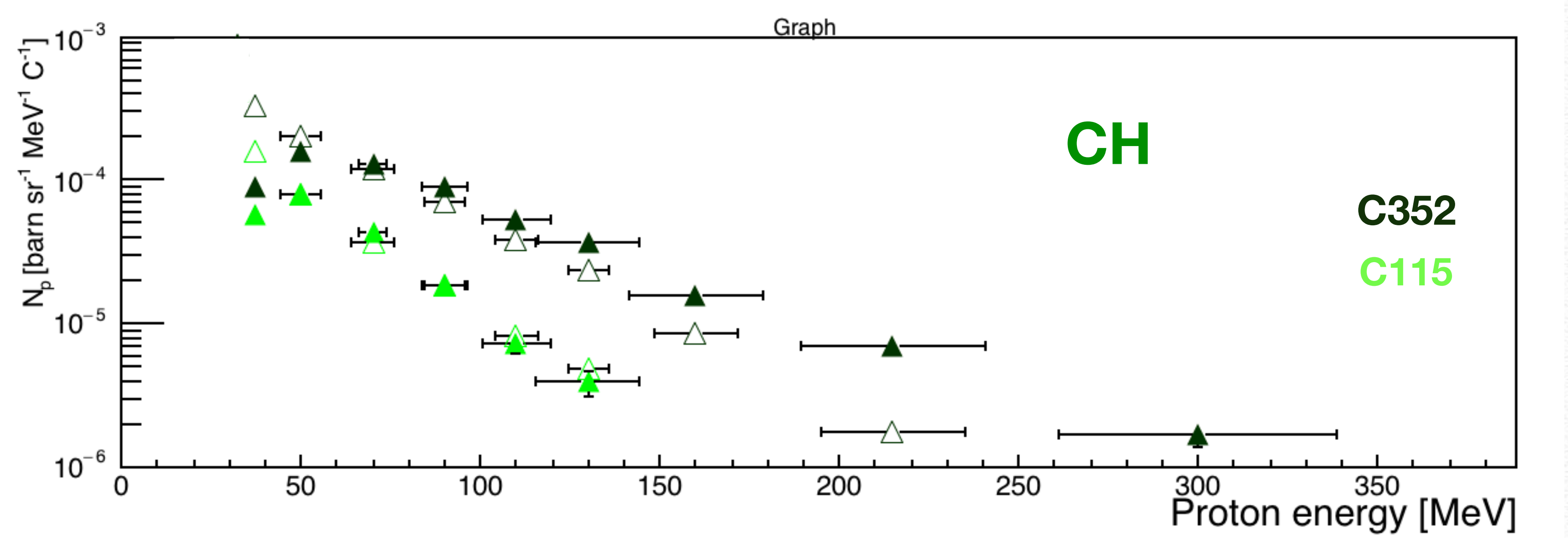

In DATA there is the contamination of deuterons in the proton signal, especially at large Ekin

Differential cross section for proton production from C on PMMA, CH, C vs Eprotons
- FLUKA (open) vs DATA (filled) -

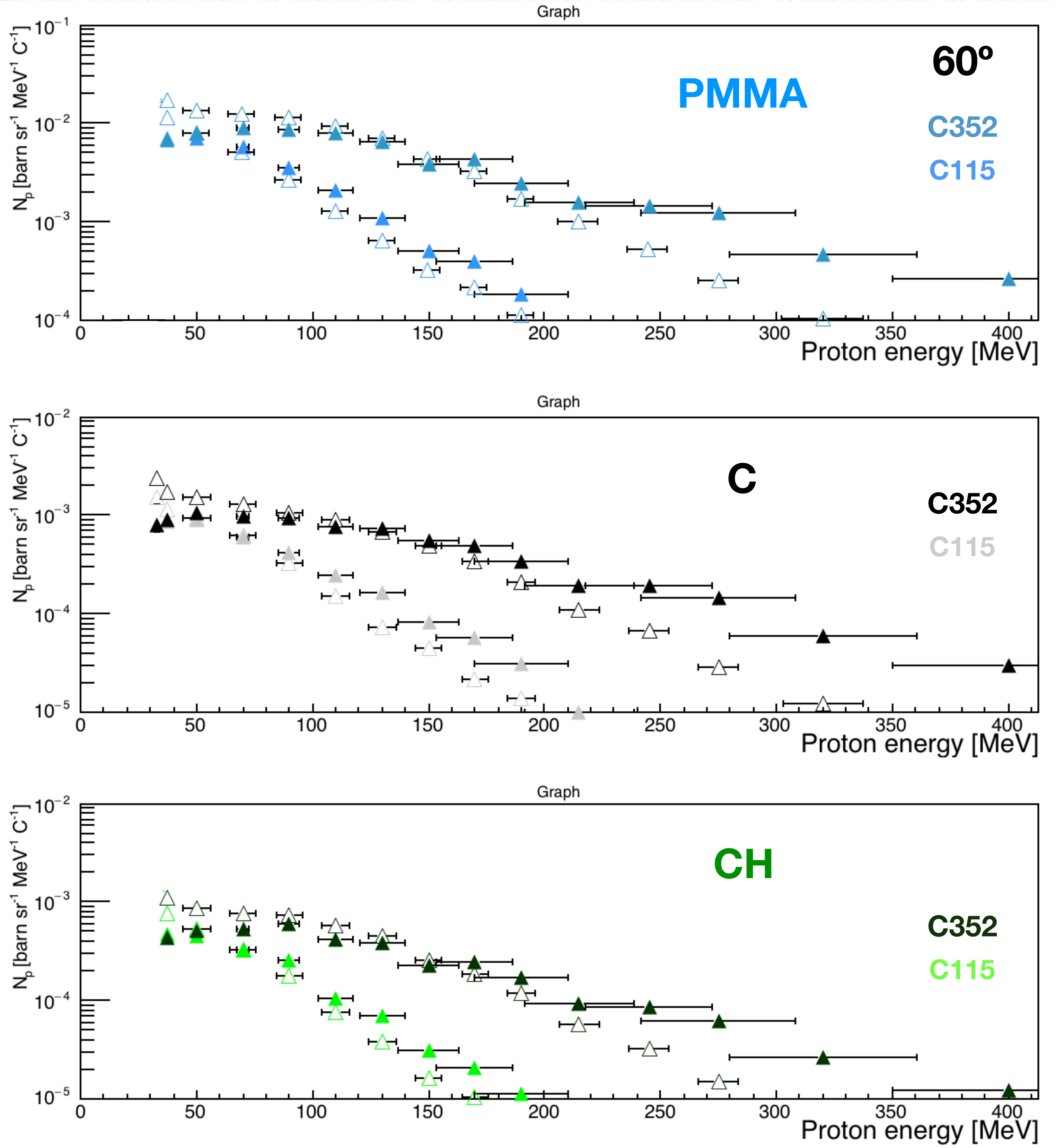

The comparison seems more in agreement at 115 MeV/u wrt 352 MeV/u but it could be due to the deuterons and tritons contamination at high energies (low ToF) and/or to the BME-rQMD models transition => to be investigated

Differential Cross Section for proton production from C on O, H, C vs Eproton

- FLUKA (open) vs DATA (filled) -

C

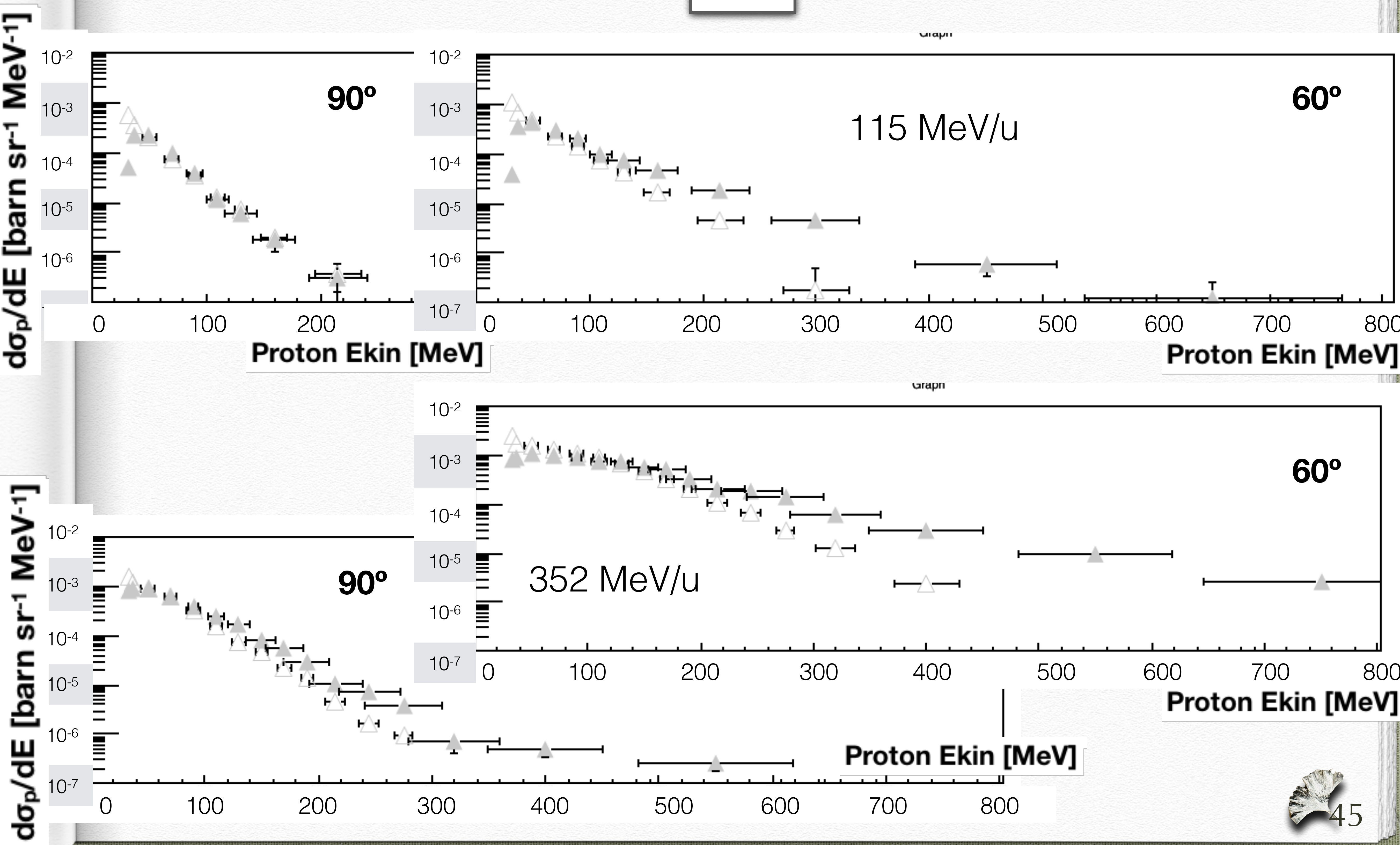

Differential Cross Section for proton production from C on O, H, C vs Eproton

- FLUKA (open) vs DATA (filled) -

O

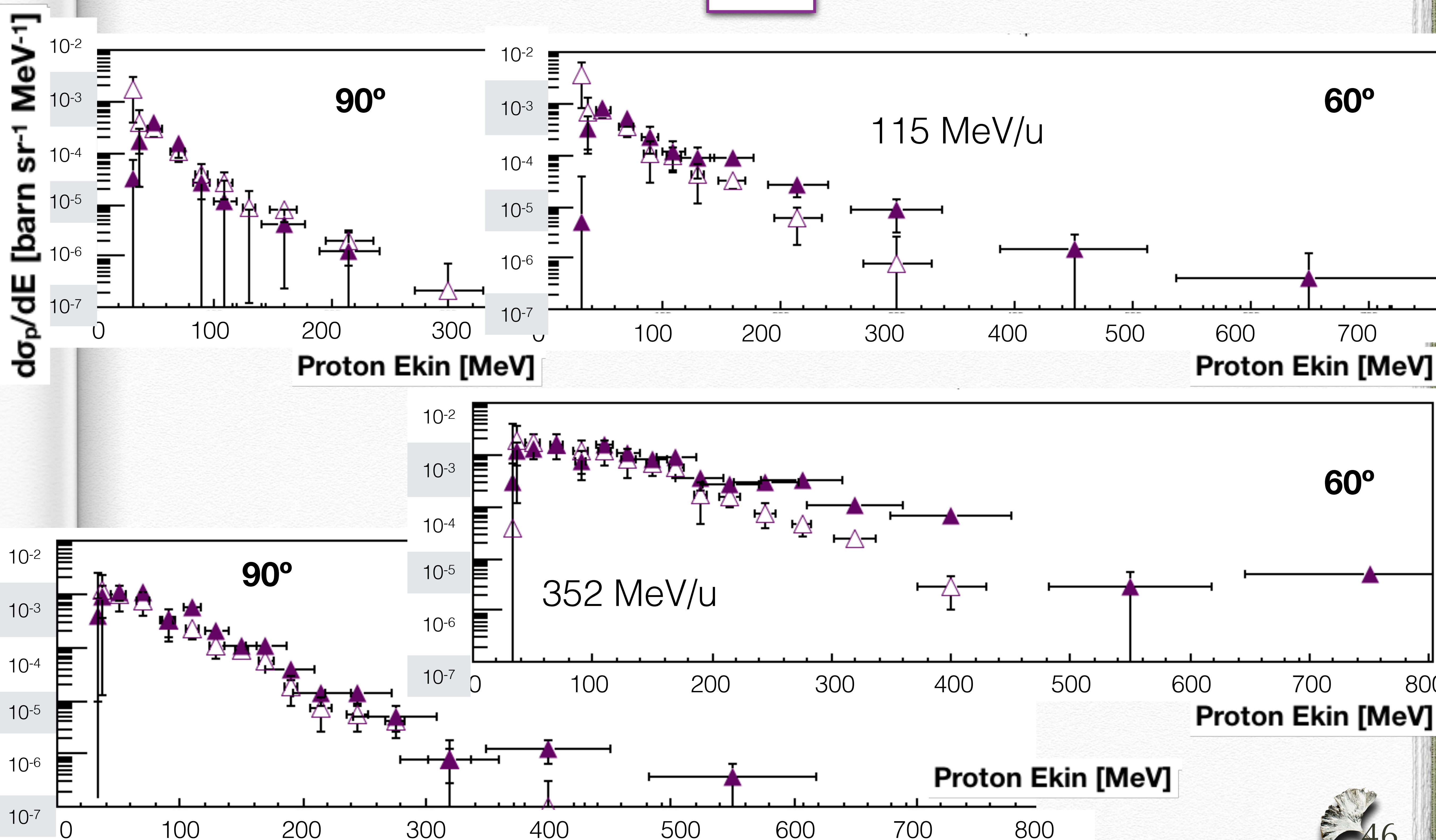

Total Cross Section for proton production from C on O, H, C vs Ebeam

- FLUKA (open) vs DATA (filled) -

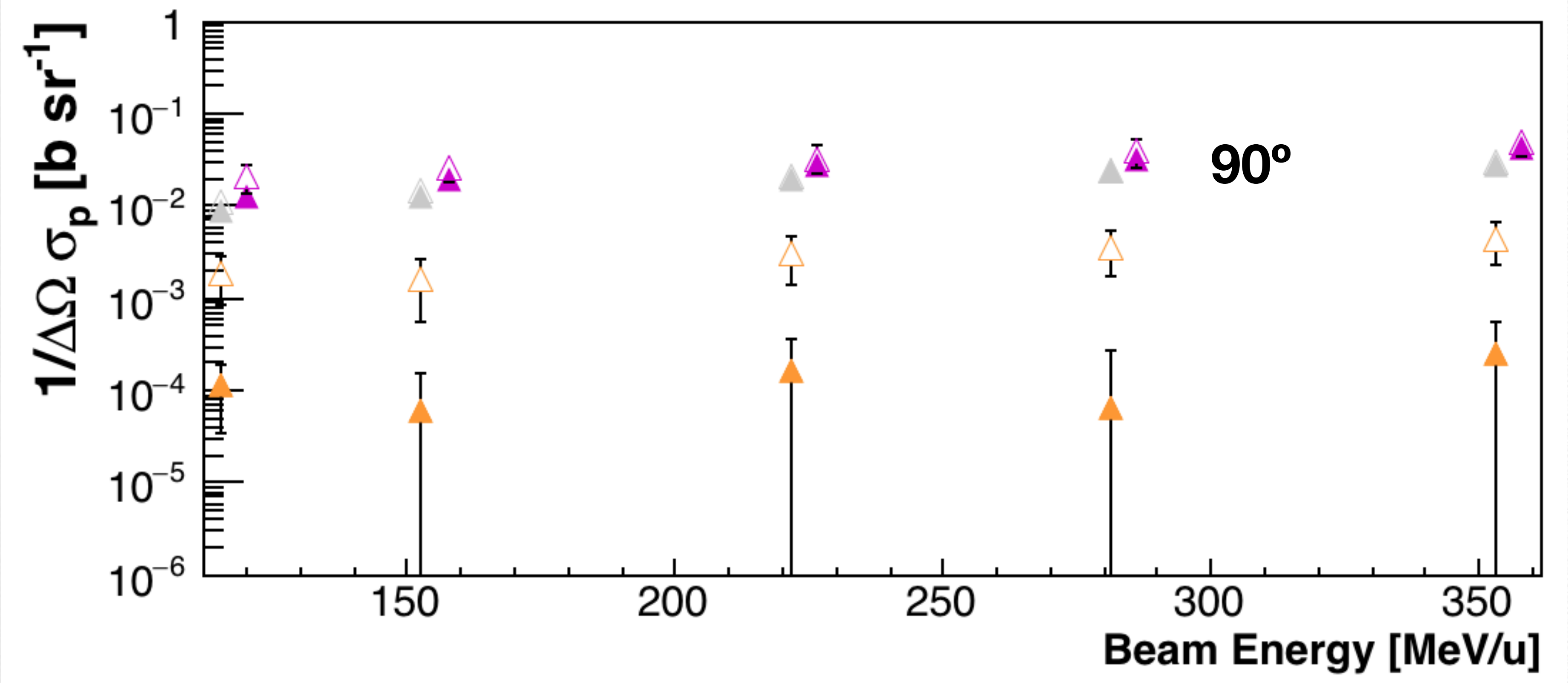

C

O

H

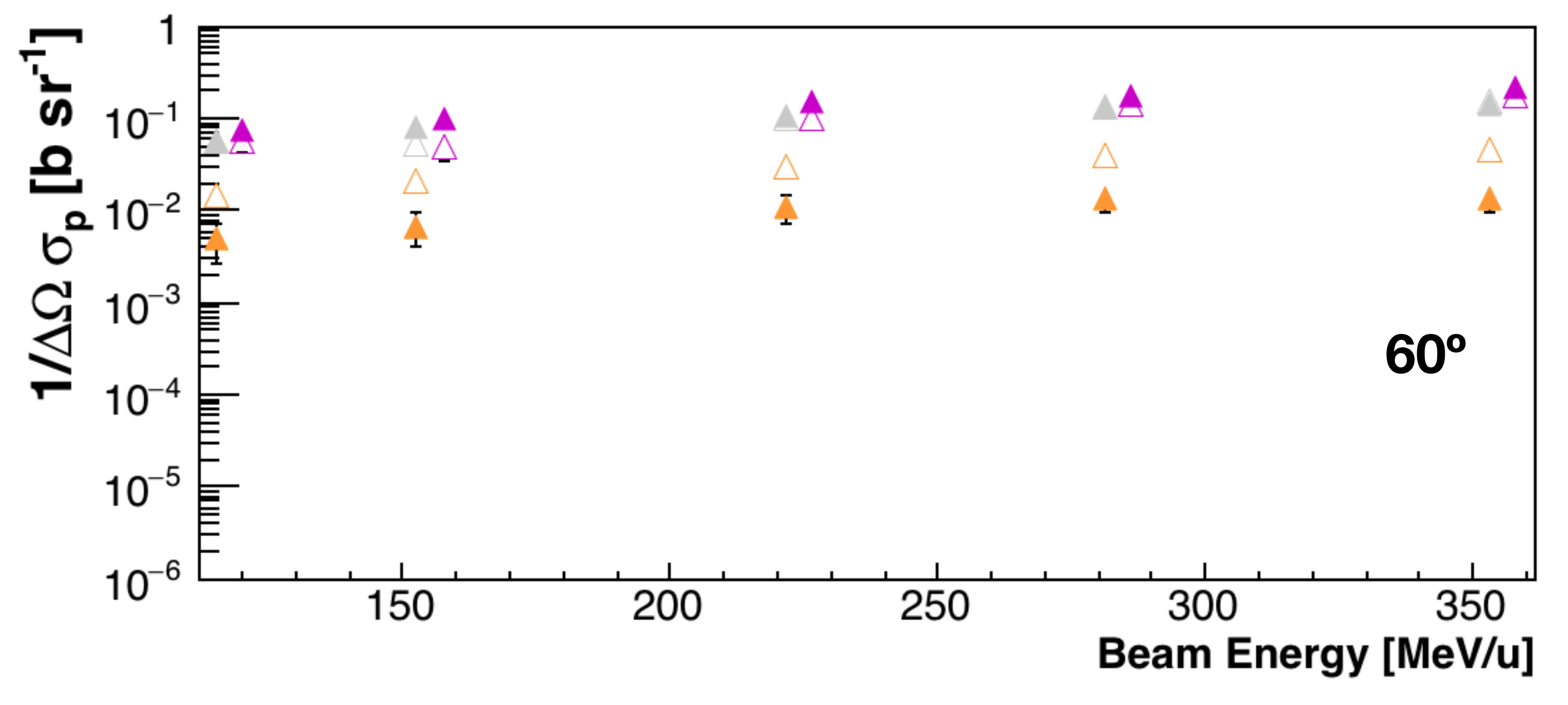

Here DATA have been corrected for the contamination of deuterons in the proton signal

Total Cross Section for proton production from C on O, H, C vs ANGLE

- FLUKA (open) vs DATA (filled) -

C **O** **H**